TECHNICAL
REPORT
NCSL TR 327-78

FEBRUARY 1978

PREDICTION OF ACCELERATION HYDRODYNAMIC COEFFICIENTS FOR UNDERWATER VEHICLES FROM GEOMETRIC PARAMETERS

D. E. HUMPHREYS
K. W. WATKINSON

NAVAL COASTAL SYSTEMS LABORATORY
NCSL
PANAMA CITY, FLORIDA 32407

NAVAL COASTAL SYSTEMS LABORATORY
PANAMA CITY, FLORIDA 32407

CAPT JAMES V. JOLLIFF, USN
Commanding Officer

GERALD G. GOULD
Technical Director

ADMINISTRATIVE INFORMATION

This work was performed under the joint sponsorship of the projects Vehicle Hydrodynamics, Task Area Number ZF 61-112-001, Work Unit Number 00112-50-1A; Analytical Investigations of Countermeasure Launchers, Task Area Number SF 34-371-208, Work Unit Number 16436; and the Advanced Submarine Control Program, Subproject Number S0207, Work Unit 20259.

63561N

Released by
M. J. Wynn, Head
Coastal Technology Department
February 1978

Under Authority of
G. G. Gould
Technical Director

UNCLASSIFIED

SECURITY CLASSIFICATION OF THIS PAGE (When Data Entered)

REPORT DOCUMENTATION PAGE

READ INSTRUCTIONS BEFORE COMPLETING FORM

1. REPORT NUMBER: NCSL-TR-327-78
2. GOVT ACCESSION NO.
3. RECIPIENT'S CATALOG NUMBER

4. TITLE (and Subtitle): See Cover
[redacted]
5. TYPE OF REPORT & PERIOD COVERED: Technical Report
6. PERFORMING ORG. REPORT NUMBER

7. AUTHOR(s)
D. E. Humphreys
K. W. Watkinson

8. CONTRACT OR GRANT NUMBER(s)

9. PERFORMING ORGANIZATION NAME AND ADDRESS
Naval Coastal Systems Laboratory
Panama City, Florida 32407

10. PROGRAM ELEMENT, PROJECT, TASK AREA & WORK UNIT NUMBERS

11. CONTROLLING OFFICE NAME AND ADDRESS

12. REPORT DATE: February 1978
13. NUMBER OF PAGES: 108

14. MONITORING AGENCY NAME & ADDRESS (if different from Controlling Office)
F61112, F34371

15. SECURITY CLASS. (of this report): UNCLASSIFIED
15a. DECLASSIFICATION/DOWNGRADING SCHEDULE: N/A

16. DISTRIBUTION STATEMENT (of this Report)

Approved for Public Release: Distribution Unlimited.

17. ZF61112001, SF34371298

Prediction of Acceleration Hydrodynamic Coefficients for Underwater Vehicles from Geometric Parameters

different from Report)

DDC
APR 17 1978
F

18. SUPPLEMENTARY NOTES

19. KEY WORDS (Continue on reverse side if necessary and identify by block number)

Hydrodynamic coefficients	Simulation	Identifiers:
Underwater vehicles	Hydrodynamics	Acceleration
Dynamic response	Equations of motion	hydrodynamic coefficient
Analytic functions	Fluid mechanics	
Coefficients		

20. ABSTRACT (Continue on reverse side if necessary and identify by block number)

A compilation of methods for analytically calculating the acceleration hydrodynamic coeff cients from the geometric and mass distribution characteristics of an underwater vehicle is presented. Each of the coefficients in the longitudinal and lateral planes are treated in the order introductory description; relative importance in characterizing the vehicle dynamic response; causal relationship; and analytical expression for calculating

DD FORM 1 JAN 73 1473 EDITION OF 1 NOV 65 IS OBSOLETE
S/N 0102-LF-014-6601

407 216 UNCLASSIFIED B

SECURITY CLASSIFICATION OF THIS PAGE (When Data Entered)

10.

Task Area No. ZF 61-112-001, Work Unit No. 00112-50-1A
Task Area No. SF 34-371-208, Work Unit Number 16436
Subproject No. S0207, Work Unit 20259

20.

the value of the coefficient. Relationships for cross-coupled and non-linear hydrodynamic coefficients arising from potential flow theory are derived. All of the techniques have been implemented as part of the computer program GEORGE, a program for computing underwater vehicle dynamic stability characteristics in use at NCSL since 1972. Comparison of experimental and computed results is presented, along with a physical description of the generalized underwater vehicle used as the basis for the calculations and graphic representations contained in the report.

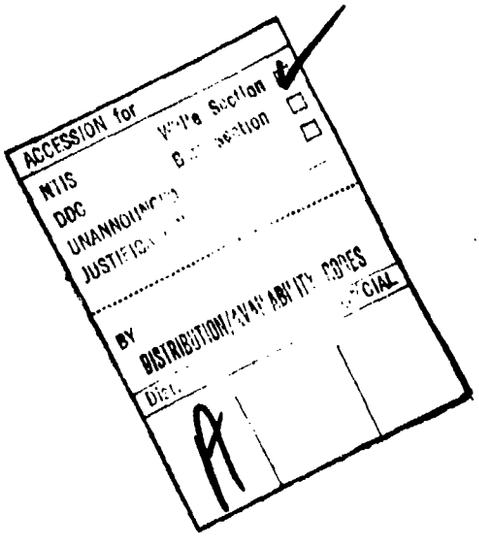

GLOSSARY OF TERMS

All symbols, subscripts, and nondimensionalized hydrodynamic coefficient expressions appearing in the body of this report are defined below. Any dimensions involved will be consistent with the foot-pound-second system of units. All angles are in degrees.

SYMBOLS

Symbol	Definition
AR	Aspect ratio of surface = b^2/s.
B	Buoyancy force which is positive upwards, B = $\rho\nabla$ (except where used in fluid kinetic energy equations).
b	Exposed root-to-tip span of surface.
c	Chord.
$\bar{c}$	Mean chord of surface = s/b = b/AR.
c_r	Root chord of surface.
c_t	Tip chord of surface.
I_a	Added moment of inertia.
I_x	Moment of inertia of an underwater vehicle about the x-axis.
I_{x_a}	Added moment of inertia about the x-axis.
I_y	Moment of inertia of an underwater vehicle about the y-axis.
$I_{y_{df}}$	Moment of inertia about the y-axis of the fluid displaced by the body.
I_z	Moment of inertia of an underwater vehicle about the z-axis.
K	Moment about the x-axis exerted on the body by the dynamic pressure of the surrounding fluid.
k_1	Lamb's inertial coefficient for a prolate ellipsoid in axial flow.

Symbol (Continued)	Definition
k_2	Lamb's inertial coefficient for a prolate ellipsoid in cross flow.
k'_p	Coefficient for added moment of inertia for a flat plate.
k'_b	Lamb's coefficient for added moment of inertia for a prolate ellipsoid body.
ℓ	Overall length of the vehicle.
M	Moment about the y-axis exerted on the body by the dynamic pressure of the surrounding fluid.
m	Mass of the vehicle including the water in the free-flooding spaces.
m_a	Additional mass.
m_{df}	Mass of fluid displaced by hull envelope.
N	Moment about the z-axis exerted on the body by the dynamic pressure of the surrounding fluid.
p	Component of angular velocity about the body fixed x-axis.
q	Component of angular velocity about the body fixed y-axis.
r	Component of angular velocity about the body fixed z-axis.
s	Exposed planform area of surface.
s_b	Maximum cross-sectional area of the body.
T	Total kinetic energy of the body-fluid system.
T_f	Kinetic energy of the fluid representing the system of impulsive pressures exerted by the surface of the body on the fluid during acceleration.
T_{veh}	Kinetic energy of the vehicle representing linear and angular momentum of the body.
t	Time.
U	Linear velocity of origin of body axes relative to a fluid-fixed axis system.

Symbol (Continued)	Definition
u	Component of U along the body x-axis.
$\forall$	Displaced volume of the hull envelope.
v	Component of U along the body y-axis.
w	Component of U along the body z-axis.
X	Force along the x-axis exerted on the body by the dynamic pressure of the surrounding fluid.
X_{ncb}	x-distance from nose to cb.
X_{ncg}	x-distance from nose to cg.
X_{nht}	x-distance from nose to centroid of the horizontal tail fins.
x	Longitudinal axis of the body fixed coordinate axis system.
Y	Force along the y-axis exerted on the body by the dynamic pressure of the surrounding fluid.
y	Transverse axis of the body fixed coordinate axis system.
Z	Force along the z-axis exerted on the body by the dynamic pressure of the surrounding fluid.
z	Vertical axis of the body fixed coordinate axis system.
z_{cb}	The z-distance to the center of buoyancy (cb) from the center of gravity (cg), positive down.
α	Angle of attack.
β	Angle of side-slip.
δ_{bp}	Deflection angle of bowplane (or sailplane).
δ_r	Deflection angle of rudder.
δ_s	Deflection angle of sternplane.

Symbol (Continued)	Definition
λ	Planform taper ratio of surface = c_t/c_r.
ω	Angular velocity.
ψ	Yaw angle.
ϕ	Roll angle.
ρ	Mass density of seawater.
θ	Pitch angle.
ℓ	The component in the plane of a surface of the perpendicular distance between the axis of rotation and the centroid of the area of the surface.
'	A prime over any symbol signifies nondimensionalization.
.	A dot over any symbol signifies differentiation with respect to time.

SUBSCRIPTS

Subscript	Definition
a	Added or additional inertia.
b	Body.
bp	Bow plane.
cb	Distance from cg to cb.
cg	Distance to cg.
df	Displaced fluid.
f	Fluid.
ht	Horizontal tail.
&vt	Lower vertical tail section.

Subscript (Continued)	Definition
n( )	Referenced from nose to some point, ( ), e.g., ncb implies nose-to-cb.
p	Plate.
r	Rudder.
s	Sternplane.
sh	Shroud.
t	Tip.
uvt	Upper vertical tail section.
veh	Vehicle.
x	Pertaining to the x-axis.
y	Pertaining to the y-axis.
z	Pertaining to the z-axis.

NONDIMENSIONALIZED HYDRODYNAMIC COEFFICIENT EXPRESSIONS

$$X'_{\dot{u}} = \frac{X_{\dot{u}}}{(\frac{1}{2})\rho \ell^3}, \qquad X'_{\dot{v}} = \frac{X_{\dot{v}}}{(\frac{1}{2})\rho \ell^3}, \qquad X'_{\dot{w}} = \frac{X_{\dot{w}}}{(\frac{1}{2})\rho \ell^3}$$

$$Y'_{\dot{u}} = \frac{Y_{\dot{u}}}{(\frac{1}{2})\rho \ell^3}, \qquad Y'_{\dot{v}} = \frac{Y_{\dot{v}}}{(\frac{1}{2})\rho \ell^3}, \qquad Y'_{\dot{w}} = \frac{Y_{\dot{w}}}{(\frac{1}{2})\rho \ell^3}$$

$$Z'_{\dot{u}} = \frac{Z_{\dot{u}}}{(\frac{1}{2})\rho \ell^3}, \qquad Z'_{\dot{v}} = \frac{Z_{\dot{v}}}{(\frac{1}{2})\rho \ell^3}, \qquad Z'_{\dot{w}} = \frac{Z_{\dot{w}}}{(\frac{1}{2})\rho \ell^3}$$

$$X'_{\dot{p}} = \frac{X_{\dot{p}}}{(\frac{1}{2})\rho \ell^4}, \qquad X'_{\dot{q}} = \frac{X_{\dot{q}}}{(\frac{1}{2})\rho \ell^4}, \qquad X'_{\dot{r}} = \frac{X_{\dot{r}}}{(\frac{1}{2})\rho \ell^4}$$

$$Y'_{\dot{p}} = \frac{Y_{\dot{p}}}{(\frac{1}{2})\rho \ell^4}, \qquad Y'_{\dot{q}} = \frac{Y_{\dot{q}}}{(\frac{1}{2})\rho \ell^4}, \qquad Y'_{\dot{r}} = \frac{Y_{\dot{r}}}{(\frac{1}{2})\rho \ell^4}$$

$$Z'_{\dot{p}} = \frac{Z_{\dot{p}}}{(\frac{1}{2})\rho \ell^4}, \qquad Z'_{\dot{q}} = \frac{Z_{\dot{q}}}{(\frac{1}{2})\rho \ell^4}, \qquad Z'_{\dot{r}} = \frac{Z_{\dot{r}}}{(\frac{1}{2})\rho \ell^4}$$

$$K'_{\dot{u}} = \frac{K_{\dot{u}}}{(\frac{1}{2})\rho \ell^4}, \qquad K'_{\dot{v}} = \frac{K_{\dot{v}}}{(\frac{1}{2})\rho \ell^4}, \qquad K'_{\dot{w}} = \frac{K_{\dot{w}}}{(\frac{1}{2})\rho \ell^4}$$

$$M'_{\dot{u}} = \frac{M_{\dot{u}}}{(\frac{1}{2})\rho \ell^4}, \qquad M'_{\dot{v}} = \frac{M_{\dot{v}}}{(\frac{1}{2})\rho \ell^4}, \qquad M'_{\dot{w}} = \frac{M_{\dot{w}}}{(\frac{1}{2})\rho \ell^4}$$

$$N'_{\dot{u}} = \frac{N_{\dot{u}}}{(\frac{1}{2})\rho \ell^4}, \qquad N'_{\dot{v}} = \frac{N_{\dot{v}}}{(\frac{1}{2})\rho \ell^4}, \qquad N'_{\dot{w}} = \frac{N_{\dot{w}}}{(\frac{1}{2})\rho \ell^4}$$

$$K'_{\dot{p}} = \frac{K_{\dot{p}}}{(\frac{1}{2})\rho \ell^5}, \qquad K'_{\dot{q}} = \frac{K_{\dot{q}}}{(\frac{1}{2})\rho \ell^5}, \qquad K'_{\dot{r}} = \frac{K_{\dot{r}}}{(\frac{1}{2})\rho \ell^5}$$

$$M'_{\dot{p}} = \frac{M_{\dot{p}}}{(\frac{1}{2})\rho \ell^5}, \qquad M'_{\dot{q}} = \frac{M_{\dot{q}}}{(\frac{1}{2})\rho \ell^5}, \qquad M'_{\dot{r}} = \frac{M_{\dot{r}}}{(\frac{1}{2})\rho \ell^5}$$

$$N'_{\dot{p}} = \frac{N_{\dot{p}}}{(\frac{1}{2})\rho \ell^5}, \qquad N'_{\dot{q}} = \frac{N_{\dot{q}}}{(\frac{1}{2})\rho \ell^5}, \qquad N'_{\dot{r}} = \frac{N_{\dot{r}}}{(\frac{1}{2})\rho \ell^5}$$

Note that $X'_{\dot{u}} = \partial X'/\partial \dot{u}'$, $X'_{\dot{p}} = \partial X'/\partial \dot{p}'$, etc.

TABLE OF CONTENTS

TABLE OF CONTENTS (Cont'd)

LIST OF ILLUSTRATIONS

LIST OF ILLUSTRATIONS (Cont'd)

LIST OF ILLUSTRATIONS (Cont'd)

LIST OF ILLUSTRATIONS (Cont'd)

LIST OF TABLES

LIST OF TABLES (Cont'd)

LIST OF TABLES (Cont'd)

LIST OF TABLES (Cont'd)

LIST OF TABLES (Cont'd)

INTRODUCTION

BACKGROUND

This report is primarily a compilation of methods for analytically predicting the acceleration hydrodynamic coefficients from the geometric and mass distribution characteristics of an underwater vehicle. It represents the current results of an effort to find the most generally applicable and accurate techniques for calculating these coefficients.

The need for such analytical techniques grew from the many unique underwater vehicle requirements inherent to the Naval Coastal Systems Laboratory mission areas. Typically these requirements include design, modification, or simulation of towed, tethered, or free vehicles for which analytical calculation of the hydrodynamic coefficients is necessary. This necessity arises from the need for some combination of the following:

1. Flexibility. The user's project is in a design phase where vehicle requirements imposed by hardware subsystems are subject to change and it is desirable to assess the effect of many more vehicle configurations than would be practical for experimental determination.

2. Responsiveness. The project is of a research and development nature such that there is a requirement for rapid and frequent updating of the vehicle's predicted performance in response to changes in performance goals and/or subsystem hardware.

3. Economy. Cost constraints on the project will not permit use (or extensive use) of model basin testing, but the project still requires some degree of assurance that there are no potential catastrophic failures due to problems such as dynamic instability.

To more effectively meet each of these requirements, all of the methods presented herein, as well as methods for computing all of the remaining hydrodynamic coefficients, have been computer-implemented in the complete stability and control analysis program GEORGE. The GEORGE computer program uses vehicle geometric and mass distribution information to compute vehicle dynamic characteristics.

It should be pointed out that the procedure yielding the highest degree of confidence for an underwater vehicle design involves the use of both model basin testing and analytical techniques. An example of a desirable sequence of design steps would be the implementation of a computerized hydrodynamic math model of the proposed vehicle using conceptual information available in the very early design phases. Using this model and incorporating updated information as it becomes available, the effect of various sizing, distributing, and shaping ideas on the vehicle dynamics can be assessed.

As soon as a reasonably firm design configuration is laid out, model basin tests can be performed to validate the computer modeling. These tests can be much less extensive than those necessary to produce the parametric information required as a basis for new design techniques—techniques sufficiently general to maintain predictive accuracy for the redesigns or modifications frequently necessary in vehicle design. This reduction in model testing requirements is primarily the result of having a computer model to use in defining what needs to be verified experimentally, and in providing a sophisticated tool for describing complicated trends, thus reducing data requirements.

The validated computer simulation model can then be used in many ways to support the project. Trajectory simulations can be made for given operational conditions so that motion information can be generated for performance evaluation or definition of hardware specifications. Examples of work performed using simulations in this manner are trajectory analyses of submarine-launched acoustic countermeasure devices and motion prediction of a swimmer delivery vehicle to assess the motion influence on the design of a high-resolution, side-looking sonar.*

Another use has been to provide the hydrodynamic coefficients for analog or hybrid simulation models to study man-machine interface problems or to provide training. An example of recent work in this area is the implementation of a hybrid model of the Mine Neutralization Vehicle (MNV) as a performance evaluation and training device. The MNV simulation solves the nonlinear equations of motion for a tethered vehicle (including four propulsors, bowplanes, and cable tension) and produces a motion display for either body or inertial reference frame, all in real time. Of course, the computer simulation model is most often used to assess the influence of design variations of the vehicle hydrodynamic and control system parameters on dynamic stability and control characteristics.

---

*Trajectory simulations have usually been performed using suitable modified versions of the standard six-degrees-of-freedom submarine simulation computer program, ZZMN, developed by DTNSRDC.

Having briefly stated the background for the prediction and simulation capability regarding the stability and control of underwater vehicles at NCSL, attention will now be focused on the analytical techniques for assigning a value to acceleration, nonlinear, and cross-coupled hydrodynamic coefficients.* These techniques have been applied to a wide variety of body types, including torpedoes, submarines, swimmer delivery vehicles (SDV's), and many other special purpose vehicles such as the Deep Submergence Rescue Vehicle (DSRV), the Shipboard Minehunting System (SMS) towed sonar body, and submarine-launched torpedo countermeasures devices.

Generality in applicability has been sought; that is, use of a method that yields accurate results for only a specific class of vehicles, such as torpedoes, has been avoided. A more generally applicable and, in the experience of the authors, more accurate, formulation based on theoretical derivation and experimental verification is presented. The relative importance of each hydrodynamic coefficient as it contributes to the responsive motion of the vehicle is noted. In addition, important relationships between acceleration, cross-coupled, and nonlinear hydrodynamic coefficients are derived from potential flow theory.

ACCELERATION COEFFICIENTS

The forces represented by acceleration hydrodynamic coefficients are attributed to the acceleration of fluid particles surrounding a submerged body. Some of the forces appear in the equations of motion as additions to terms representing the inertia of the body. They are known as added mass or mass accession terms and, when combined with the inertial parameters of a body, have been called apparent, virtual, and hydrodynamic mass.

Analytical methods for estimating the acceleration coefficients of the bare hull differ from the methods used for the contributions of appendages in that they are not estimated using semi-empirical formulae. Rather, the body is assumed to be moving through an infinite, inviscid, circulation-free fixed fluid. For these conditions, Lamb[1] derives the complete expression for the kinetic energy of the body-fluid system which, coupled with inertia coefficients for prolate ellipsoids[1], yields estimates of body bare-hull acceleration derivatives.

---

*Although techniques are also available for the prediction of static and dynamic velocity terms with viscous effects included, the scope of this report is limited to the acceleration coefficients.

[1]Lamb, Sir Horace, *Hydrodynamics,* Dover Publications, New York, Sixth Edition, 1932. pps 172 and 154.

The basis for the added masses and moments due to body appendages, such as fins and bowplanes, is largely semi-empirical. Theoretical expressions for thin, flat plates moving in a perfect fluid have been derived from hydrodynamic theory with experimentally determined correction factors for non-ideal conditions and shapes. A great deal of the primary work done in this area was accomplished by Munk[2][3], with later significant experimental work by Gracey[4], and Malvestuto and Gale[5].

ACCELERATION COEFFICIENTS IN POTENTIAL FLOW THEORY

The forces and moments represented by the acceleration hydrodynamic coefficients can, to a very great extent, be modeled as potential flow phenomena. Neglecting the details of the boundary layer in modeling acceleration-dependent forces and moments acting on a submerged body yields quite satisfactory results for most stability and control simulation. Coefficient contributions due to appendages are most noticeably influenced by boundary layer effects. Acceleration coefficient values predicted using potential flow theory are probably most suspect in their application to fins that have a significant portion of their planform area in separated flow. There are a few considerations concerning these sources of error that should be mentioned before launching into further development.

Acceleration-dependent forces can arise from changes in the boundary layer, resulting, in turn, from changes in angle-of-attack or drift angle. There are several interesting facts in this regard. One is that the speed/power relationship for underwater vehicles generally encourages a designer to fair his vehicle so that the boundary layer has a significant thickness over as little of the vehicle as possible. The result

---

[2] National Advisory Committee for Aeronautics T.N. No. 197, *Some Tables of the Factor of Apparent Additional Mass,* by Max M. Munk, 1924.

[3] Munk, Max M., Fluid Mechanics, Part II, *Aerodynamic Theory,* Vol. 1, edited by W. F. Durand, Dover Publications, Inc., New York, 1934.

[4] National Advisory Committee for Aeronautics T.N. No. 707, *The Additional-Mass Effect of Plates as Determined by Experiments,* by William Gracey, 1941.

[5] National Advisory Committee for Aeronautics T.N. No. 1187, *Formulas for Additional-Mass Corrections to the Moments of Inertia of Airplanes,* by Frank S. Malvestuto, Jr. and Lawrence J. Gale, 1946.

is that the pressure distribution over 80 percent of the surface area of a typical underwater vehicle can be described very accurately by potential flow theory. Consequently, the acceleration coefficients most important to the description of underwater vehicle dynamics can usually be accurately computed as potential flow phenomena. Some less important acceleration coefficients, especially those resulting from the imbalance of added mass effects distributed fore and aft of the cg, can be significantly erroneous if the boundary layer is neglected. Unfortunately, those coefficients influenced by boundary layer effects suffer from similar problems in experimental model testing; e.g., improper Reynolds number scaling leads to nondynamic similarity in the modeled boundary layer.

Describing acceleration-dependent effects on fins is simplified somewhat by the vehicle designer's avoidance of the sizing and placement of fins so that they lose effectiveness in regions of separated flow. Consequently, more often than not, treatment of the added mass effects of fins as if they are in unspoiled flow provides good results. Tube-launched devices are often exceptions to this rule. They are generally constrained by tail size and after-body taper so that large portions of the fins are in separated flow.

Decisions on "effective" fin aspect ratios based on past experience with similar vehicles may be necessary to achieve accuracy in those coefficients with significant fin contributions. Since the fins on a torpedo are generally small, their contributions to the major coefficients of importance are less significant than is the case with other types of underwater vehicles. Roll coefficients are an important exception since they are due almost completely to fin contributions.

The acceleration, cross-coupled, and nonlinear coefficient equalities derived in Appendix A must be used with great caution when simulating vehicle trajectories. The NCSL approach has been to assess the importance of coefficient accuracy using two computer-implemented tools. One computer program performs root locus sensitivity studies for the linear coefficients on the vehicle of interest. The required accuracy is determined on a coefficient-by-coefficient basis, taking advantage of the insight that can be gained by a control system analysis approach to the vehicle system.

A more thorough evaluation of the math model simulating the vehicle fluid system, including the nonlinear and cross-coupled terms, must be done on a maneuver-by-maneuver basis. To assess the relative importance of each contributing force and moment, the authors have modified the standard six-degrees-of-freedom submarine simulation computer program[6]

---

[6] Naval Ship Research and Development Center Test and Evaluation Report P-433-H-01, *User's Guide NSRDC Digital Program for Simulating Submarine Motion ZZMN-Revision 1.0,* by Ronald W. Richards, June 1971.

to plot the following on any maneuver: (1) time histories of the force (or moment) of each contributing coefficient, propulsor, buoyancy/gravity, and control surface term together with the total force (or moment); and (2) time histories of the motions of the vehicle with the contribution of a single term removed, and repeated for each term. Knowing the degree of accuracy expected in the computed value for each coefficient, one can analyze the plots on the maneuvers of interest and assign a level of confidence. This procedure will give an indication of which coefficients are most critical in achieving accurate simulation on a given maneuver.

Using these techniques and a multitude of comparisons with planar motion mechanism and rotating arm results, the methods presented in this report are, on the basis of the authors' experience, considered to be quite accurate on any hydrodynamically-faired vehicle for all but extreme maneuvers. This is especially true for linear models, as will be shown by examples in Appendix B.

The modeling accuracy achieved for acceleration terms under these assumptions is quite contrary to the extremely poor results obtained when the same assumptions are applied to velocity-dependent terms. The assumptions are: (1) the body is submerged so that there are no near-surface or near-bottom effects; (2) the fluid is inviscid; and (3) there is zero circulation.

Under these conditions the momentum equations for the body-fluid system may be written in the six Lagrange equations:

$$\frac{d}{dt}\frac{\partial T}{\partial u} = r\frac{\partial T}{\partial v} - q\frac{\partial T}{\partial w} - X, \tag{1}$$

$$\frac{d}{dt}\frac{\partial T}{\partial v} = p\frac{\partial T}{\partial w} - r\frac{\partial T}{\partial u} - Y, \tag{1}$$

$$\frac{d}{dt}\frac{\partial T}{\partial w} = q\frac{\partial T}{\partial u} - p\frac{\partial T}{\partial v} - Z; \tag{1}$$

$$\frac{d}{dt}\frac{\partial T}{\partial p} = w\frac{\partial T}{\partial v} - v\frac{\partial T}{\partial w} + r\frac{\partial T}{\partial q} - q\frac{\partial T}{\partial r} - K, \tag{2}$$

$$\frac{d}{dt}\frac{\partial T}{\partial q} = u\frac{\partial T}{\partial w} - w\frac{\partial T}{\partial u} + p\frac{\partial T}{\partial r} - r\frac{\partial T}{\partial p} - M, \tag{2}$$

$$\frac{d}{dt}\frac{\partial T}{\partial r} = v\frac{\partial T}{\partial u} - u\frac{\partial T}{\partial v} + q\frac{\partial T}{\partial p} - p\frac{\partial T}{\partial q} - N, \tag{2}$$

where X, Y, Z, K, M, and N represent the forces and moments exerted on the body by the pressure of the surrounding fluid, and the total kinetic energy T may be written

$$T = T_{veh} + T_f,$$

with T_{veh} representing the linear and angular momentum of the vehicle itself, and T_f representing the system of impulsive pressures exerted by the surface of the solid on the fluid in the supposed instantaneous generation of motion from rest.

If we rewrite Equations (1) and (2), isolating the terms due to T_f, we obtain expressions for the forces exerted on the body by the dynamic pressure of the surrounding fluid, e.g.:

$$X = -\frac{d}{dt}\frac{\partial T_f}{\partial u} + r\frac{\partial T_f}{\partial v} - q\frac{\partial T_f}{\partial w}, \tag{3}$$

and

$$K = -\frac{d}{dt}\frac{\partial T_f}{\partial p} + w\frac{\partial T_f}{\partial v} - v\frac{\partial T_f}{\partial w} + r\frac{\partial T_f}{\partial q} - q\frac{\partial T_f}{\partial r}, \tag{3}$$

etc.

The fluid kinetic energy, T_f, can be expressed as a quadratic form of the body axis velocities u, v, w, p, q, and r with no explicit time dependence.* The quadratic expression for T_f may be written[1]:

$$\begin{aligned} 2T_f = {} & Au^2 + Bv^2 + Cw^2 + 2A'vw + 2B'wu + 2C'vu + Pp^2 + Qq^2 \\ & + Rr^2 + 2P'qr + 2Q'rp + 2R'pq + 2Lup + 2Mvq + 2Nwr \\ & + 2F(vr + wq) + 2G(wp + ur) + 2H(uq + vp) + 2F'(vr - wq) \\ & + 2G'(wp - ur) + 2H'(uq - vp). \end{aligned} \tag{4}$$

The body axes are generally chosen so that the xz-plane is a plane of symmetry (port-starboard symmetry). This eliminates nine of the coefficients, A', C', P', R', L, M, N, G, and G', since by symmetry arguments, sign changes in v, p, or r should not change T_f. Letting

$$F + F' = F_1,\ F - F' = F_2,\ H + H' = H_1, \text{ and } H - H' = H_2, \tag{5}$$

---

[1] ibid.

*Recent investigations indicate that there can be significant time variant terms arising from vortices shed from the forward appendages and hull. The mathematical modeling of this phenomenon is accomplished using force and moment terms in the equations of motion that are convoluted in time. These terms are outside the set of acceleration, nonlinear, and cross-coupled hydrodynamic coefficients under consideration here.

the remaining 12 coefficients are included in the equation

$$2T_f = Au^2 + Bv^2 + Cw^2 + 2B'wu + Pp^2 + Qq^2 + Rr^2$$

$$+ 2Q'rp + 2F_1vr + 2F_2wq + 2H_1uq + 2H_2vp \ . \qquad (6)$$

The complete expressions, assuming no planes of symmetry, are presented in Appendix A.

Proceeding as indicated in Equation (3), the full six-degrees-of-freedom momentum equations can be written in terms of the 12 remaining coefficients[7]. The coefficients are written in hydrodynamic coefficient notation as follows.

Added inertia terms:

$$A = -X_{\dot{u}}, \qquad P = -K_{\dot{p}}, \qquad B = -Y_{\dot{v}}, \qquad (7)$$

$$Q = -M_{\dot{q}}, \qquad C = -Z_{\dot{w}}, \text{ and } \quad R = -N_{\dot{r}} \ . \qquad (7)$$

Inertial intermodal coupling terms:

$$F_1 = -Y_{\dot{r}} = -N_{\dot{v}}, \quad F_2 = -Z_{\dot{q}} = -M_{\dot{w}}, \text{ and } H_2 = -Y_{\dot{p}} = -K_{\dot{v}} \ . \qquad (8)$$

The remaining three are

$$B' = -X_{\dot{w}} = -Z_{\dot{u}}, \ Q' = -N_{\dot{p}} = -K_{\dot{r}}, \text{ and } H_1 = -X_{\dot{q}} = -M_{\dot{u}} \ . \qquad (9)$$

If, as shown in the complete expressions in Appendix A, there is also fore-aft symmetry (symmetry about the yz-plane), then, in addition to the aforementioned zeroed terms

$$B' = Q' = F_1 = F_2 = 0 \ .$$

Vehicles having symmetry about both the xz-plane and the xy-plane have the additional zeroed terms

$$B' = Q' = H_1 = H_2 = 0 \ .$$

---

[7] Massachusetts Institute of Technology, Instrumentation Laboratory Report R-570-A, *Deep Submergence Rescue Vehicle Simulation and Ship Control Analysis,* by Charles Broxmeyer, Pierre P. Dogan, et al, 1967, p. 31.

These relations will be used extensively in the following coefficient formulations. It should be noted that the coefficient identities, such as Equations (8) and (9), result from derivation under no assumptions of symmetry. The existence of symmetry results in some of the terms being equal to zero. The complete set of identities of acceleration, nonlinear and cross-coupled coefficients is presented in Appendix A.

METHODS FOR COMPUTING ACCELERATION HYDRODYNAMIC COEFFICIENTS

INTRODUCTION

Methods for estimating the acceleration-dependent hydrodynamic coefficients are given in this section. Each coefficient is described using the following format:

1. Introductory description.

2. Relative importance - major or minor, and under what circumstances.

3. Causal relationship - important assumptions.

4. Analytical expression - including normal range of coefficients in the expression and necessary references.

Appendix C provides a physical description of the underwater vehicle used as the basis for calculations illustrated graphically in this report, and Appendix D contains time history plots of the four maneuvers from which the trajectory simulation and percent contribution plots were obtained. Reference frame conventions are as shown in Figure 1.

A word of caution is appropriate here. When comparing computed acceleration coefficient values with experimentally determined values, attention must be given to the location of the reference frame origin. If the origin during the experimental tests is not the vehicle cg, then erroneous comparisons will result for those coefficients where distances from the cg are involved.

LONGITUDINAL COEFFICIENTS

$X'_{\dot{u}}$

1. $X'_{\dot{u}}$ is an acceleration coefficient resulting from the resisting force of the fluid on a vehicle accelerating in the x-direction. This

(Text Continued on Page 11)

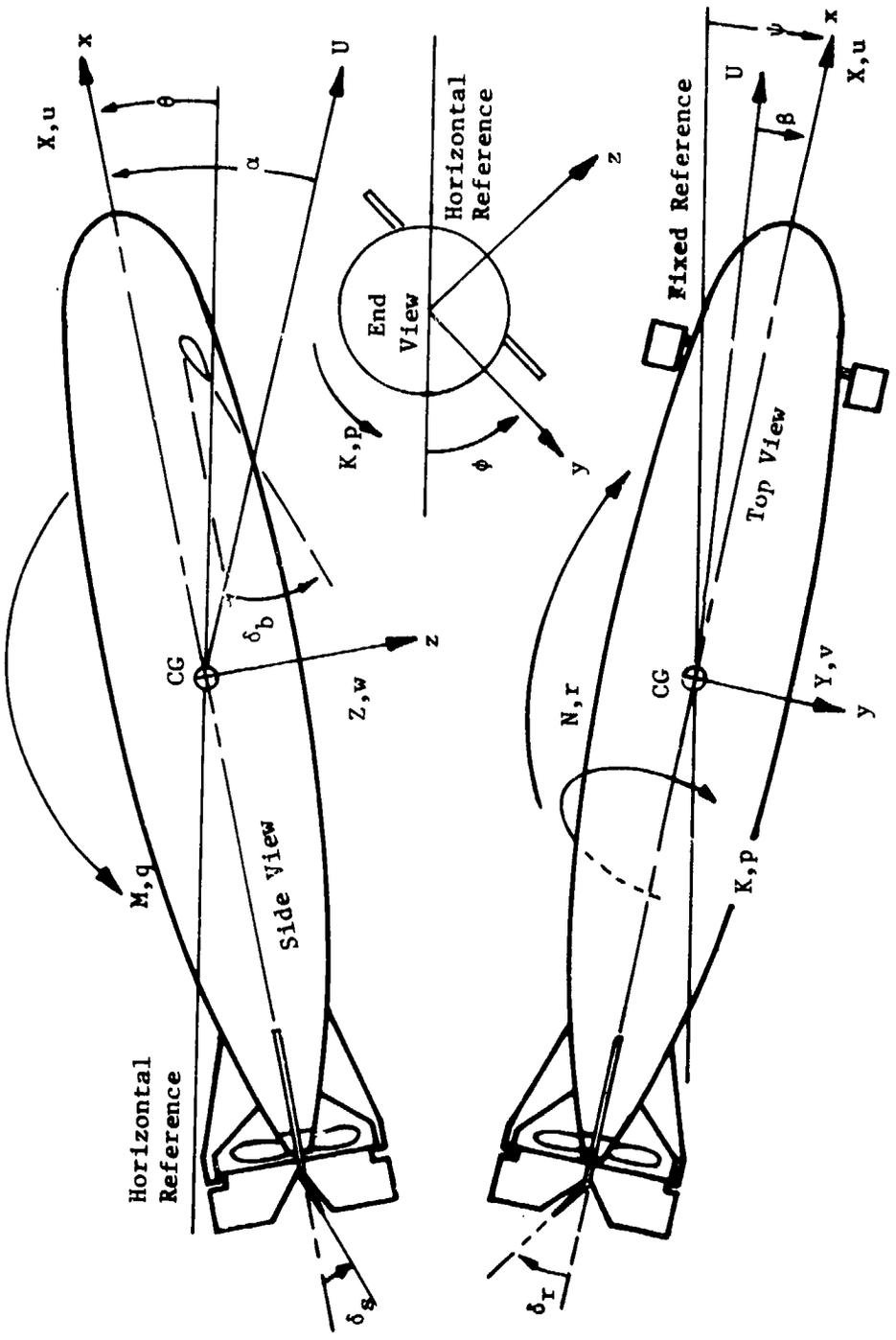

FIGURE 1. POSITIVE DIRECTIONS OF AXES, ANGLES, VELOCITIES, FORCES, AND MOMENTS

force is required to change the flow field about the vehicle, whereas the static coefficients represent the forces necessary to maintain a flow field configuration at a constant vehicle velocity. More simply, $X'_{\dot{u}}$ may be thought of as a mass of fluid that must be accelerated along with the vehicle, thus giving the vehicle an "added" or "apparent" mass which is manifest during vehicle acceleration.

2. Insight to the relative significance of $X'_{\dot{u}}$ can be gained by noting that $X'_{\dot{u}}$ appears in the linear equations of motion in the mass term

$$(m' - X'_{\dot{u}}) \ .$$

Thus, in cases where the value of $X'_{\dot{u}}$ represents a significant contribution to this term, accuracy in predicting $X'_{\dot{u}}$ is important. The $X'_{\dot{u}}$ contribution to vehicular motion during a control surface step input is generally minor, and dissipates rapidly as the vehicle attains a steady state. In control surface reversal maneuvers, as illustrated in trajectory simulation and x-force percent contribution plots in Figures 2 and 3, $X'_{\dot{u}}$ becomes slightly more significant and longer-acting, but still remains a relatively minor influence. For nearly neutrally buoyant faired vehicles having an ℓ/d ratio higher than 8.0, $X'_{\dot{u}}$ typically contributes less than 3 percent to the mass term. $X'_{\dot{u}}$ has increasing relative significance for lower ℓ/d ratios. Root locus studies for typical submarine and torpedo-like bodies has corraborated the foregoing, indicating very minor sensitivity to large percentage errors in predicting $X'_{\dot{u}}$.

When performing a two-degree-of-freedom linear analysis in the longitudinal plane (M and Z equations), three roots of the characteristic equation are obtained. The investigator may find a fourth root arising from the x-degree of freedom equation by assuming that the only significant terms are X'_{u} and $X'_{\dot{u}}$ (this is often acceptable for an axisymmetric vehicle). The fourth root is found by the relation

$$\sigma_4' = \frac{X'_u}{m' - X'_{\dot{u}}} \ . \qquad (10)$$

Tables 1A through 1D present the results of a sensitivity analysis of nondimensional roots of the characteristic equation (transfer function denominator) and u, w, and θ (numerators) for a generalized underwater vehicle, varying $X'_{\dot{u}}$ from -100 percent to +100 percent.

3. Mathematically, given the linearizing truncation of the Taylor series expansion to the first term, $X'_{\dot{u}}\dot{u}$ is the force additional to the inertial force occurring with a vehicular x-acceleration. In the computation of $X'_{\dot{u}}$, the body is approximated by a prolate ellipsoid having

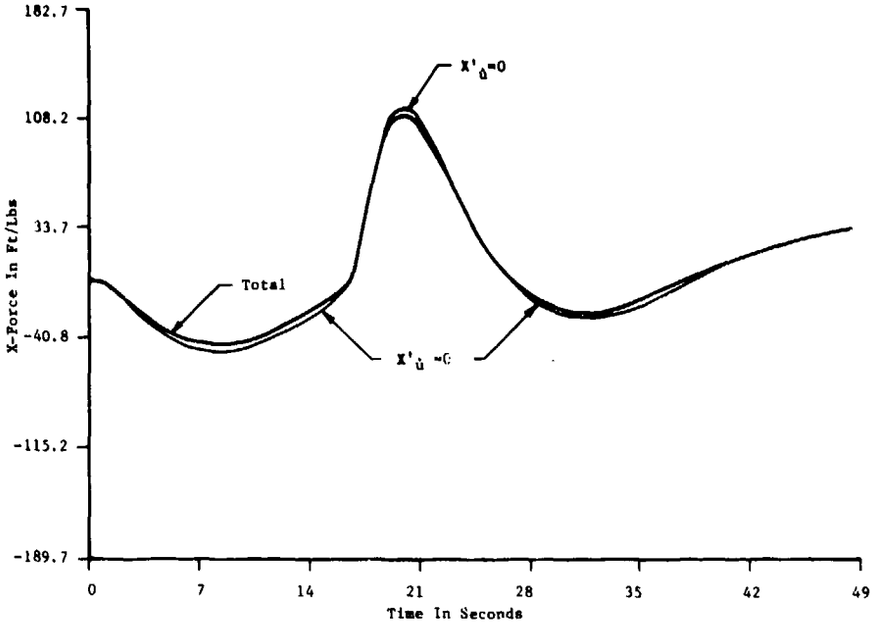

FIGURE 2. TRAJECTORY SIMULATION PLOT OF $X'_{\dot{U}}$ CONTRIBUTION TO X-FORCE DURING A $\delta_s = \pm 30°$ DIVE/CLIMB MANEUVER

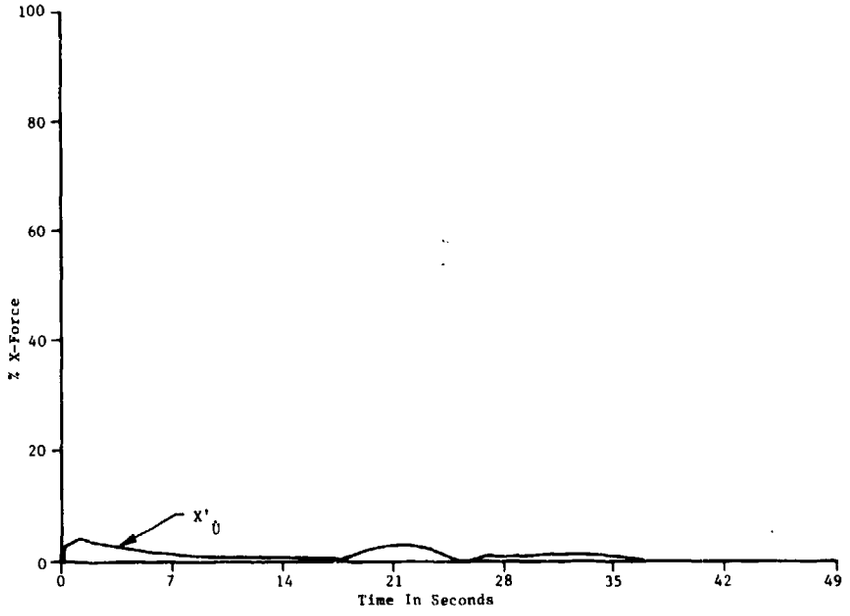

FIGURE 3. PERCENT CONTRIBUTION OF $X'_{\dot{U}}$ TO X-FORCE DURING A $\delta_s = \pm 30°$ DIVE/CLIMB MANEUVER

TABLE 1A

LONGITUDINAL SENSITIVITY ANALYSIS OF CHARACTERISTIC EQUATION NON-DIMENSIONAL ROOTS FOR A GENERALIZED UNDERWATER VEHICLE, VARYING X'_u ±100%

% VAR	ROOT 1	% CHANGE	ROOT 2	% CHANGE	ROOT 3	% CHANGE	ROOT 4	% CHANGE
-100^R_I			-.11242 0	3.3				
-50^R_I			-.11061 0	1.6				
-25^R_I			-.10972 0	.80				
-10^R_I			-.10920 0	.32				
BASE^R_I	-.043028 0		-.10885 0		-.82160 0		-4.1501 0	
$+10^R_I$			-.10851 0	-.32				
$+25^R_I$			-.10800 0	-.80				
$+50^R_I$			-.10715 0	-1.6				
$+100^R_I$			-.10551 0	-3.1				

TABLE 1B

LONGITUDINAL SENSITIVITY ANALYSIS OF U NUMERATOR NON-DIMENSIONAL ROOTS FOR A GENERALIZED UNDERWATER VEHICLE, VARYING X'_u ±100%

% VAR	ROOT 1	% CHANGE	ROOT 2	% CHANGE	ROOT 3	% CHANGE
-100^R_I						
-50^R_I						
-25^R_I						
-10^R_I						
BASE^R_I	-.049345 0		-.79158 0		-3.7580 0	
$+10^R_I$						
$+25^R_I$						
$+50^R_I$						
$+100^R_I$						

TABLE 1C

LONGITUDINAL SENSITIVITY ANALYSIS OF W NUMERATOR NON-DIMENSIONAL ROOTS FOR A GENERALIZED UNDERWATER VEHICLE, VARYING X'_u ±100%

% VAR	ROOT 1	% CHANGE	ROOT 2	% CHANGE	ROOT 3	% CHANGE
-100^R_I			-.11242 0	3.3		
-50^R_I			-.11061 0	1.6		
-25^R_I			-.10972 0	.80		
-10^R_I			-.10920 0	.32		
BASE^R_I	-.032782 0		-.10885 0		-6.3461 0	
$+10^R_I$			-.10951 0	-.32		
$+25^R_I$			-.10800 0	-.80		
$+50^R_I$			-.10715 0	-1.6		
$+100^R_I$			-.10551 0	-3.1		

TABLE 1D

LONGITUDINAL SENSITIVITY ANALYSIS OF θ NUMERATOR NON-DIMENSIONAL ROOTS FOR A GENERALIZED UNDERWATER VEHICLE, VARYING X'_u ±100%

% VAR	ROOT 1	% CHANGE	ROOT 2	% CHANGE
-100^R_I	-.11242 0	3.3		
-50^R_I	-.11061 0	1.6		
-25^R_I	-.10972 0	.80		
-10^R_I	-.10920 0	.32		
BASE^R_I	-.10885 0		-1.0199 0	
$+10^R_I$	-.10851 0	-.32		
$+25^R_I$	-.10800 0	-.80		
$+50^R_I$	-.10715 0	-1.3		
$+100^R_I$	-.10551 0	-3.1		

like length and maximum diameter, and neglecting appendages to the body due to their comparatively small frontal area. Using the results of Lamb[1], derived assuming potential flow, we have:

4. $$X'_{\dot{u}} = X'_{\dot{u}_b} = \frac{k_1 m_{df}}{\frac{1}{2}\rho \ell^3} , \tag{11}$$

where

$$k_1 = \frac{\alpha_0}{2 - \alpha_0} , \tag{12}$$

with

$$\alpha_0 = \frac{2(1 - e^2)}{e^3} \left(\tfrac{1}{2}\ell n \left[\frac{1 + e}{1 - e}\right] - e\right) , \tag{13}$$

e being the eccentricity of the rotated ellipse expressed in common terms as

$$e = \frac{2}{\ell}\left(\frac{\ell^2}{4} - \frac{s_b}{\pi}\right)^{\frac{1}{2}} . \tag{14}$$

The inertia coefficient for axial flow, k_1, ranges from 0.5 to 0 for fineness ratios of 1.0 to ∞. k_1 is graphically presented in Figure 4.

$Z'_{\dot{u}}$

1. The acceleration coefficient $Z'_{\dot{u}}$ represents a z-force resulting from an acceleration in the x-direction.

2. Root locus sensitivity studies on typical submarine and torpedo-like vehicles show extreme insensitivity to large magnitude excursions and sign changes of $Z'_{\dot{u}}$. Thus the coefficient is generally assumed negligible and set to zero.

3. Vehicles exhibiting symmetry about the xy-plane produce balanced z-forces during acceleration along x, indicating $Z'_{\dot{u}} = 0$. In potential theory, symmetry about the xy-plane or yz-plane causes $Z'_{\dot{u}} = 0$ as shown in Appendix A.

4. In the vast majority of cases, the combination of near symmetry about the xy-plane and minor influence on roots of the characteristic equation leads to setting $Z'_{\dot{u}} = 0$.

---

[1] ibid.

(Text Continued on Page 16)

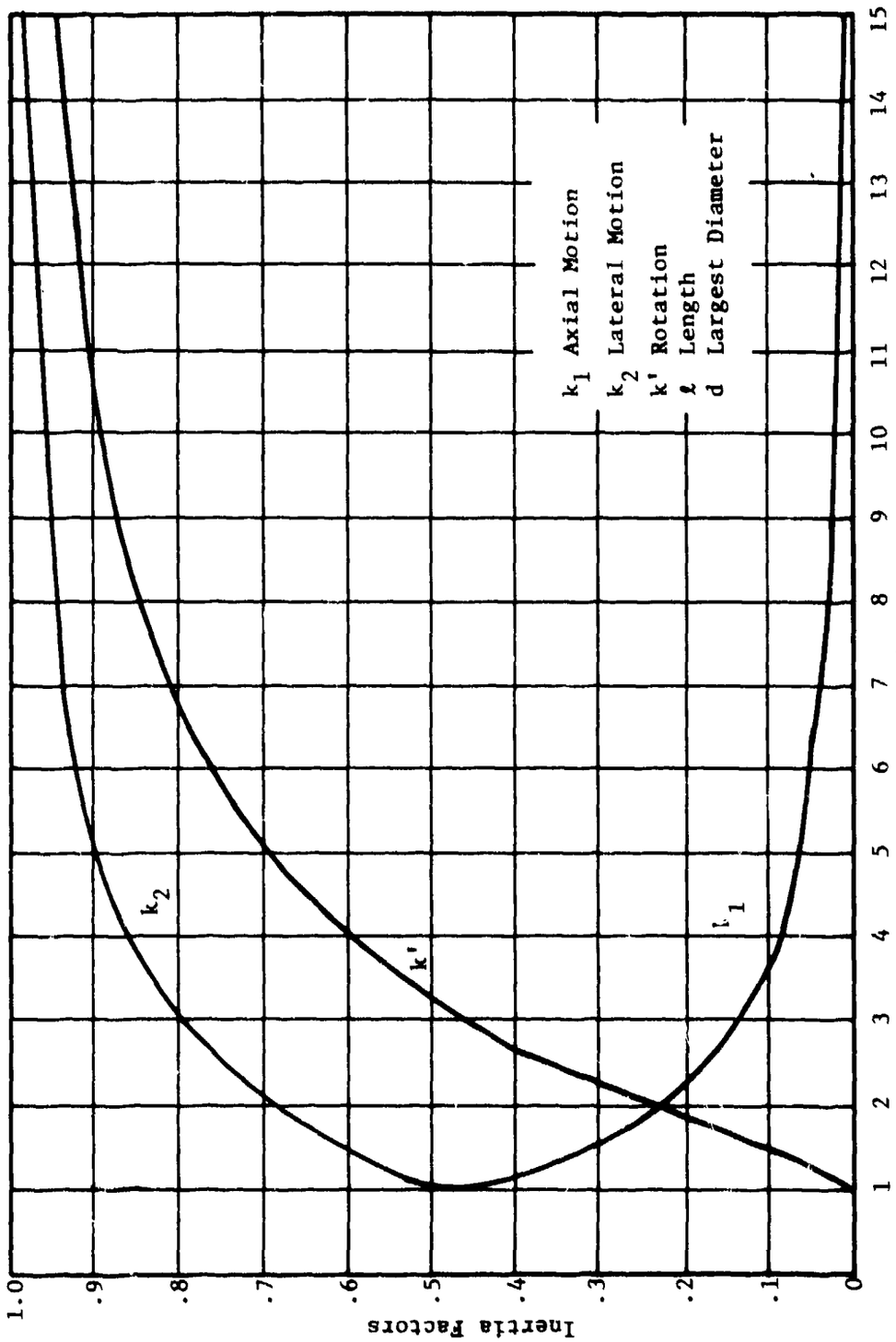

FIGURE 4. LAMB'S INERTIA COEFFICIENTS k_1, k_2 AND k' PLOTTED AS A FUNCTION OF VEHICLE ℓ/d

$M'_{\dot{u}}$

1. The term $M'_{\dot{u}}$ represents the pitching moment resulting from an acceleration parallel to the x-axis.

2. Root locus sensitivity studies on typical submarine and torpedo-like bodies show extreme insensitivity to large magnitude changes in $M'_{\dot{u}}$.

3. As was the case with $Z'_{\dot{u}}$, vehicles having symmetry or near symmetry about the xy-plane will create a negligible M-moment due to x-acceleration. Potential theory predicts $M_{\dot{u}} = 0$ for yz-plane symmetry (see Appendix A). Extreme vertical separation of the cb and cg, coupled with a large $X'_{\dot{u}}$ force (arising from low ℓ/d ratio), could conceivably cause a significantly large $M'_{\dot{u}}$. For free-flooded vehicles, launcher devices, and torpedo-like bodies, this is a highly unlikely occurrence.

4. The combination of near symmetry about the xy-plane and minor influence on the roots of the characteristic equation usually leads to setting $M'_{\dot{u}} = 0$. For a vehicle with an extremely large vertical cg - cb separation and/or an $X'_{\dot{u}}$ value that is significant when compared to m', $M'_{\dot{u}}$ is calculated as

$$M'_{\dot{u}} = X'_{\dot{u}} \frac{z_{cb}}{\ell} ,$$

where z_{cb} = z-distance from the cg to the cb, positive down.

$X'_{\dot{w}}$

1. The acceleration derivative $X'_{\dot{w}}$ represents the x-force resulting from an acceleration in the z-direction.

2. As with $Z'_{\dot{u}}$ and $M'_{\dot{u}}$, the roots of the characteristic equation show negligible change with $X'_{\dot{w}}$ set equal to zero, then varied positively and negatively over a range much greater than would be likely in reality.

3. Near balanced z-force during z-acceleration due to near fore-aft symmetry yields resultants of a large z-force component and some pitching moment, but very little x-force. It is significant to note that $Z'_{\dot{u}} = X'_{\dot{w}}$ according to potential theory (Equation (9)). If the cg and cb are significantly separated along both the x- and z-axes then, since those forces arising from potential flow theory are in a reference frame with a cb origin, the pitching moment term $M'_{\dot{w}}$ will yield an $X'_{\dot{w}}$ term when transferred to the cg. As with $Z_{\dot{u}}$, though, even variation through extreme ranges showed that setting $X'_{\dot{w}} = 0$ was justified for application to the vast majority of underwater vehicles.

4. $X'_{\dot{w}} = 0$.

$Z'_{\dot{w}}$

1. The resisting hydrodynamic force resulting from a z-acceleration is represented in the equation of motion by $Z'_{\dot{w}}$. The term $(m' - Z'_{\dot{w}})$ is the nondimensional "apparent mass" of the vehicle when one is considering heave acceleration.

2. $Z'_{\dot{w}}$ is one of the most important acceleration derivatives. Trajectory simulation and z-force percent contribution plots in Figures 5 through 10 illustrate its significance to vehicular motion during various maneuvers. The root locus plots in Figures 11, 12, and 13 illustrate the wide variation in the locations of the poles due to variation in $Z'_{\dot{w}}$. Tables 2A through 2D present the results of a sensitivity analysis of nondimensional roots of the characteristic equation (transfer function denominator) and u, w, and θ (numerators) for a generalized underwater vehicle, varying $Z'_{\dot{w}}$ from -100 percent to +100 percent. As in $X'_{\dot{u}}$ and $M'_{\dot{q}}$, insight into the influence of $Z'_{\dot{w}}$ can be gained by noting the significance of $Z'_{\dot{w}}$ in the hydrodynamic mass term $(m' - Z'_{\dot{w}})$. Vehicles with ℓ/d ratios greater than 8.5 will usually have nearly a 50 percent $Z'_{\dot{w}}$ contribution to the apparent mass. That is, the added mass will be roughly equal to the mass. Horizontal fins will contribute to $Z'_{\dot{w}}$ and frequently cause it to be larger than m'.

3. As with $X'_{\dot{u}}$, the body is approximated by a prolate ellipsoid having like length and maximum diameter. Lamb's[1] inertial coefficient for such a body in crosswise flow is used as follows:

$$Z'_{\dot{w}_b} = \frac{k_2 m_{df}}{\frac{1}{2}\rho \ell^3} = \frac{k_2 \forall}{\frac{1}{2}\ell^3} \tag{15}$$

where

$$k_2 = \frac{\beta_0}{2 - \beta_0}, \tag{16}$$

with

$$\beta_0 = \frac{1}{e^2} - \frac{1 - e^2}{2e^3} \ln \frac{1 + e}{1 - e}, \tag{17}$$

e being the eccentricity of the rotated ellipse as noted in Equation (14). k_2 is graphically presented in Figure 14. Fortunately, this very important body coefficient has proved to be accurate to ±5 percent in comparison with experimental data on the majority of underwater vehicles

---

[1] ibid.

(Text Continued on Page 23)

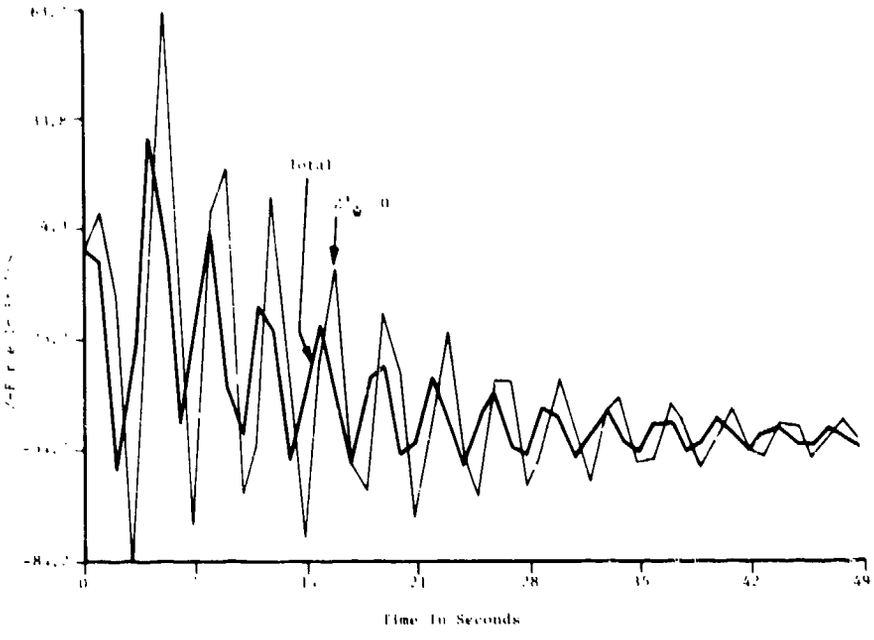

FIGURE 5. TRAJECTORY SIMULATION PLOT OF Z'_w CONTRIBUTION TO Z-FORCE DURING A δ_r = 30° STEADY TURN (AUTOMATIC DEPTH-KEEPING)

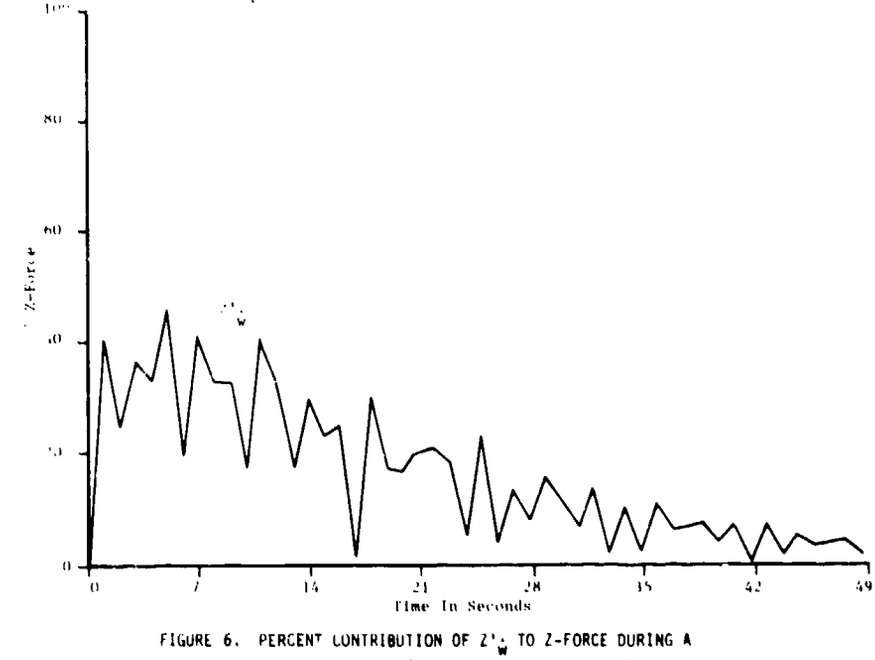

FIGURE 6. PERCENT CONTRIBUTION OF Z'_w TO Z-FORCE DURING A δ_r = 30° STEADY TURN (AUTOMATIC DEPTH-KEEPING)

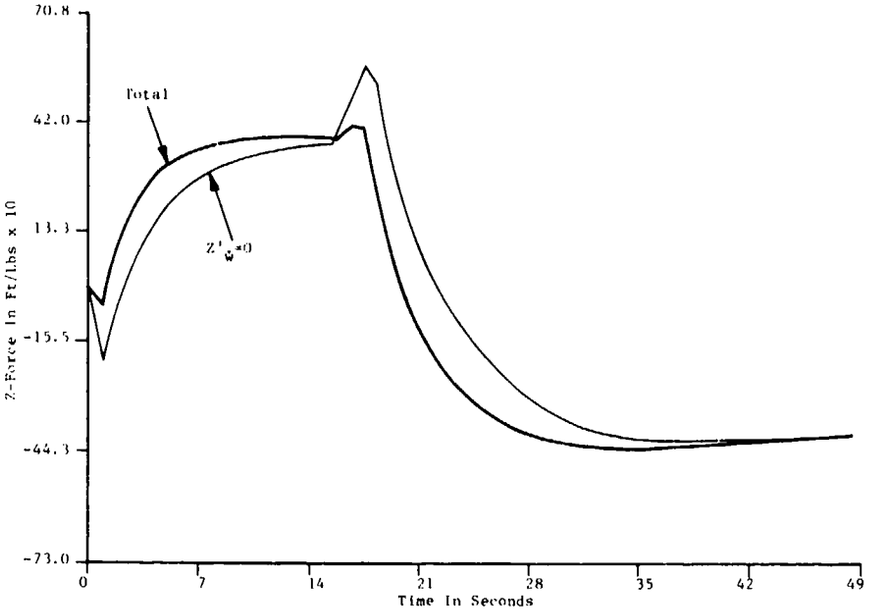

FIGURE 7. TRAJECTORY SIMULATION PLOT OF $Z'_{\dot{w}}$ CONTRIBUTION TO Z-FORCE DURING A δ_s = ±30° DIVE/CLIMB MANEUVER

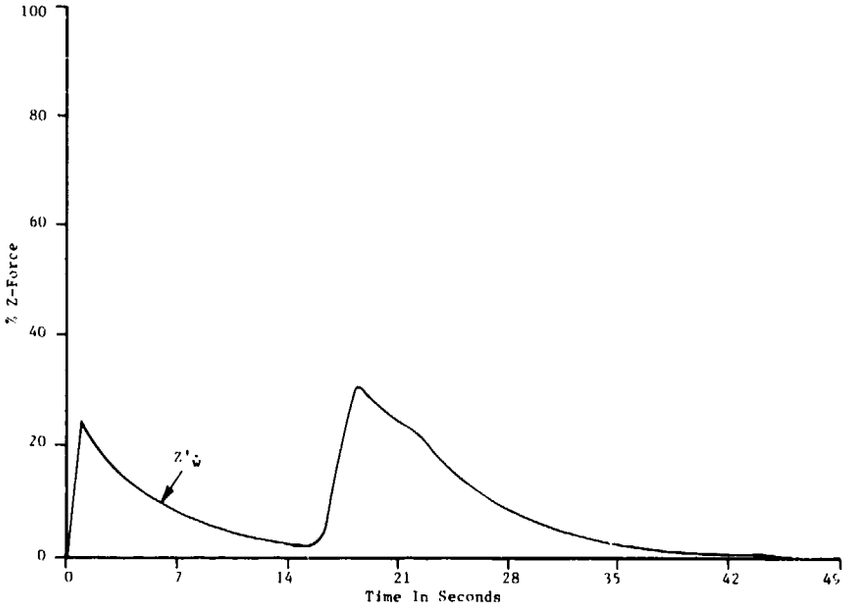

FIGURE 8. PERCENT CONTRIBUTION OF $Z'_{\dot{w}}$ TO Z-FORCE DURING A δ_s = ±30° DIVE/CLIMB MANEUVER

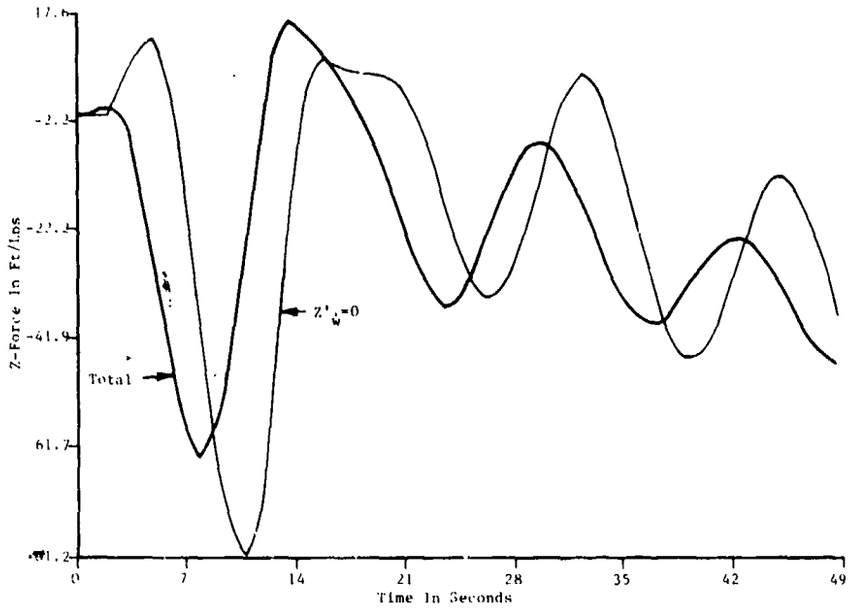

FIGURE 9. TRAJECTORY SIMULATION PLOT OF $Z'_{\dot{w}}$ CONTRIBUTION TO Z-FORCE DURING A $\delta_r = \pm 30°$ TURN REVERSAL MANEUVER (AUTOMATIC DEPTH-KEEPING)

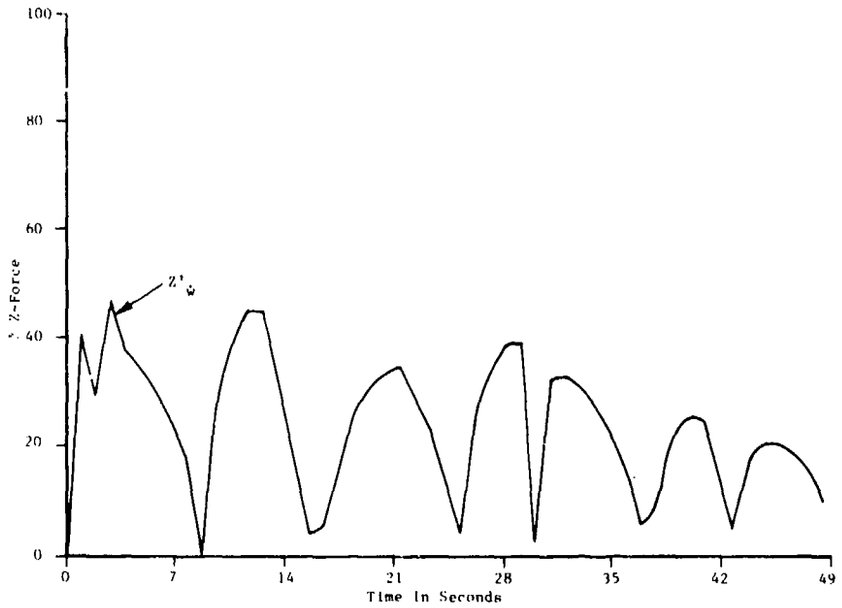

FIGURE 10. PERCENT CONTRIBUTION OF $Z'_{\dot{w}}$ TO Z-FORCE DURING A $\delta_r = \pm 30°$ TURN REVERSAL MANEUVER (AUTOMATIC DEPTH-KEEPING)

Z'_w variation using the formula

$$\frac{(100+\text{Constant})}{100} \times (Z'_w),$$

where Constant = ±100.

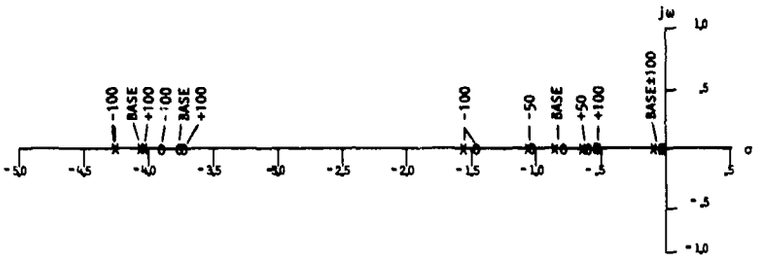

FIGURE 11. ROOT LOCUS PLOT OF u/δ_s FOR A GENERALIZED UNDERWATER VEHICLE, VARYING Z'_w

Z'_w variation using the formula

$$\frac{(100+\text{Constant})}{100} \times (Z'_w),$$

where Constant = ±100.

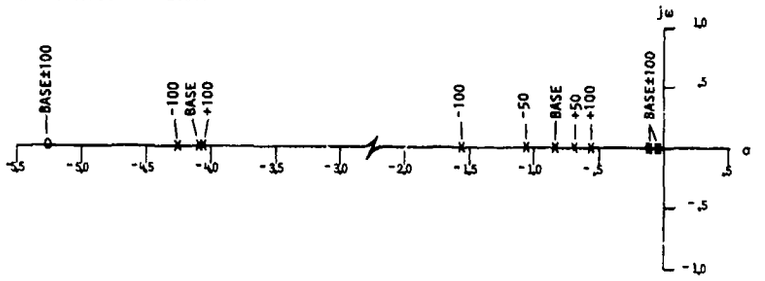

FIGURE 12. ROOT LOCUS PLOT OF w/δ_s FOR A GENERALIZED UNDERWATER VEHICLE, VARYING Z'_w

Z'_w variation using the formula

$$\frac{(100+\text{Constant})}{100} \times (Z'_w),$$

where Constant = ±100.

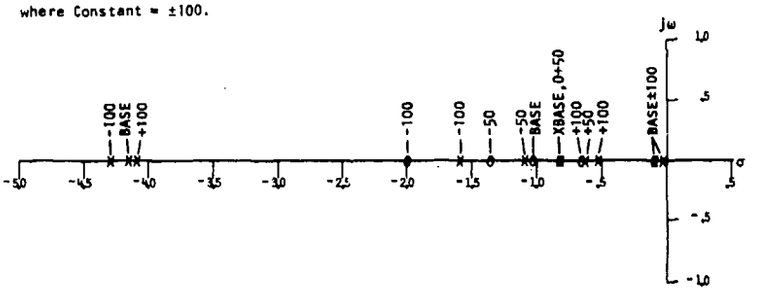

FIGURE 13. ROOT LOCUS PLOT OF θ/δ_s FOR A GENERALIZED UNDERWATER VEHICLE, VARYING Z'_w

TABLE 2A

LONGITUDINAL SENSITIVITY ANALYSIS OF CHARACTERISTIC EQUATION NON-DIMENSIONAL ROOTS FOR A GENERALIZED UNDERWATER VEHICLE, VARYING Z'_w ±100%

% VAR	ROOT 1	% CHANGE	ROOT 2	% CHANGE	ROOT 3	% CHANGE	ROOT 4	% CHANGE
-100^R_I	-.042977 0	-.12			-1.5211 0	91.2	-4.2485 0	2.4
-50^R_I	-.043001 0	-.06			-1.0805 0	31.5	-4.1731 0	.67
-25^R_I	-.043014 0	-.03			-.93360 0	13.6	-4.1616 0	.28
-10^R_I	-.043021 0	-.01			-.86304 0	5.0	-4.1548 0	.10
$BASE^R_I$	-.043026 0		-.10885 0		-.82160 0		-4.1521 0	
$+10^R_I$	-.043031 0	.01			-.78353 0	-4.6	-4.1465 0	-.09
$+25^R_I$	-.043038 0	.03			-.73346 0	-10.7	-4.1417 0	-.20
$+50^R_I$	-.043051 0	.06			-.66223 0	-19.4	-4.1352 0	-.36
$+100^R_I$	-.043077 0	.12			-.55452 0	-32.5	-4.1259 0	-.58

TABLE 2B

LONGITUDINAL SENSITIVITY ANALYSIS OF U NUMERATOR NON-DIMENSIONAL ROOTS FOR A GENERALIZED UNDERWATER VEHICLE, VARYING Z'_w ±100%

% VAR	ROOT 1	% CHANGE	ROOT 2	% CHANGE	ROOT 3	% CHANGE
-100^R_I	-.049241 0	-.21	-1.4303 0	82.3	-3.8076 0	4.0
-50^R_I	-.049293 0	-.11	-1.0368 0	31.0	-3.7467 0	2.1
-25^R_I	-.049319 0	-.05	-.83600 0	13.4	-3.7336 0	.47
-10^R_I	-.049335 0	-.02	-.83100 0	5.0	-3.7623 0	.17
$BASE^R_I$	-.049345 0		-.79156 0		-3.7560 0	
$+10^R_I$	-.049356 0	-.02	-.75564 0	-4.5	-3.7504 0	-.15
$+25^R_I$	-.049373 0	.06	-.70746 0	-10.6	-3.7431 0	-.34
$+50^R_I$	-.049400 0	.11	-.63930 0	-19.2	-3.7333 0	-.60
$+100^R_I$	-.049457 0	.23	-.53578 0	-32.3	-3.7133 0	-.99

TABLE 2C

LONGITUDINAL SENSITIVITY ANALYSIS OF W NUMERATOR NON-DIMENSIONAL ROOTS FOR A GENERALIZED UNDERWATER VEHICLE, VARYING Z'_w ±100%

% VAR	ROOT 1	% CHANGE	ROOT 2	% CHANGE	ROOT 3	% CHANGE
-100^R_I						
-50^R_I						
-25^R_I						
-10^R_I						
$BASE^R_I$	-.032752 0		-.10885 0		-6.3461 0	
$+10^R_I$						
$+25^R_I$						
$+50^R_I$						
$+100^R_I$						

TABLE 2D

LONGITUDINAL SENSITIVITY ANALYSIS OF θ NUMERATOR NON-DIMENSIONAL ROOTS FOR A GENERALIZED UNDERWATER VEHICLE, VARYING Z'_w ±100%

% VAR	ROOT 1	% CHANGE	ROOT 2	% CHANGE
-100^R_I			-2.3085 0	97.0
-50^R_I			-1.3529 0	32.7
-25^R_I			-1.1630 0	14.0
-10^R_I			-1.0199 0	5.2
$BASE^R_I$	-.10885 0		-1.0139 0	
$+10^R_I$			-.97201 0	-4.7
$+25^R_I$			-.90810 0	-11.0
$+50^R_I$			-.81841 0	-19.8
$+100^R_I$			-.69341 0	-33.0

compared. In application to a wide variety of underwater vehicles, it has been our experience that if a body is nearly axisymmetric then Lamb's inertial coefficient is a reliable formulation for $Z'_{\dot{w}_b}$. This is especially true for large ℓ/d ratios.

This is the first hydrodynamic coefficient with significant contribution from appendages to the body. The discussion and formulations that follow can be applied to any surface projecting from the body that can be approximated as a flat plate in accelerated fluid flow normal to its surface. The equations given will be for horizontal tail fins, but they are applicable to any horizontal surfaces such as bowplanes, sailplanes, fairwater planes, depressors, wings, faired struts, sails, etc. Tail contributions to other longitudinal hydrodynamic coefficients are formulated using the expressions given below. Theoretical values of the additional mass of a number of types of bodies (bodies of infinite length, bodies of revolution, ellipsoids or elliptic plates of finite dimensions) have been derived by Lamb[1] and Munk[2][3]. Values for bodies of finite dimensions not covered by the theory; for example, rectangular plates and wings, have been the object of many experimental research programs on the phenomenon.

Extensive test programs on additional-mass and additional-moment effects were conducted by the National Advisory Committee for Aeronautics (NACA) from 1933 to 1940. The coefficients given here are based on the results of these tests as reported by Gracey[4], and Malvestuto and Gale[5]. A very similar formulation is given by Pastor and Abkowitz[8].

For a thin flat plate of infinite span moving in a perfect fluid at constant velocity, V, along the normal to its surface, the momentum imparted to the fluid per unit span is given by hydrodynamic theory as

$$\frac{\pi\rho c^2 V}{4} .$$

For plates of finite span, this expression must be corrected by the introduction of coefficients whose values depend on the dimensions of

---

[1] ibid.

[2] ibid.

[3] ibid.

[4] ibid.

[5] ibid.

[8] Naval Underwater Ordnance Station T.N. No. 120, *Hydrodynamic Stability and Control Derivatives,* by D. L. Pastor and M. A. Abkowitz, 1957.

the plate. The additional mass, m_a, for translation of a plate of span b, V is thus determined from the equation of linear momentum

$$m_a V = \frac{k\pi\rho c^2 b V}{4} ,$$

so that

$$m_a = \frac{k\pi\rho c^2 b}{4} , \tag{18}$$

where k is the coefficient of additional mass shown in Figure 14. This formulation is for one fin. So, with the proper nondimensionalizing terms added, the expression for two identical horizontal fin surfaces in a tail configuration is written

$$Z'_{\dot{w}_{ht}} = \frac{1}{\frac{1}{2}\rho \ell^3} \frac{k\pi\rho c^2 b}{2} = \frac{k\pi c^2 b}{\ell^3} . \tag{19}$$

Note: Pastor and Abkowitz substituted a curve fitted expression for k:

$$k = \frac{1}{(1 + 1/AR)^{\frac{1}{2}}} .$$

An effective chord, $\bar{c}$, is usually used since most surfaces are not simple rectangular shapes. If a sternplane or any movable horizontal tail surface is present and is an extension of the fixed horizontal tail surface, then it should be included in the area for calculating $\bar{c}$ and s. If it is not a part of the fin, then its contribution to $Z'_{\dot{w}}$ can be calculated separately, as can the bowplane contribution, by using Equation 19 to yield $Z'_{\dot{w}_s}$ and $Z'_{\dot{w}_{bp}}$. For completeness and clarification, Figure 15 and the following relationships are given.

AR = aspect ratio of surface = b^2/s

b = root-to-tip span of surface

s = planform area of surface

c_r = root chord of surface

c_t = tip chord of surface

$\bar{c}$ = mean chord of surface = $s/b = b/AR$

λ = planform taper ratio of surface = c_t/c_r .

(Text Continued on Page 26)

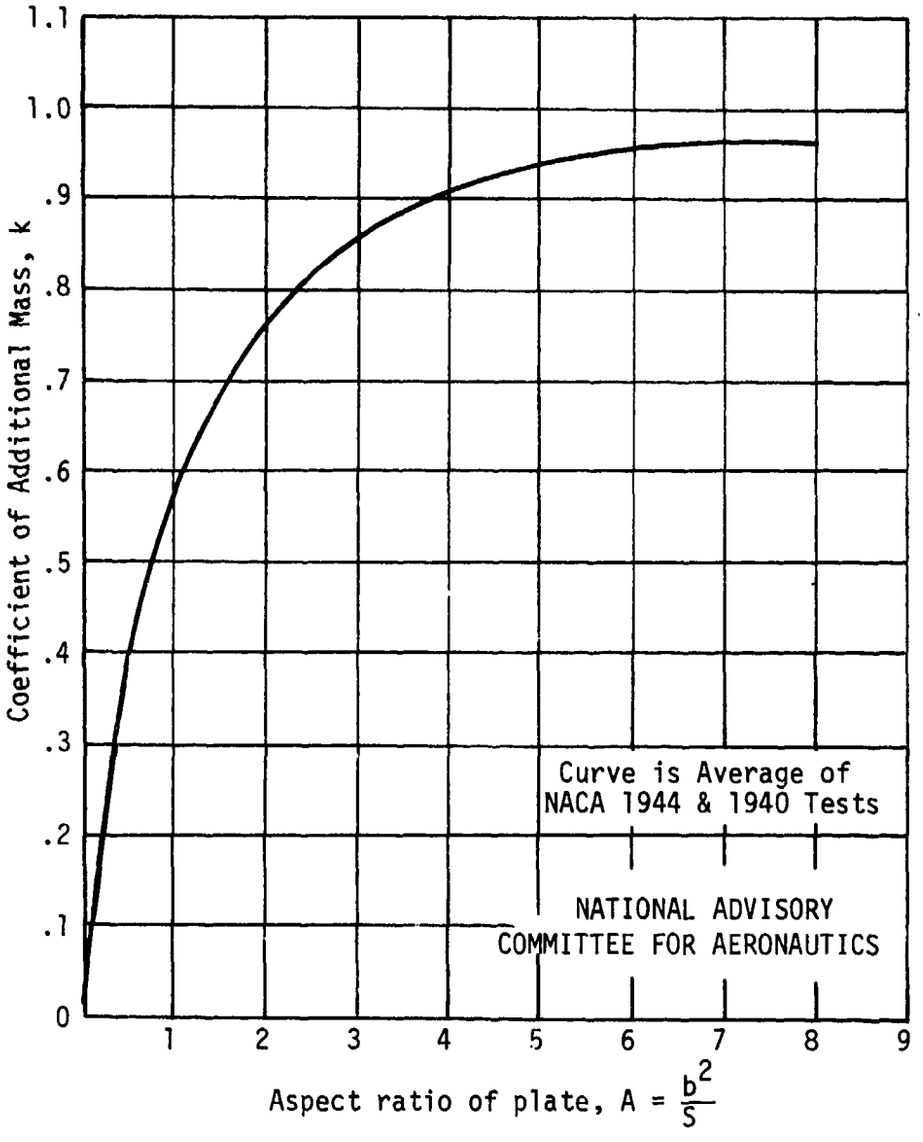

FIGURE 14. COEFFICIENTS OF ADDITIONAL MASS FOR RECTANGULAR PLATES

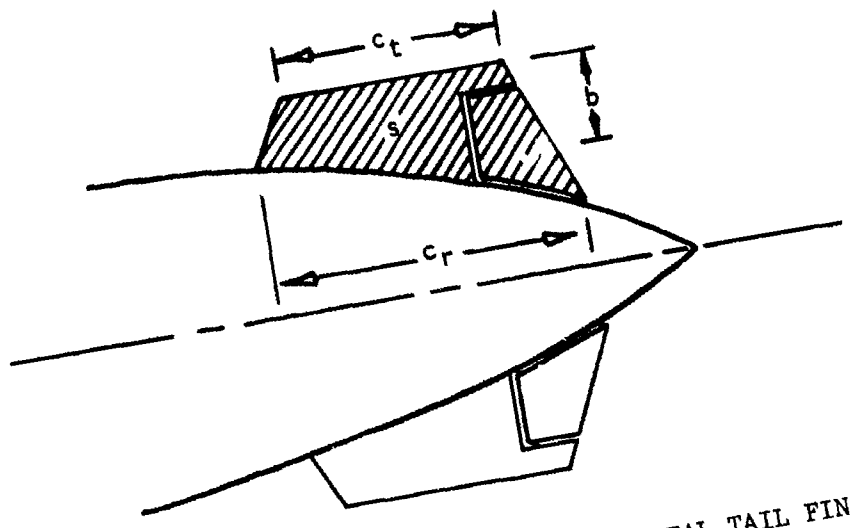

FIGURE 15. TOP VIEW OF BODY AND HORIZONTAL TAIL FIN CONFIGURATION WITH DESCRIPTIVE DIMENSIONS

A common way of computing the shroud contribution to $Z'_{\dot{w}}$ is to treat it as a flat plate in projection. That is, project the shroud into the xy-plane and treat its projection as a flat plate.

$$Z'_{\dot{w}_s} = \frac{k\pi c^2 r}{\ell^3} \tag{20}$$

where c = chord of the shroud and r = radius of the shroud. The complete $Z'_{\dot{w}}$ equation is the sum of the component contributions; e.g.,

$$Z'_{\dot{w}} = Z'_{\dot{w}_b} + Z'_{\dot{w}_{ht}} + Z'_{\dot{w}_{bp}} + Z'_{\dot{w}_s} .$$

$M'_{\dot{w}}$

1. When a vehicle undergoing an acceleration in the z-direction experiences a pitching moment proportional to the acceleration, this moment is represented in the equations of motion as $M'_{\dot{w}}$.

2. $M'_{\dot{w}}$ usually has a minor influence on the characteristic equation of the vehicle. Unlike $Z'_{\dot{u}}$, $M'_{\dot{u}}$, and $X'_{\dot{w}}$, though, it should not be ignored. It is most important on vehicles that have large stern configurations and/or cg locations well forward on the vehicle.

Tables 3A through 3D present the results of a sensitivity analysis of nondimensional roots of the characteristic equation (transfer function denominator) and u, w, and θ (numerators) for a generalized underwater vehicle, varying $M'_{\dot{w}}$ from -100 percent to +100 percent.

3. The cg and cb of a submerged vehicle are generally in vertical alignment to achieve level trim at zero speed. Since the body additional mass effects are lumped as acting through the body cb (caution must be exercised when the cb is not coincident with the centroid of the volume displaced by the outer hull surface—as with "wet" vehicles) and the vehicle equations of motion are typically written about a cg origin, the resisting force to a z-acceleration is a pure $Z'_{\dot{w}_b}\dot{w}$ term. That is, there is no x-moment arm to cause the generation of a moment $M'_{\dot{w}}\dot{w}$. The added mass and moment effects of the horizontal surfaces generally are the primary contributors to $M'_{\dot{w}}$. Just as any force on a moment arm is calculated to produce a moment, so with $M'_{\dot{w}}$ we have

4.
$$M'_{\dot{w}_b} = Z'_{\dot{w}_b}\frac{(X_{ncb} - X_{ncg})}{\ell} \tag{21}$$

$$M'_{\dot{w}_t} = Z'_{\dot{w}_{ht}}\frac{(X_{nht} - X_{ncg})}{\ell} \tag{22}$$

where

X_{ncb} = x-distance from nose to cb

X_{ncg} = x-distance from nose to cg

X_{nht} = x-distance from nose to centroid of the horizontal tail fins .

Note: The distances are all positive numbers.

Substituting the x-distance to bowplanes or shroud into Equation (22) yields $M'_{\dot{w}_{bp}}$ and $M'_{\dot{w}_s}$. The complete expression is the sum of the component contributions; e.g.,

$$M'_{\dot{w}} = M'_{\dot{w}_b} + M'_{\dot{w}_{ht}} + M'_{\dot{w}_{bp}} + M'_{\dot{w}_s} .$$

(Text Continued on Page 29)

TABLE 3A

LONGITUDINAL SENSITIVITY ANALYSIS OF CHARACTERISTIC EQUATION NON-DIMENSIONAL ROOTS FOR A GENERALIZED UNDERWATER VEHICLE, VARYING M'_w ±100%

% VAR	ROOT 1	% CHANGE	ROOT 2	% CHANGE	ROOT 3	% CHANGE	ROOT 4	% CHANGE
-100^R_I	-.043121 0	-.01			-.82361 0	.27	-4.1382 0	-.28
-50^R_I	-.043023 0	-.007			-.82279 0	.13	-4.1441 0	-.14
-25^R_I	-.043025 0	-.002			-.82215 0	.07	-4.1471 0	-.07
-10^R_I	-.043025 0	-.002			-.82182 0	.03	-4.1489 0	-.03
$BASE^R_I$	-.043026 0		-.10885 0		-.82160 0		-4.1501 0	
$+10^R_I$	-.043026 0	0			-.82138 0	-.03	-4.1512 0	.03
$+25^R_I$	-.043027 0	.002			-.82105 0	-.07	-4.1531 0	.07
$+50^R_I$	-.043028 0	.005			-.82050 0	-.13	-4.1561 0	.14
$+100^R_I$	-.043031 0	.01			-.81940 0	-.27	-4.1621 0	.29

TABLE 3B

LONGITUDINAL SENSITIVITY ANALYSIS OF U NUMERATOR NON-DIMENSIONAL ROOTS FOR A GENERALIZED UNDERWATER VEHICLE, VARYING M'_w ±100%

% VAR	ROOT 1	% CHANGE	ROOT 2	% CHANGE	ROOT 3	% CHANGE
-100^R_I	-.049335 0	-.02	-.79443 0	.43	-3.7325 0	-.44
-50^R_I	-.049340 0	-.01	-.79324 0	.21	-3.7478 0	-.22
-25^R_I	-.049343 0	-.004	-.79240 0	.11	-3.7519 0	-.11
-10^R_I	-.049344 0	-.002	-.79189 0	.04	-3.7543 0	-.05
$BASE^R_I$	-.049345 0		-.79166 0		-3.7600 0	
$+10^R_I$	-.049346 0	.002	-.79122 0	-.04	-3.7576 0	.04
$+25^R_I$	-.049348 0	.006	-.79072 0	-.11	-3.7650 0	.11
$+50^R_I$	-.049351 0	.01	-.78965 0	-.21	-3.7641 0	.22
$+100^R_I$	-.049356 0	.02	-.78822 0	-.42	-3.7723 0	.42

TABLE 3C

LONGITUDINAL SENSITIVITY ANALYSIS OF W NUMERATOR NON-DIMENSIONAL ROOTS FOR A GENERALIZED UNDERWATER VEHICLE, VARYING M'_w ±100%

% VAR	ROOT 1	% CHANGE	ROOT 2	% CHANGE	ROOT 3	% CHANGE
-100^R_I						
-50^R_I						
-25^R_I						
-10^R_I						
$BASE^R_I$	-.032752 0		-.10885 0		-5.3461 0	
$+10^R_I$						
$+25^R_I$						
$+50^R_I$						
$+100^R_I$						

TABLE 3D

LONGITUDINAL SENSITIVITY ANALYSIS OF θ NUMERATOR NON-DIMENSIONAL ROOTS FOR A GENERALIZED UNDERWATER VEHICLE, VARYING M'_w ±100%

% VAR	ROOT 1	% CHANGE	ROOT 2	% CHANGE
-100^R_I			-1.0118 0	-.79
-50^R_I			-1.0158 0	-.40
-25^R_I			-1.0179 0	-.21
-10^R_I			-1.0191 0	-.08
$BASE^R_I$	-.10885 0		-1.0199 0	
$+10^R_I$			-1.0207 0	.08
$+25^R_I$			-1.0219 0	.20
$+50^R_I$			-1.0232 0	.39
$+100^R_I$			-1.0280 0	.79

$X'_{\dot{q}}$

1. Forces along the x-direction caused by angular acceleration in pitch are represented by $X'_{\dot{q}}$.

2. & 3. $X'_{\dot{q}}$ is usually an insignificant term as is its near-equal, $M'_{\dot{u}}$ (Equation (9)).

4. $X'_{\dot{q}} = 0$.

$Z'_{\dot{q}}$

1. z-forces arising from pitch angle accelerations are termed $Z'_{\dot{q}}$.

2. $Z'_{\dot{q}}$, as its counterpart $M'_{\dot{w}}$, is a minor derivative, yet it can have some influence over the characteristic equation of a vehicle. It should therefore be calculated. Tables 4A through 4D present the results of a sensitivity analysis of nondimensional roots of the characteristic equation (transfer function denominator) and u, w, and θ (numerators) for a generalized underwater vehicle, varying $Z'_{\dot{q}}$ from -100 percent to +100 percent.

3. & 4. $Z'_{\dot{q}} = M'_{\dot{w}}$.

$M'_{\dot{q}}$

1. When a submerged body is accelerated in pitch, it must change the flow pattern in the surrounding fluid. The added moment needed to effect this change in flow pattern is represented in the equations of motion as an apparent moment of inertia, $(I'_y - M'_{\dot{q}})$.

2. $M'_{\dot{q}}$ is a major derivative in influence on the characteristic equation. As with $Z'_{\dot{w}}$ and $X'_{\dot{u}}$, M'_q enters the equations of motion as an addition to the vehicle inertia term, in this case the moment of inertia about the y-axis. Trajectory simulation and pitch moment percent contribution plots in Figures 16 through 21 illustrate its significance to vehicular motion during various maneuvers. The root locus plots in Figures 22, 23, and 24 illustrate the wide variation in the locations of the poles due to variations in $M'_{\dot{q}}$. Tables 5A through 5D present the results of a sensitivity analysis of nondimensional roots of the characteristic equation (transfer function denominator) and u, w, and θ (numerators) for a generalized underwater vehicle, varying M'_q from -100 percent to +100 percent.

(Text Continued on Page 36)

TABLE 4A

LONGITUDINAL SENSITIVITY ANALYSIS OF CHARACTERISTIC EQUATION NON-DIMENSIONAL ROOTS FOR A GENERALIZED UNDERWATER VEHICLE, VARYING $Z'_{\dot{q}}$ ±100%

% VAR	ROOT 1	% CHANGE	ROOT 2	% CHANGE	ROOT 3	% CHANGE	ROOT 4	% CHANGE
-100^R_I	-.043023 0	-.007			-.82311 0	.18	-4.1415 0	-.21
-50^R_I	-.043024 0	-.005			-.82235 0	.09	-4.1458 0	-.10
-25^R_I	-.043025 0	-.002			-.82197 0	.05	-4.1480 0	-.05
-10^R_I	-.043026 0	0			-.82175 0	.02	-4.1493 0	-.02
$BASE^R_I$	-.043026 0		-.10885 0		-.82160 0		-4.1501 0	
$+10^R_I$	-.043026 0	0			-.82145 0	-.02	-4.1510 0	.02
$+25^R_I$	-.043027 0	.002			-.82122 0	-.05	-4.1523 0	.05
$+50^R_I$	-.043027 0	.002			-.82085 0	-.09	-4.1544 0	.10
$+100^R_I$	-.043029 0	.007			-.82010 0	-.18	-4.1587 0	.21

TABLE 4B

LONGITUDINAL SENSITIVITY ANALYSIS OF U NUMERATOR NON-DIMENSIONAL ROOTS FOR A GENERALIZED UNDERWATER VEHICLE, VARYING $Z'_{\dot{q}}$ ±100%

% VAR	ROOT 1	% CHANGE	ROOT 2	% CHANGE	ROOT 3	% CHANGE
-100^R_I	-.049341 0	-.008	-.79321 0	.21	-3.7474 0	-.28
-50^R_I	-.049343 0	-.004	-.79238 0	.10	-3.7517 0	-.11
-25^R_I	-.049344 0	-.002	-.79197 0	.05	-3.7538 0	-.22
-10^R_I	-.049345 0	0	-.79172 0	.02	-3.7551 0	-.22
$BASE^R_I$	-.049345 0		-.79156 0		-3.7560 0	
$+10^R_I$	-.049346 0	.002	-.79139 0	-.02	-3.7569 0	.02
$+25^R_I$	-.049347 0	.004	-.79115 0	-.05	-3.7581 0	.06
$+50^R_I$	-.049348 0	.006	-.79074 0	-.10	-3.7603 0	.11
$+100^R_I$	-.049350 0	.01	-.78992 0	-.21	-3.7646 0	.23

TABLE 4C

LONGITUDINAL SENSITIVITY ANALYSIS OF W NUMERATOR NON-DIMENSIONAL ROOTS FOR A GENERALIZED UNDERWATER VEHICLE, VARYING $Z'_{\dot{q}}$ ±100%

% VAR	ROOT 1	% CHANGE	ROOT 2	% CHANGE	ROOT 3	% CHANGE
-100^R_I	-.032760 0	.02			-5.1334 0	-4.0
-50^R_I	-.032756 0	.01			-5.2376 0	-2.0
-25^R_I	-.032754 0	.006			-5.2913 0	-1.0
-10^R_I	-.032752 0	0			-5.3240 0	-.41
$BASE^R_I$	-.032752 0		-.10886 0		-5.3461 0	
$+10^R_I$	-.032751 0	-.003			-5.3683 0	.42
$+25^R_I$	-.032750 0	-.006			-5.4020 0	1.0
$+50^R_I$	-.032747 0	-.02			-5.4591 0	2.1
$+100^R_I$	-.032743 0	-.03			-5.5770 0	4.3

TABLE 4D

LONGITUDINAL SENSITIVITY ANALYSIS OF θ NUMERATOR NON-DIMENSIONAL ROOTS FOR A GENERALIZED UNDERWATER VEHICLE, VARYING $Z'_{\dot{q}}$ ±100%

% VAR	ROOT 1	% CHANGE	ROOT 2	% CHANGE
-100^R_I				
-50^R_I				
-25^R_I				
-10^R_I				
$BASE^R_I$	-.10885 0		-1.0199 0	
$+10^R_I$				
$+25^R_I$				
$+50^R_I$				
$+100^R_I$				

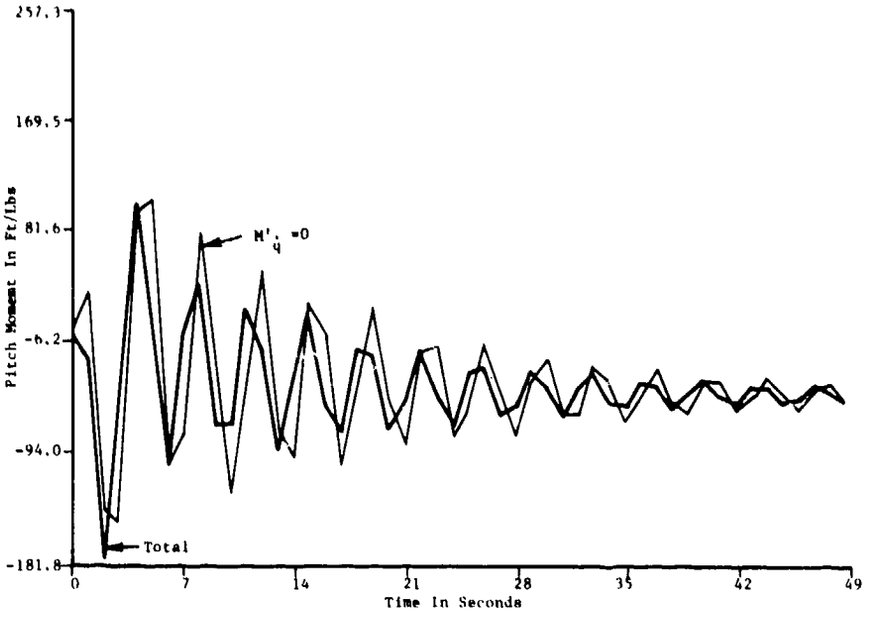

FIGURE 16. TRAJECTORY SIMULATION PLOT OF $M'_{\dot{q}}$ CONTRIBUTION TO PITCH MOMENT DURING A δ_r = 30° STEADY TURN (AUTOMATIC DEPTH-KEEPING)

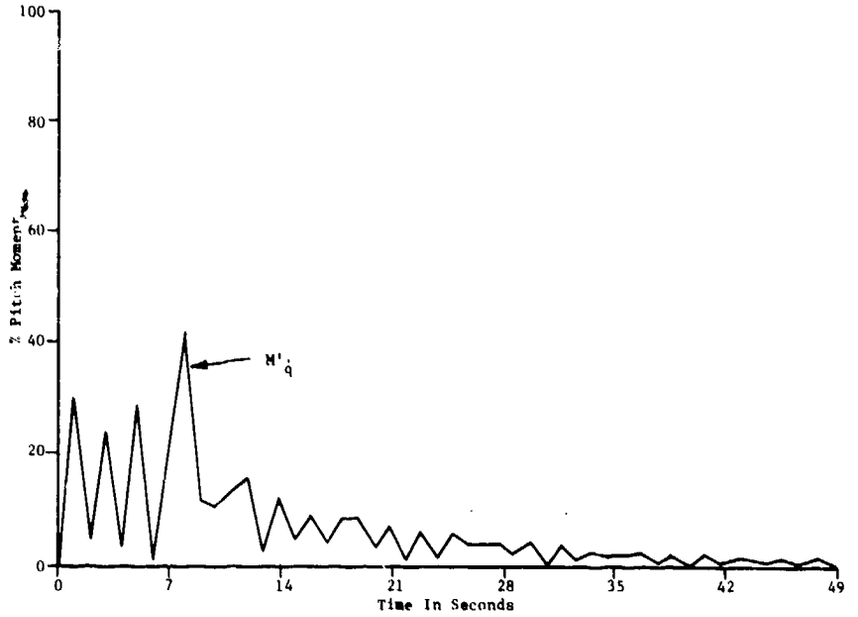

FIGURE 17. PERCENT CONTRIBUTION OF $M'_{\dot{q}}$ TO PITCH MOMENT DURING A δ_r = 30° STEADY TURN (AUTOMATIC DEPTH-KEEPING)

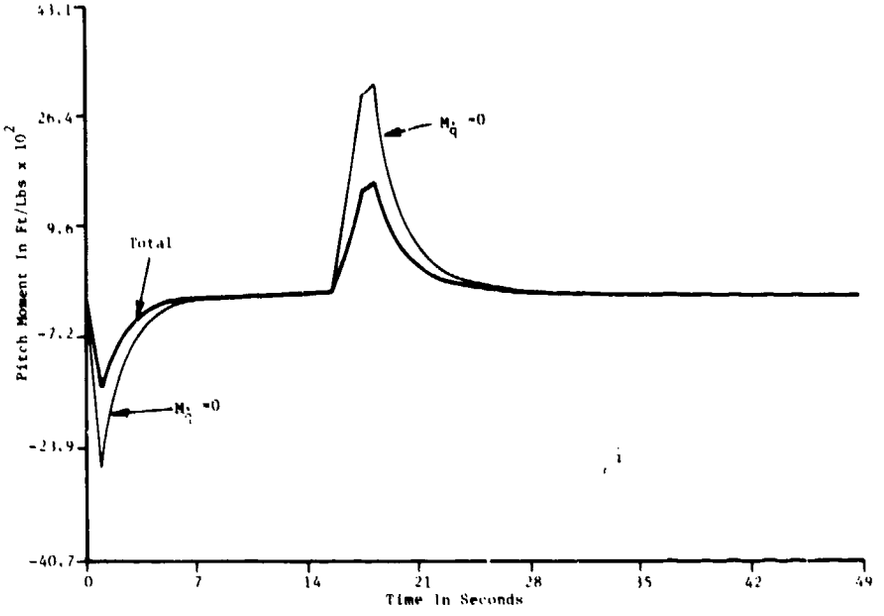

FIGURE 18. TRAJECTORY SIMULATION PLOT OF $M'_{\dot{q}}$ CONTRIBUTION TO PITCH MOMENT DURING A δ_s = ±30° DIVE/CLIMB MANEUVER

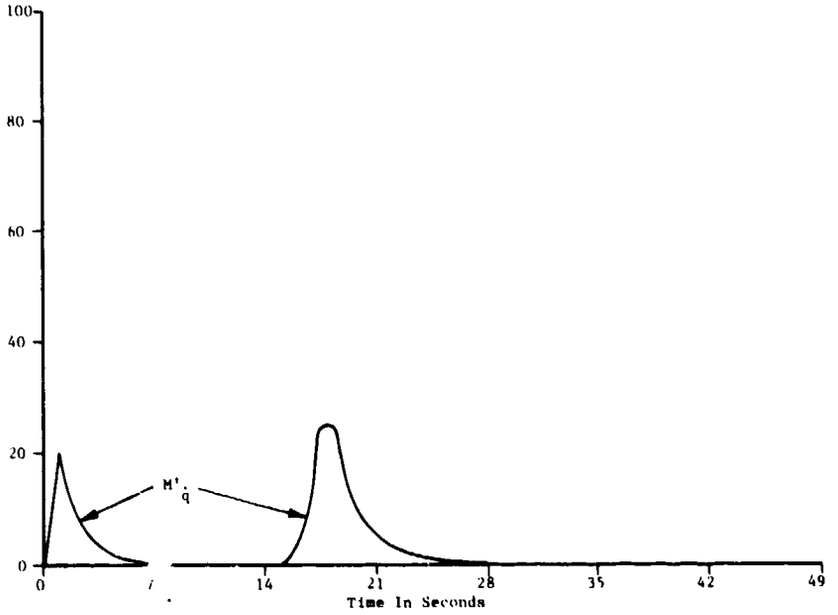

FIGURE 19. PERCENT CONTRIBUTION OF $M'_{\dot{q}}$ TO PITCH MOMENT DURING A δ_s = ±30° DIVE/CLIMB MANEUVER

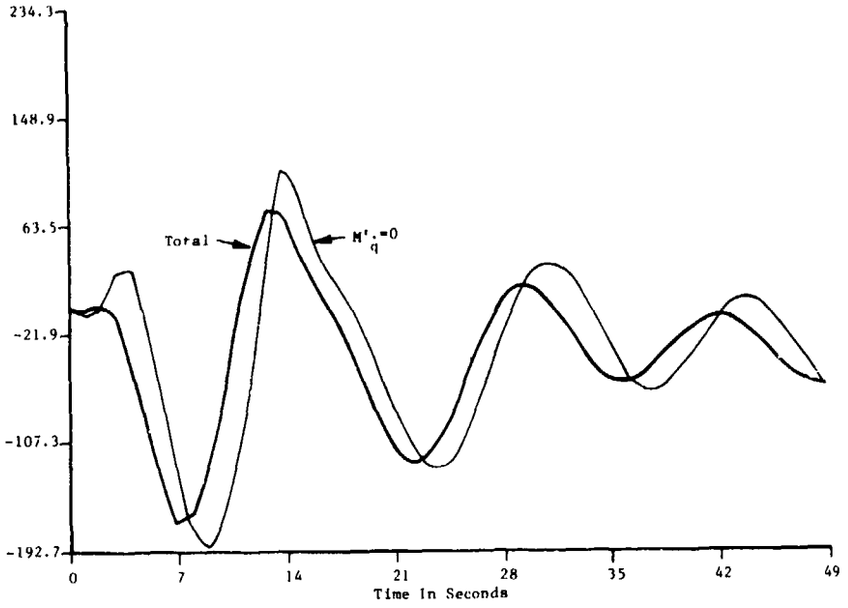

FIGURE 20. TRAJECTORY SIMULATION PLOT OF $M'_{\dot{q}}$ CONTRIBUTION TO PITCH MOMENT DURING A $\delta_r = \pm 30°$ TURN REVERSAL MANEUVER (AUTOMATIC DEPTH-KEEPING)

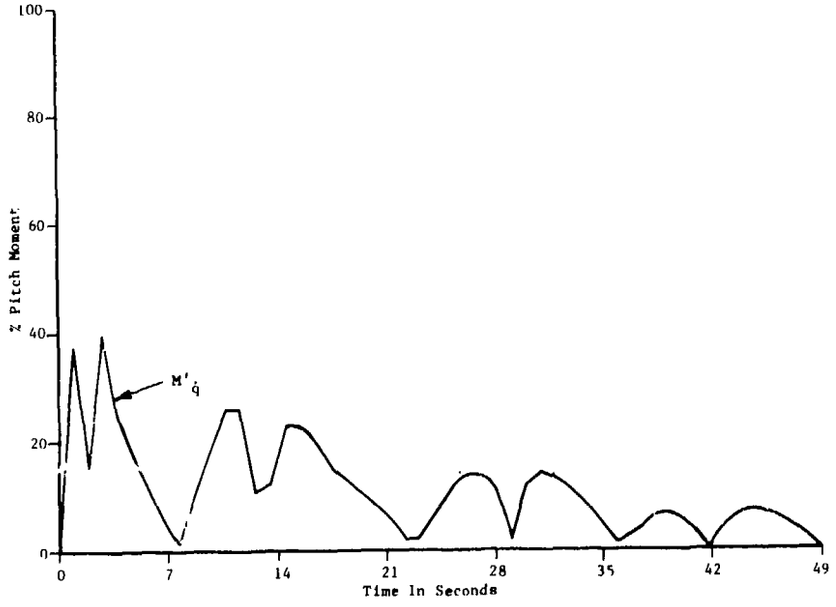

FIGURE 21. PERCENT CONTRIBUTION OF $M'_{\dot{q}}$ TO PITCH MOMENT DURING A $\delta_r = \pm 30°$ TURN REVERSAL MANEUVER (AUTOMATIC DEPTH-KEEPING)

M'_q variation using the formula

$$\frac{(100+\text{Constant})}{100} \times (M'_q),$$

where Constant = ±100.

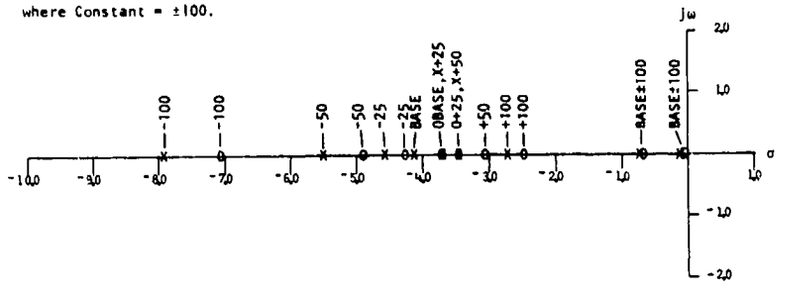

FIGURE 22. ROOT LOCUS PLOT OF u/δ_s FOR A GENERALIZED UNDERWATER VEHICLE, VARYING M'_q

M'_q variation using the formula

$$\frac{(100+\text{Constant})}{100} \times (M'_q),$$

where Constant = ±100.

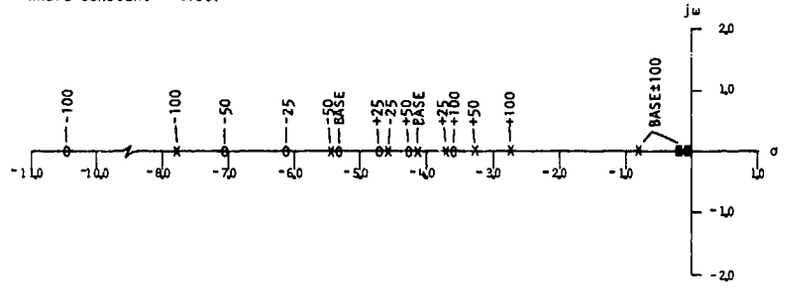

FIGURE 23. ROOT LOCUS PLOT OF w/δ_s FOR A GENERALIZED UNDERWATER VEHICLE, VARYING M'_q

M'_q variation using the formula

$$\frac{(100+\text{Constant})}{100} \times (M'_q),$$

where Constant = ±100.

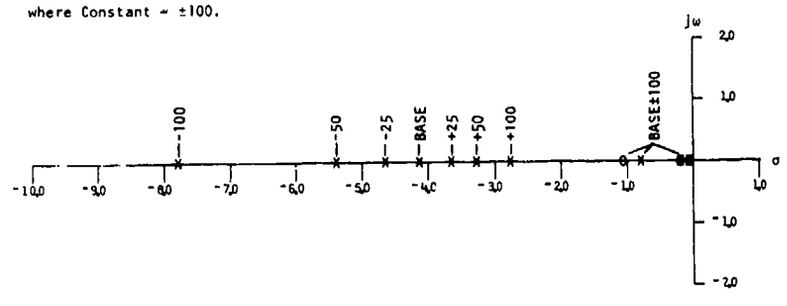

FIGURE 24. ROOT LOCUS PLOT OF θ/δ_s FOR A GENERALIZED UNDERWATER VEHICLE, VARYING M'_q

TABLE 5A

LONGITUDINAL SENSITIVITY ANALYSIS OF CHARACTERISTIC EQUATION NON-DIMENSIONAL ROOTS FOR A GENERALIZED UNDERWATER VEHICLE, VARYING M'_q ±100%

% VAR	ROOT 1	% CHANGE	ROOT 2	% CHANGE	ROOT 3	% CHANGE	ROOT 4	% CHANGE
-100^R_I	-.042802 0	-.22			-.82717 0	.68	-7.8464 0	88.1
-50^R_I	-.042913 0	-.26			-.82453 0	.36	-5.4266 0	30.8
-25^R_I	-.042969 0	-.13			-.82311 0	.18	-4.7028 0	13.3
-10^R_I	-.043003 0	-.05			-.82221 0	.07	-4.3547 0	4.9
$BASE^R_I$	-.043026 0		-.10885 0		-.82160 0		-4.1501 0	
$+10^R_I$	-.043049 0	.05			-.82097 0	-.08	-3.9641 0	- 4.5
$+25^R_I$	-.043083 0	.13			-.82000 0	-.19	-3.7145 0	-10.5
$+50^R_I$	-.043140 0	.26			-.81831 0	-.40	-3.3625 0	-19.0
$+100^R_I$	-.043255 0	.53			-.81460 0	-.85	-2.8286 0	-31.8

TABLE 5B

LONGITUDINAL SENSITIVITY ANALYSIS OF U NUMERATOR NON-DIMENSIONAL ROOTS FOR A GENERALIZED UNDERWATER VEHICLE, VARYING M'_q ±100%

% VAR	ROOT 1	% CHANGE	ROOT 2	% CHANGE	ROOT 3	% CHANGE
-100^R_I	-.049007 0	-.68	-.80122 0	1.2	-7.0748 0	88.4
-50^R_I	-.049175 0	-.34	-.79667 0	.65	-4.2012 0	30.5
-25^R_I	-.049260 0	-.17	-.79419 0	.33	-4.2516 0	13.2
-10^R_I	-.049311 0	-.07	-.79263 0	.14	-3.9394 0	4.9
$BASE^R_I$	-.049345 0		-.79156 0		-3.7560 0	
$+10^R_I$	-.049380 0	.07	-.79046 0	- .14	-3.5892 0	- 4.4
$+25^R_I$	-.049432 0	.18	-.78877 0	- .35	-3.3656 0	-10.4
$+50^R_I$	-.049518 0	.35	-.78581 0	- .73	-3.0505 0	-18.8
$+100^R_I$	-.049694 0	.71	-.77932 0	-1.5	-2.5737 0	-31.5

TABLE 5C

LONGITUDINAL SENSITIVITY ANALYSIS OF W NUMERATOR NON-DIMENSIONAL ROOTS FOR A GENERALIZED UNDERWATER VEHICLE, VARYING M'_q ±100%

% VAR	ROOT 1	% CHANGE	ROOT 2	% CHANGE	ROOT 3	% CHANGE
-100^R_I	-.032653 0	-.30			-10.538 0	97.1
-50^R_I	-.032702 0	-.15			- 7.0970 0	32.6
-25^R_I	-.032727 0	-.08			- 6.0990 0	14.1
-10^R_I	-.032742 0	-.03			- 5.6239 0	5.2
$BASE^R_I$	-.032752 0		-.10885 0		-5.3461 0	
$+10^R_I$	-.032762 0	.03			-5.0942 0	- 4.7
$+25^R_I$	-.032776 0	.07			-4.7578 0	-11.0
$+50^R_I$	-.032801 0	.15			-4.2858 0	-19.8
$+100^R_I$	-.032851 0	.30			-3.5743 0	-33.1

TABLE 5D

LONGITUDINAL SENSITIVITY ANALYSIS OF θ NUMERATOR NON-DIMENSIONAL ROOTS FOR A GENERALIZED UNDERWATER VEHICLE, VARYING M'_q ±100%

% VAR	ROOT 1	% CHANGE	ROOT 2	% CHANGE
-100^R_I				
-50^R_I				
-25^R_I				
-10^R_I				
$BASE^R_I$	-.10885 0		-1.0199 0	
$+10^R_I$				
$+25^R_I$				
$+50^R_I$				
$+100^R_I$				

3. & 4. The body contribution to $M'_{\dot{q}}$ is calculated assuming the body is a prolate ellipsoid. Thus, we use Lamb's coefficient for added moment of inertia and the parallel axis theorem

$$M'_{\dot{q}_b} = \frac{-k'_b I_{y_{df}}}{\frac{1}{2}\rho \ell^5} + Z'_{\dot{w}_b} \frac{(X_{ncb} - X_{ncg})^2}{\ell^2}$$

where

$$k'_b = \frac{e^4(\beta_0 - \alpha_0)}{(2 - e^2)\{2e^2 - (2 - e^2)(\beta_0 - \alpha_0)\}}$$

α_0 and β_0 are defined in Equations (13) and (17). These equations are repeated here for convenience:

$$\alpha_0 = \frac{2(1 - e^2)}{e^3}\left(\tfrac{1}{2}\ell n \left[\frac{1 + e}{1 - e}\right] - e\right), \tag{13}$$

$$\beta_0 = \frac{1}{e^2} - \frac{1 - e^2}{2e^3} \ell n \frac{1 + e}{1 - e}, \tag{17}$$

$I_{y_{df}}$ = moment of inertia about the y-axis of the mass of the fluid displaced by the body.

The tail contribution to $M'_{\dot{q}}$ is in the same form as the body terms. That is, there is an added moment of inertia term and a term representing an added mass acting on a moment arm from the cg. The added moment of inertia of a flat plate resulting from rotation about an axis in the plane of the plate and parallel to the span is given by

$$I_a = \frac{k'_p \pi \rho b^2 c^3}{48}$$

where k'_p is the coefficient of added moment of inertia for a flat plate plotted on Figure 25. When c/b is sufficiently small (AR sufficiently large), this term becomes negligible compared with the second term in $M'_{\dot{q}_t}$ given as

$$Z'_{\dot{w}_{ht}} \frac{(X_{nht} - X_{ncg})^2}{\ell^2}.$$

(Text Continued on Page 38)

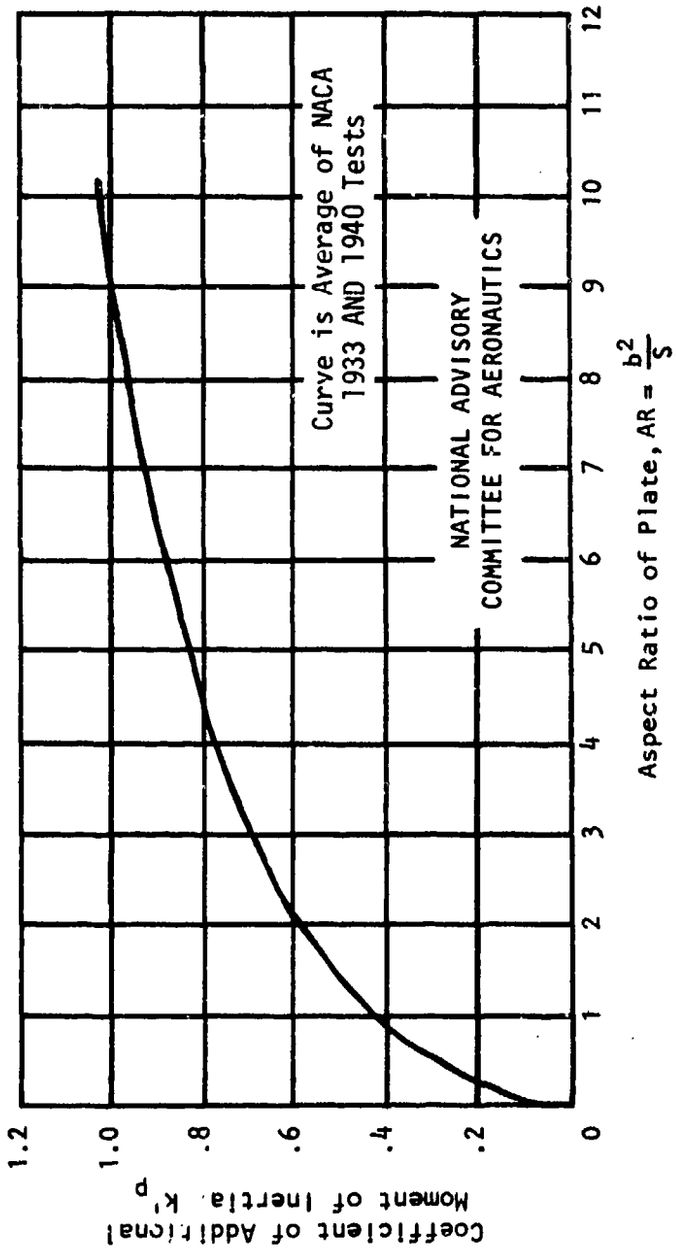

FIGURE 25. COEFFICIENT OF ADDITIONAL MOMENT OF INERTIA FOR RECTANGULAR PLATES

The horizontal tail surface contribution is then

$$M'_{\dot{q}_{ht}} = -\frac{1}{\frac{1}{2}\rho\ell^5}\frac{(k'_p \pi\rho b^{2-3}_c)}{48} + Z'_{\dot{w}_{ht}}\frac{(X_{nht} - X_{ncg})^2}{\ell^2} \quad .$$

Similar expressions may be written for bowplanes and a shroud so that the complete $M'_{\dot{q}}$ formula would be

$$M'_{\dot{q}} = M'_{\dot{q}_b} + M'_{\dot{q}_{ht}} + M'_{\dot{q}_{bp}} + M'_{\dot{q}_{sh}} \quad .$$

LATERAL COEFFICIENTS

$\underline{Y'_{\dot{v}}}$

1. Forces along the y-axis proportional to accelerations along the same axis are characterized by the added mass term $Y'_{\dot{v}}$. This term is the lateral counterpart of $Z'_{\dot{w}}$ in the longitudinal equations.

2. Just as $Z'_{\dot{w}}$ was seen to be a major stability derivative in the longitudinal plane, $Y'_{\dot{v}}$ is a very important coefficient in the lateral characteristic equation. Trajectory simulation and y-force percent contribution plots in Figures 26 through 29 illustrate its significance to vehicular motion during various maneuvers. The root locus plots in Figures 30, 31, and 32 illustrate the wide variation in the locations of the poles due to variation in $Y'_{\dot{v}}$. Tables 6A through 6D present the results of a sensitivity analysis of nondimensional roots of the characteristic equation (transfer function denominator) and v, ψ, and ϕ (numerators) for a generalized underwater vehicle, varying $Y'_{\dot{v}}$ from -100 percent to +100 percent.

3. & 4. For axisymmetric bodies

$$Y'_{\dot{v}_b} = Z'_{\dot{w}_b} \quad .$$

Most underwater vehicles have nearly axisymmetric hull forms. Of those whose shapes are not a body of revolution, quite often good approximations can be made by treating the body as everywhere circular in cross-section with a cross-sectional area equal to the actual body. This approximation is often used in the analysis of underwater vehicles.

Appendages that contribute to $Y'_{\dot{v}}$ are those with significant projections onto the xz-plane. Usually these consist of vertical tail fins

(Text Continued on Page 43)

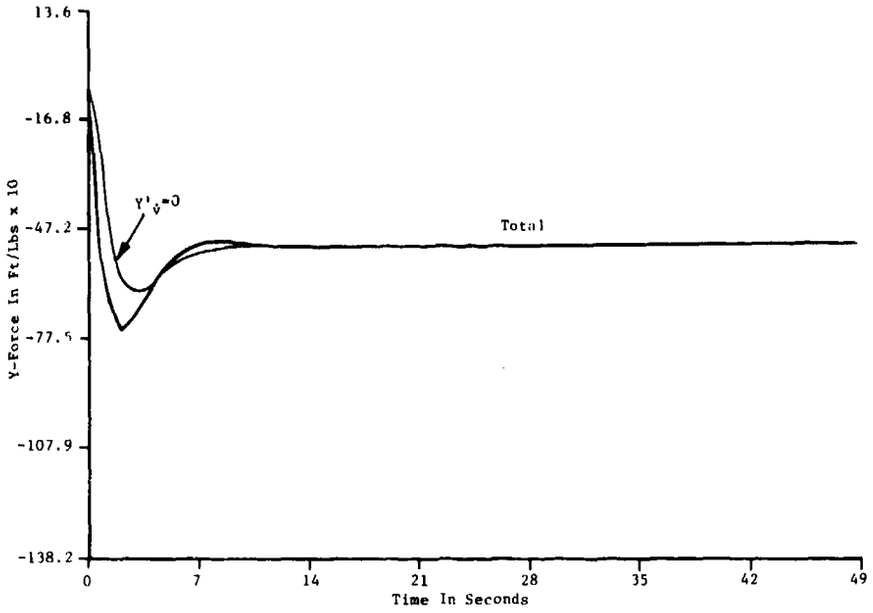

FIGURE 26. TRAJECTORY SIMULATION PLOT OF $Y'_{\dot{v}}$ CONTRIBUTION TO Y-FORCE DURING A δ_r = 30° STEADY TURN

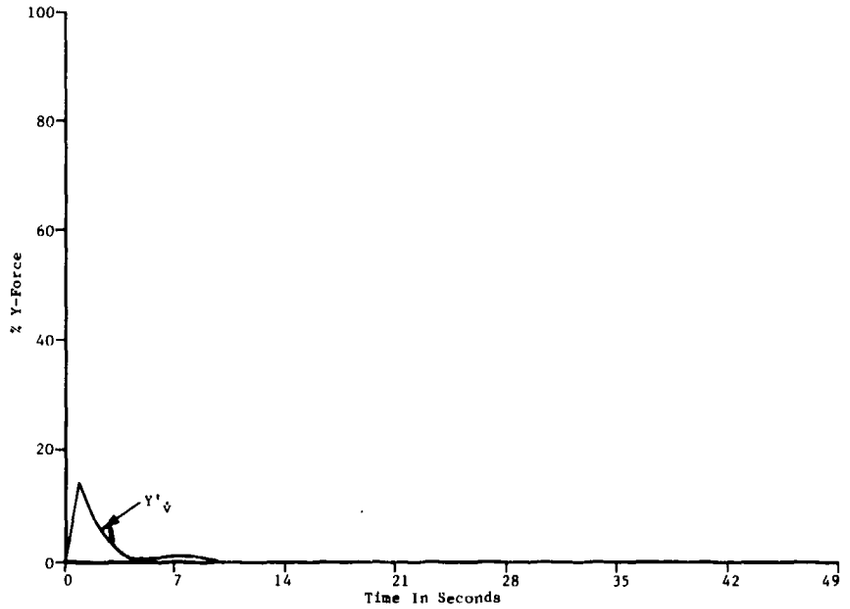

FIGURE 27. PERCENT CONTRIBUTION OF $Y'_{\dot{v}}$ TO Y-FORCE DURING A δ_r = 30° STEADY TURN

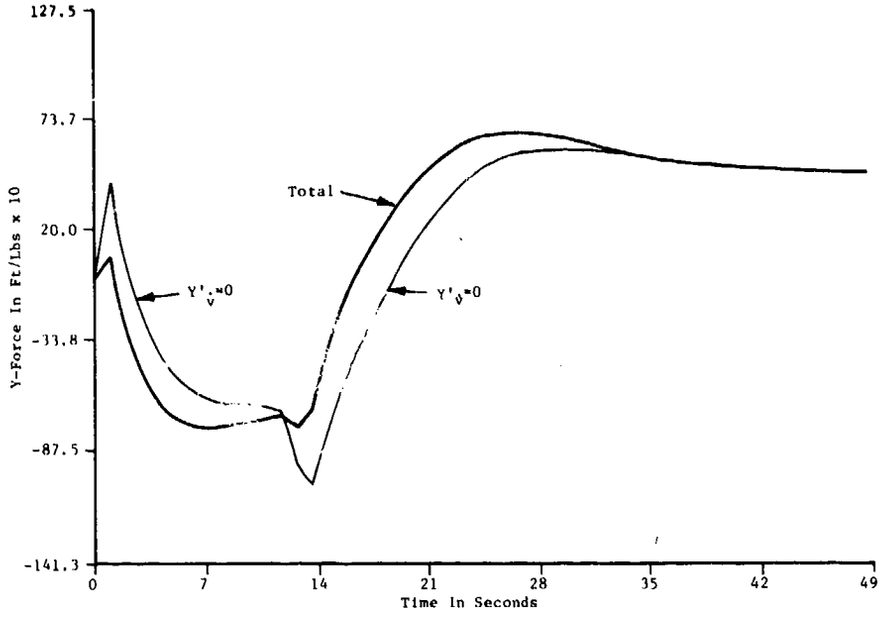

FIGURE 28. TRAJECTORY SIMULATION PLOT OF $Y'_{\dot{v}}$ CONTRIBUTION TO Y-FORCE DURING A δ_r = ±30° TURN REVERSAL MANEUVER

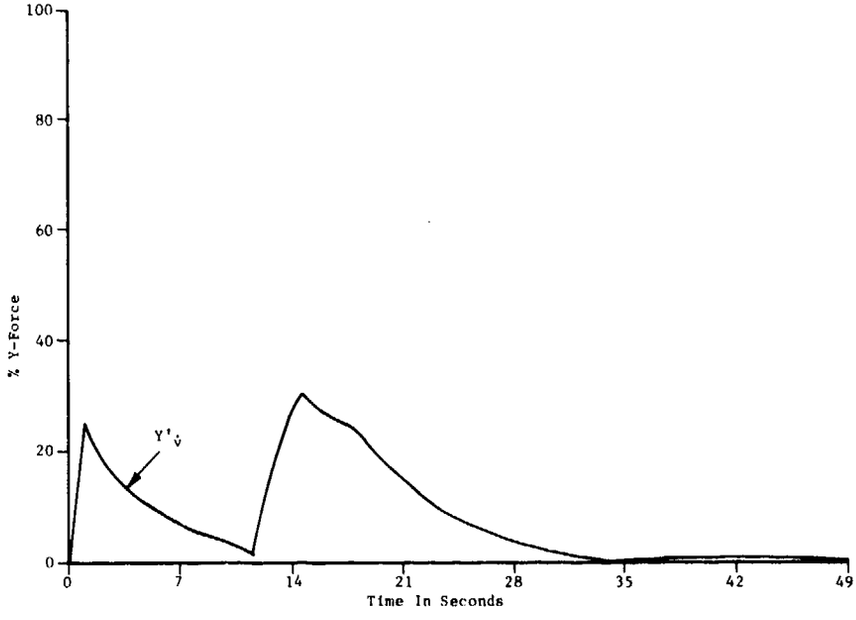

FIGURE 29. PERCENT CONTRIBUTION OF $Y'_{\dot{v}}$ TO Y-FORCE DURING A δ_r = ±30° TURN REVERSAL MANEUVER

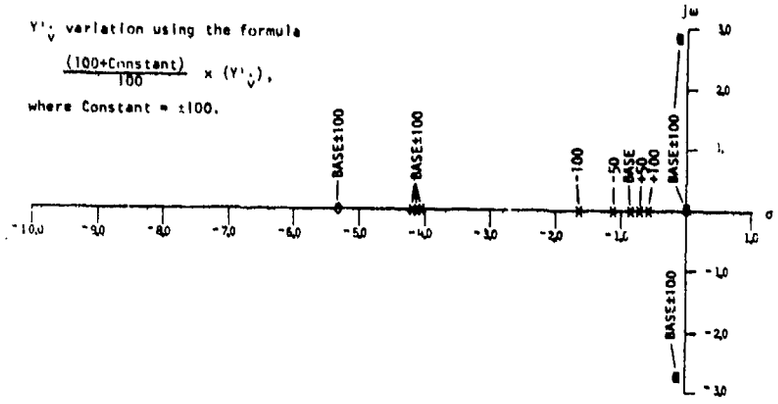

FIGURE 30. ROOT LOCUS PLOT OF v/δ_r FOR A GENERALIZED UNDERWATER VEHICLE, VARYING Y'_v

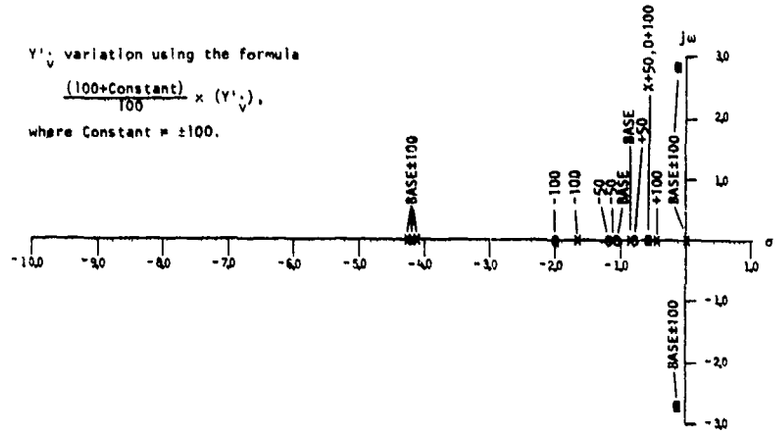

FIGURE 31. ROOT LOCUS PLOT OF ψ/δ_r FOR A GENERALIZED UNDERWATER VEHICLE, VARYING Y'_v

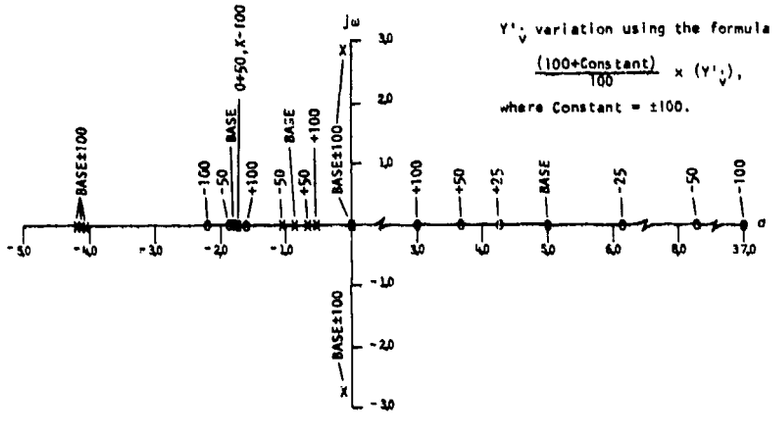

FIGURE 32. ROOT LOCUS PLOT OF ϕ/δ_r FOR A GENERALIZED UNDERWATER VEHICLE, VARYING Y'_v

TABLE 6A

LATERAL SENSITIVITY ANALYSIS OF CHARACTERISTIC EQUATION NON-DIMENSIONAL ROOTS FOR A GENERALIZED UNDERWATER VEHICLE, VARYING $Y'_{\dot{v}}$ ±100%

% VAR	ROOT 1	% CHANGE	ROOT 2	% CHANGE	ROOT 3	% CHANGE	ROOT 4	% CHANGE
-100^{R}_{I}	-.17646	-3.9	-.17646	-3.9	-4.2845	2.1	-1.6222	91.5
	-2.8541	-.18	2.8541	-.18	0		0	
-50^{R}_{I}	-.18130	-1.2	-.18130	-1.2	-4.2218	.59	-1.1147	31.6
	-2.8570	-.08	2.8570	-.08	0		0	
-25^{R}_{I}	-.18263	-.51	-.18263	-.51	-4.2072	.24	-.96285	13.7
	-2.8582	-.03	2.8582	-.03	0		0	
-10^{R}_{I}	-.18323	-.19	-.18323	-.19	-4.2007	.09	-.88996	5.1
	-2.8588	-.01	2.8588	-.01	0		0	
$BASE^{R}_{I}$	-.18357		-.18357		-4.1970		-.84717	*
	-2.8592		2.8592		0		0	
$+10^{R}_{I}$	-.18387	.16	-.18387	.16	-4.1938	-.08	-.80828	-4.6
	-2.8596	.01	2.8596	.01	0		0	
$+25^{R}_{I}$	-.18426	.38	-.18426	.38	-4.1895	-.18	-.75618	-10.7
	-2.8601	.03	2.8601	.03	0		0	
$+50^{R}_{I}$	-.18478	.66	-.18478	.66	-4.1838	-.31	-.68278	-19.4
	-2.8609	.06	2.8609	.06	0		0	
$+100^{R}_{I}$	-.18556	1.1	-.18550	1.1	-4.1755	-.51	-.57170	-32.5
	-2.86241	.10	2.8621	.10	0		0	

* A fifth set of real and imaginary roots exists, which has a base ±100% variation value of zero.

TABLE 6B

LATERAL SENSITIVITY ANALYSIS OF V NUMERATOR NON-DIMENSIONAL ROOTS FOR A GENERALIZED UNDERWATER VEHICLE, VARYING $Y'_{\dot{v}}$ ±100%

% VAR	ROOT 1	% CHANGE	ROOT 2	% CHANGE	ROOT 3	% CHANGE	ROOT 4	% CHANGE
-100^{R}_{I}								
-50^{R}_{I}								
-25^{R}_{I}								
-10^{R}_{I}								
$BASE^{R}_{I}$	-5.3392		-.17756		-.17756		0	
	0		-2.8702		2.8702		0	
$+10^{R}_{I}$								
$+25^{R}_{I}$								
$+50^{R}_{I}$								
$+100^{R}_{I}$								

TABLE 6C

LATERAL SENSITIVITY ANALYSIS OF ϕ NUMERATOR NON-DIMENSIONAL ROOTS FOR A GENERALIZED UNDERWATER VEHICLE, VARYING $Y'_{\dot{v}}$ ±100%

% VAR	ROOT 1	% CHANGE	ROOT 2	% CHANGE	ROOT 3	% CHANGE
-100^{R}_{I}	-.18251	-1.5	-.18251	-1.5	-2.0114	96.9
	-2.8603	-.20	2.8603	-.20	0	
-50^{R}_{I}	-.18401	-.33	-.18401	-.33	-1.3551	32.7
	-2.8637	-.08	2.8637	-.08	0	
-25^{R}_{I}	-.18501	-.12	-.18501	-.12	-1.1648	14.0
	-2.8650	-.03	2.8650	-.03	0	
-10^{R}_{I}	-.18516	-.04	-.18516	-.04	-1.0743	5.2
	-2.8656	-.01	2.8656	-.01	0	
$BASE^{R}_{I}$	-.18523		-.18523		-1.0214	
	-2.8660		2.8660		0	
$+10^{R}_{I}$	-.18528	.03	-.18528	.03	-.97344	-4.7
	-2.8663	.01	2.8663	.01	0	
$+25^{R}_{I}$	-.18533	.05	-.18533	.05	-.90939	-11.0
	-2.8668	.03	2.8668	.03	0	
$+50^{R}_{I}$	-.18537	.08	-.18537	.08	-.81951	-19.8
	-2.8675	.05	2.8675	.05	0	
$+100^{R}_{I}$	-.18538	.07	-.18536	.07	-.68425	-33.0
	-2.8685	.09	2.8685	.09	0	

TABLE 6D

LATERAL SENSITIVITY ANALYSIS OF ϕ NUMERATOR NON-DIMENSIONAL ROOTS FOR A GENERALIZED UNDERWATER VEHICLE, VARYING $Y'_{\dot{v}}$ ±100%

% VAR	ROOT 1	% CHANGE	ROOT 2	% CHANGE
-100^{R}_{I}	-2.1989	24.0	36.982	640.4
	0		0	
-50^{R}_{I}	-1.9349	9.1	8.2590	65.3
	0		0	
-25^{R}_{I}	-1.8462	4.1	6.1751	23.6
	0		0	
-10^{R}_{I}	-1.8010	1.6	5.4013	8.1
	0		0	
$BASE^{R}_{I}$	-1.7725		4.9963	*
	0		0	
$+10^{R}_{I}$	-1.7478	-1.4	4.6548	-6.8
	0		0	
$+25^{R}_{I}$	-1.7123	-3.5	4.2320	-15.3
	0		0	
$+50^{R}_{I}$	-1.6598	-6.4	3.6930	-26.1
	0		0	
$+100^{R}_{I}$	-1.5735	-11.3	2.9777	-40.4
	0		0	

% VAR	ROOT 2	% CHANGE
-96^{R}_{I}	28.230	
	0	
-92^{R}_{I}	22.924	
	0	
-88^{R}_{I}	19.363	
	0	
-84^{R}_{I}	16.805	
	0	
-80^{R}_{I}	14.878	
	0	
-70^{R}_{I}	11.654	
	0	
-60^{R}_{I}	9.6334	
	0	

* A third set of real and imaginary roots exists, which has a base ±100% variation value of zero.

(or stabilizers), rudders, canards, and shrouds. The contributions of these and any other surfaces that can be treated as flat plates in accelerated fluid flow normal to its surface can be calculated using Equation (18). It is repeated here for convenience.

$$m_a = \frac{k\pi\rho c^2 b}{4} \tag{18}$$

Since it is common to have unequal upper and lower vertical fins in the tail, the two will not be combined as were the two horizontal tail fins. The expressions for the upper and lower vertical tail fins are written as

$$Y'_{\dot{v}_{uvt(\ell vt)}} = -\frac{k\pi c^2 b}{2\ell^3} \quad .$$

If the rudder is an extension of the vertical tail fins, then it should be included in the area for calculation of c. If the rudder is separate, then it can be treated separately using the same expression.

Since the bowplanes have no significant vertical surface area, they do not contribute to $Y'_{\dot{v}}$. The shroud has the same projection in the vertical plane as in the horizontal plane, so

$$Y'_{\dot{v}_s} = Z'_{\dot{w}_{sh}} \quad .$$

The complete expression of $Y'_{\dot{v}}$ for a typical underwater vehicle is written

$$Y'_{\dot{v}} = Y'_{\dot{v}_b} + Y'_{\dot{v}_{uvt}} + Y'_{\dot{v}_{\ell vt}} + Y'_{\dot{v}_{sh}} \quad .$$

$\underline{Y'_{\dot{p}}}$

1. y-forces on a submerged vehicle that are due to angular acceleration in roll are represented in the equations of motion as $Y'_{\dot{p}}$.

2. This term can be significant on vehicles with large Z_{cb}/ℓ, Z_{uct}/ℓ, and $Z_{\ell ct}/\ell$ ratios, where

Z_{cb} = z-distance from body cg to cb

Z_{uct} = z-distance from the x-axis to the centroid of the upper vertical tail, and

$Z_{\ell ct}$ = z-distance from the x-axis to the centroid of the lower vertical tail.

Tables 7A through 7D present the results of a sensitivity analysis of nondimensional roots of the characteristic equation (transfer function denominator) and v, ψ, and ϕ (numerators) for a generalized underwater vehicle, varying $Y'_{\dot{p}}$ from -100 percent to +100 percent.

3. Due to intermodal coupling, $Y'_{\dot{p}} = K'_{\dot{v}}$ as shown in Equation (8). Since the conceptual description of the physical phenomenon causing $K'_{\dot{v}}$ moments is more easily understood than that for $Y'_{\dot{p}}$, only the equality relationship is given here; that is

4. $Y'_{\dot{p}} = K'_{\dot{v}}$ (See below).

$\underline{Y'_{\dot{r}}}$

1. When an angular acceleration in yaw results in a force in the y-direction, the y-force is represented in the equations of motion by the term $Y'_{\dot{r}}$. The longitudinal counterpart of $Y'_{\dot{r}}$ is $Z'_{\dot{q}}$.

2. Tables 8A through 8D present the results of a sensitivity analysis of nondimensional roots of the characteristic equation (transfer function denominator) and v, ψ, and ϕ (numerators) for a generalized underwater vehicle, varying $Y'_{\dot{r}}$ from -100 percent to +100 percent.

3. Intermodal coupling yields the relationships in Equation (8). That is,

4. $Y'_{\dot{r}} = N'_{\dot{v}}$.

$\underline{K'_{\dot{v}}}$

1. Rolling moment due to acceleration along the y-axis is termed $k'_{\dot{v}}$.

2. $K'_{\dot{v}}$ couples the roll and yaw motions of a vehicle. As a vehicle enters a turn, the changes in the drift angle, β, will appear as a change in the sway velocity, v; i.e., an acceleration $\dot{v}$. The rolling moment produced by $\dot{v}$ in this situation can be significant on a vehicle with unsymmetrical vertical fin arrangements, like a submarine's sail. Trajectory simulation and roll moment percent contribution plots in Figures 33 and 34 illustrate its significance to vehicular motion during a turn reversal maneuver. The root locus plot in Figure 35 illustrates the variation in the locations of the poles due to variation in $K'_{\dot{v}}$. Tables 9A through 9D present the results of a sensitivity analysis of nondimensional roots of the characteristic equation (transfer function denominator) and v, ψ, and ϕ (numerators) for a generalized underwater vehicle, varying $K'_{\dot{v}}$ from -100 percent to +100 percent.

(Text Continued on Page 50)

TABLE 7A

LATERAL SENSITIVITY ANALYSIS OF CHARACTERISTIC EQUATION NON-DIMENSIONAL ROOTS FOR A GENERALIZED UNDERWATER VEHICLE, VARYING $Y'_{\dot{p}}$ ±100%

% VAR	ROOT 1	% CHANGE	ROOT 2	% CHANGE	ROOT 3	% CHANGE	ROOT 4	% CHANGE
-100^R_I	-.18172	-1.0	-.18172	-1.0	-4.1983	.03	-.84664	-.06
	-2.8662	.24	2.8662	.24	0		0	
-50^R_I	-.18265	-.50	-.18265	-.50	-4.1977	.02	-.84690	-.03
	-2.8627	.12	2.8627	.12	0		0	
-25^R_I	-.18311	-.25	-.18311	-.25	-4.1973	.007	-.84704	-.02
	-2.8610	.06	2.8610	.06	0		0	
-10^R_I	-.18338	-.10	-.18338	-.10	-4.1971	.002	-.84711	-.007
	-2.8599	.02	2.8599	.02	0		0	
$BASE^R_I$	-.18357		-.18357		-4.1970		-.84717	*
	-2.8592		2.8592		0		0	
$+10^R_I$	-.18375	.10	-.18375	.10	-4.1969	-.002	-.84722	.006
	-2.8585	-.02	2.8585	-.02	0		0	
$+25^R_I$	-.18403	.25	-.18403	.25	-4.1967	-.007	-.84730	.02
	-2.8575	-.06	2.8575	-.06	0		0	
$+50^R_I$	-.18449	.50	-.18449	.50	-4.1964	-.01	-.84743	.03
	-2.8558	-.12	2.8558	-.12	0		0	
$+100^R_I$	-.18540	1.0	-.18540	1.0	-4.1957	-.03	-.84769	.06
	-2.8523	-.24	2.8523	-.24	0		0	

* A fifth set of real and imaginary roots exists, which has a base ±100% variation value of zero.

TABLE 7B

LATERAL SENSITIVITY ANALYSIS OF v NUMERATOR NON-DIMENSIONAL ROOTS FOR A GENERALIZED UNDERWATER VEHICLE, VARYING $Y'_{\dot{p}}$ ±100%

% VAR	ROOT 1	% CHANGE	ROOT 2	% CHANGE	ROOT 3	% CHANGE	ROOT 4	% CHANGE
-100^R_I	-.18354	3.4	-.13354	3.4	-6.3773	.71		
	-2.8728	.13	2.8738	.13	0			
-50^R_I	-.18054	1.7	-.18054	1.7	-6.3582	.36		
	-2.8720	.06	2.8720	.06	0			
-25^R_I	-.17905	.84	-.17905	.84	-6.3497	.18		
	-2.8711	.03	2.8711	.03	0			
-10^R_I	-.17815	.33	-.17815	.33	-6.3430	.07		
	-2.8706	.01	2.8706	.01	0			
$BASE^R_I$	-.17756		-.17756		-6.3392		0	
	-2.8702		2.8702		0		0	
$+10^R_I$	-.17696	-.34	-.17696	-.34	-6.3355	-.07		
	-2.8698	-.01	2.8698	-.01	0			
$+25^R_I$	-.17607	-.84	-.17607	-.84	-6.3299	-.17		
	-2.8693	-.03	2.8693	-.03	0			
$+50^R_I$	-.17459	-1.7	-.17459	-1.7	-6.3205	-.35		
	-2.8684	-.06	2.8684	-.06	0			
$+100^R_I$	-.17165	-3.3	-.17165	-3.3	-6.3020	-.70		
	-2.8666	-.13	2.8666	-.13	0			

TABLE 7C

LATERAL SENSITIVITY ANALYSIS OF ϕ NUMERATOR NON-DIMENSIONAL ROOTS FOR A GENERALIZED UNDERWATEK VEHICLE, VARYING $Y'_{\dot{p}}$ ±100%

% VAR	ROOT 1	% CHANGE	ROOT 2	% CHANGE	ROOT 3	% CHANGE
-100^R_I	-.18354	-.91	-.18354	-.91	-1.0207	-.07
	-2.8734	.26	2.8734	.26	0	
-50^R_I	-.18438	-.46	-.18438	-.46	-1.0211	-.03
	-2.8697	.13	2.8697	.13	0	
-25^R_I	-.18481	-.23	-.18481	-.23	-1.0212	-.02
	-2.8678	.06	2.8678	.06	0	
-10^R_I	-.18506	-.09	-.18506	-.09	-1.0213	-.01
	-2.8667	.02	2.8667	.02	0	
$BASE^R_I$	-.18523		-.18523		-1.0214	
	-2.8660		2.8660		0	
$+10^R_I$	-.18539	.09	-.18539	.09	-1.0215	.01
	-2.8652	-.03	2.8652	-.03	0	
$+25^R_I$	-.18565	.23	-.18565	.23	-1.0216	.02
	-2.8641	-.07	2.8641	-.07	0	
$+50^R_I$	-.18606	.45	-.18606	.45	-1.0217	.03
	-2.8623	-.13	2.8623	-.13	0	
$+100^R_I$	-.18690	.90	-.18690	.90	-1.0221	.07
	-2.8586	-.26	2.8586	-.26	0	

TABLE 7D

LATERAL SENSITIVITY ANALYSIS OF ϕ NUMERATOR NON-DIMENSIONAL ROOTS FOR A GENERALIZED UNDERWATER VEHICLE, VARYING $Y'_{\dot{p}}$ ±100%

% VAR	ROOT 1	% CHANGE	ROOT 2	% CHANGE	ROOT 3	% CHANGE
-100^R_I						
-50^R_I						
-25^R_I						
-10^R_I						
$BASE^R_I$	-1.7735		4.9963		0	
	0		0		0	
$+10^R_I$						
$+25^R_I$						
$+50^R_I$						
$+100^R_I$						

TABLE 8A

LATERAL SENSITIVITY ANALYSIS OF CHARACTERISTIC EQUATION NON-DIMENSIONAL ROOTS FOR A GENERALIZED UNDERWATER VEHICLE, VARYING Y'_r ±100%

% VAR	ROOT 1	% CHANGE	ROOT 2	% CHANGE	ROOT 3	% CHANGE	ROOT 4	% CHANGE
-100^R_I	-.18348 -2.8593	-.05 .003	-.18348 2.8593	-.05 .003	-4.1890 0	-.19	-.84248 0	.15
-50^R_I	-.18352 -2.8593	-.03 .003	-.18352 2.8593	-.03 .003	-4.1930 0	-.10	-.84782 0	.08
-25^R_I	-.18355 -2.8592	-.01 0	-.18355 2.8592	-.01 0	-4.1950 0	-.05	-.84749 0	.04
-10^R_I	-.18356 -2.8592	-.005 0	-.18356 2.8592	-.005 0	-4.1962 0	-.02	-.84730 0	.02
BASE^R_I	-.18357 -2.8592		-.18357 2.8592		-4.1970 0		-.84717 0	
$+10^R_I$	-.18358 -2.8592	.005 0	-.18358 -2.8592	.005 0	-4.1978 0	.02	-.84704 0	-.02
$+25^R_I$	-.18359 -2.8592	.01 0	-.18359 2.8592	.01 0	-4.1990 0	.05	-.84684 0	-.04
$+50^R_I$	-.18361 -2.8592	.02 0	-.18361 2.8592	.02 0	-4.2010 0	.10	-.84651 0	-.08
$+100^R_I$	-.18366 -2.8592	.05 0	-.18366 2.8592	.05 0	-4.2050 0	.19	-.84586 0	-.15

* *A fifth set of real and imaginary roots exists, which has a base ±100% variation value of zero.*

TABLE 8B

LATERAL SENSITIVITY ANALYSIS OF V NUMERATOR NON-DIMENSIONAL ROOTS FOR A GENERALIZED UNDERWATER VEHICLE, VARYING Y'_r ±100%

% VAR	ROOT 1	% CHANGE	ROOT 2	% CHANGE	ROOT 3	% CHANGE	ROOT 4	% CHANGE
-100^R_I	-.17767 -2.8701	.06 .003	-.17767 2.8701	.06 -.003	-5.1303 0	-3.9		
-50^R_I	-.17762 -2.8702	.03 0	-.17762 2.8702	.03 0	-5.2327 0	-2.0		
-25^R_I	-.17759 -2.8702	.02 0	-.17759 2.8702	.02 0	-5.2854 0	-1.0		
-10^R_I	-.17757 -2.8702	.006 0	-.17757 2.8702	.006 0	-5.3176 0	-.40		
BASE^R_I	-.17756 -2.8702		-.17756 2.8702		-5.3392 0		0 0	
$+10^R_I$	-.17755 -2.8702	-.006 0	-.17755 2.8702	-.006 0	-5.3611 0	.41		
$+25^R_I$	-.17753 -2.8702	-.02 0	-.17753 2.8702	-.02 0	-5.3942 0	1.0		
$+50^R_I$	-.17750 -2.8702	-.03 0	-.17750 2.8702	-.03 0	-5.4502 0	2.1		
$+100^R_I$	-.17744 -2.8703	-.07 .003	-.17744 2.8703	-.07 .003	-5.5653 0	4.2		

TABLE 8C

LATERAL SENSITIVITY ANALYSIS OF ϕ NUMERATOR NON-DIMENSIONAL ROOTS FOR A GENERALIZED UNDERWATER VEHICLE, VARYING Y'_r ±100%

% VAR	ROOT 1	% CHANGE	ROOT 2	% CHANGE	ROOT 3	% CHANGE
-100^R_I						
-50^R_I						
-25^R_I						
-10^R_I						
BASE^R_I	-.19523 -2.8660		-.18523 2.8660		-1.0214 0	
$+10^R_I$						
$+25^R_I$						
$+50^R_I$						
$+100^R_I$						

TABLE 8D

LATERAL SENSITIVITY ANALYSIS OF ϕ NUMERATOR NON-DIMENSIONAL ROOTS FOR A GENERALIZED UNDERWATER VEHICLE, VARYING Y'_r ±100%

% VAR	ROOT 1	% CHANGE	ROOT 2	% CHANGE	ROOT 3	% CHANGE
-100^R_I	-1.7688 0	-.27	5.1823 0	3.7		
-50^R_I	-1.7711 0	-.14	5.0877 0	1.8		
-25^R_I	-1.7723 0	-.07	5.0418 0	.91		
-10^R_I	-1.7730 0	-.03	5.0163 0	.36		
BASE^R_I	-1.7735 0		4.9963 0		0 0	
$+10^R_I$	-1.7739 0	.02	4.9783 0	-.36		
$+25^R_I$	-1.7746 0	.06	4.9517 0	-.89		
$+50^R_I$	-1.7758 0	.13	4.9079 0	-1.8		
$+100^R_I$	-1.7781 0	.26	4.8224 0	-3.5		

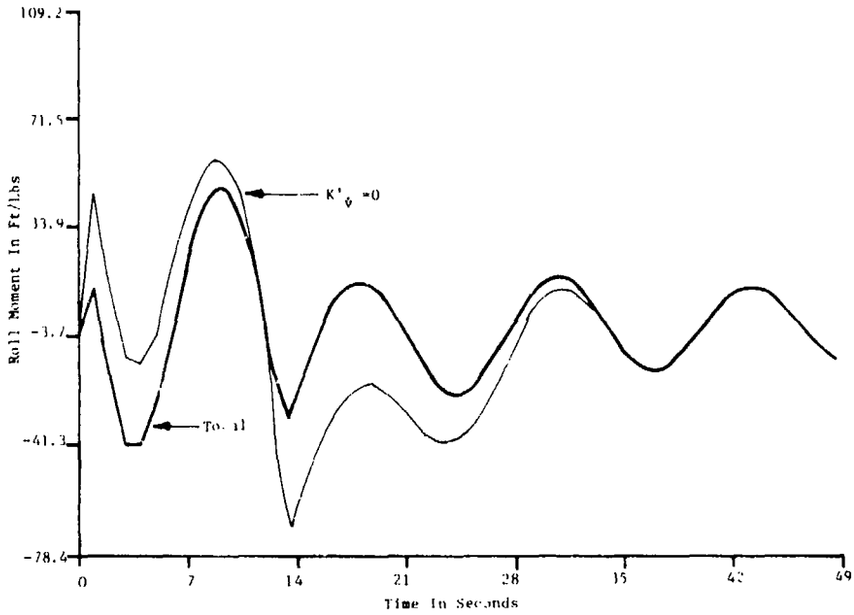

FIGURE 33. TRAJECTORY SIMULATION PLOT OF $K'_{\dot{v}}$ CONTRIBUTION TO ROLL MOMENT DURING A δ_r = ±30° TURN REVERSAL MANEUVER

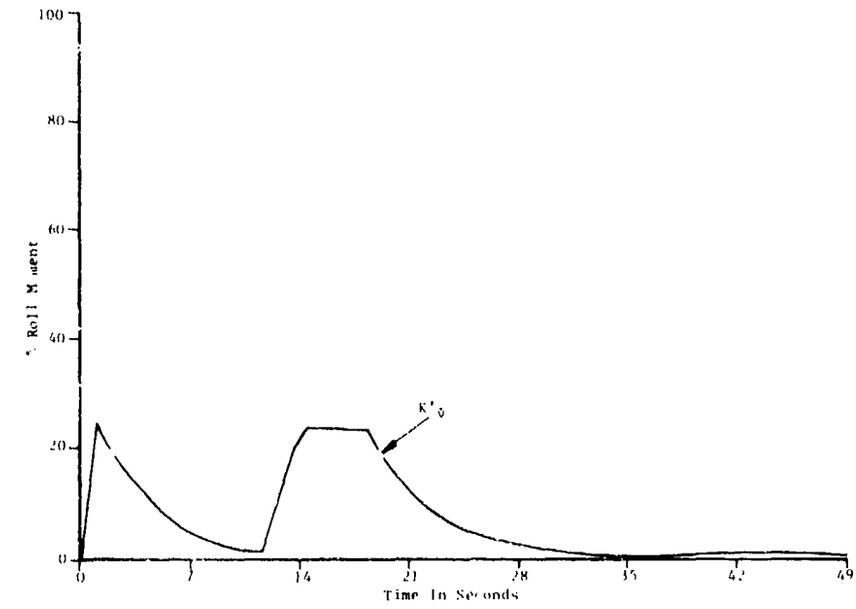

FIGURE 34. PERCENT CONTRIBUTION OF $K'_{\dot{v}}$ TO ROLL MOMENT DURING A δ_r = ±30° TURN REVERSAL MANEUVER

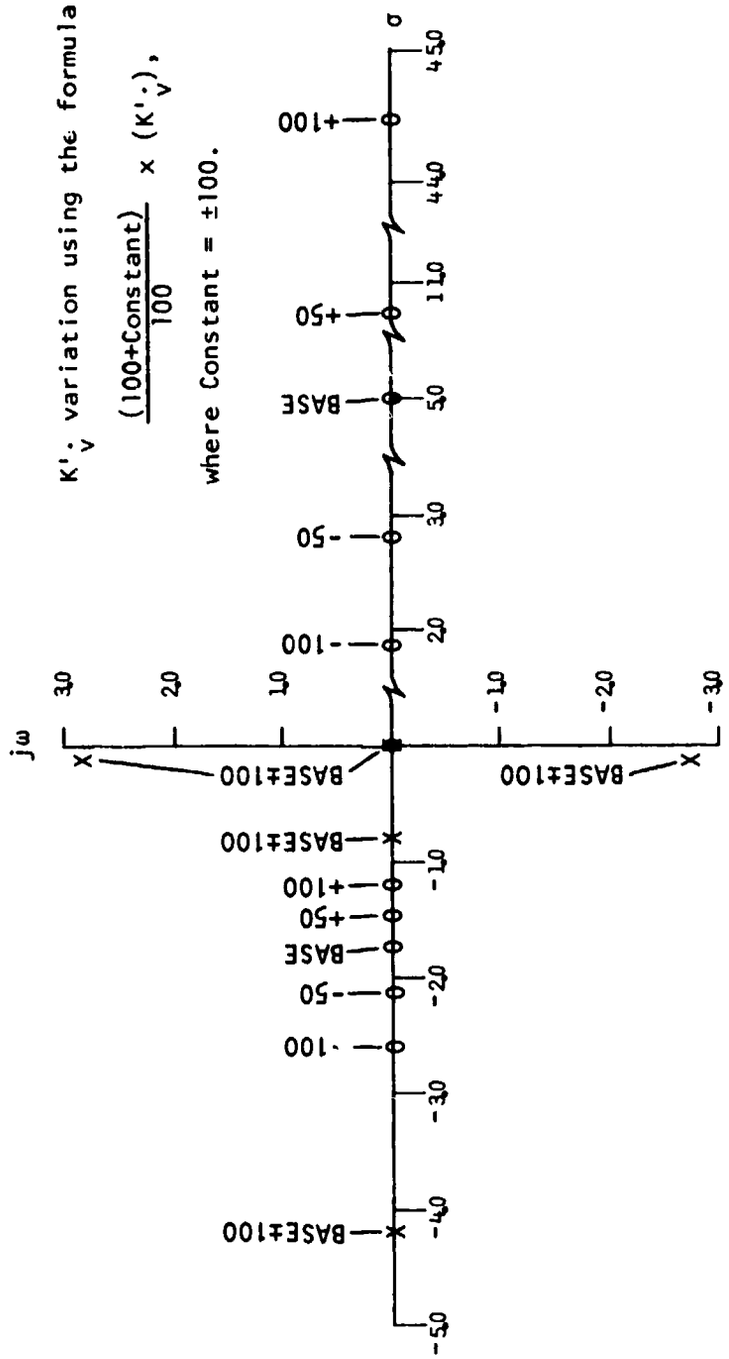

FIGURE 35. ROOT LOCUS PLOT OF ϕ/δ_r FOR A GENERALIZED UNDERWATER VEHICLE, VARYING K'_v.

TABLE 9A

LATERAL SENSITIVITY ANALYSIS OF CHARACTERISTIC EQUATION NON-DIMENSIONAL ROOTS FOR A GENERALIZED UNDERWATER VEHICLE, VARYING K'_v ±100%

% VAR	ROOT 1	% CHANGE	ROOT 2	% CHANGE	ROOT 3	% CHANGE	ROOT 4	% CHANGE
-100	-.19159	4.4	-.19159	4.4	-4.1960	-.05	-.84354	.16
	-2.8635	.15	2.8635	.15	0		0	
-50	-.18757	2.2	-.18757	2.2	-4.1960	-.02	-.84785	.08
	-2.8613	.07	2.8613	.07	0		0	
-25	-.18557	1.1	-.18557	1.1	-4.1965	-.01	-.84751	.04
	-2.8603	.04	2.8603	.04	0		0	
-10	-.18437	.44	-.18437	.44	-4.1958	-.005	-.84320	.02
	-2.8596	.01	2.8596	.01	0		0	
BASE	-.18357		-.18357		-4.1970		-.84717	
	-2.8592		2.8592		0		0	
+10	-.18277	-.44	-.18277	-.44	-4.1972	.005	-.84703	-.02
	-2.8588	-.01	2.8588	-.01	0		0	
+25	-.18158	-1.1	-.18158	-1.1	-4.1975	.01	-.84682	-.04
	-2.8582	-.03	2.8582	-.03	0		0	
+50	-.17958	-2.2	-.17959	-2.2	-4.1980	.02	-.84642	-.08
	-2.8571	-.07	2.8571	-.07	0		0	
+100	-.17562	-4.3	-.17562	-4.3	-4.1990	.05	-.84580	-.16
	-2.8550	-.15	2.8550	-.15	0		0	

* A fifth set of real and imaginary roots exists, which has a base ±100% variation value of zero.

TABLE 9B

LATERAL SENSITIVITY ANALYSIS OF V NUMERATOR NON-DIMENSIONAL ROOTS FOR A GENERALIZED UNDERWATER VEHICLE, VARYING Y'_v ±100%

% VAR	ROOT 1	% CHANGE	ROOT 2	% CHANGE	ROOT 3	% CHANGE	ROOT 4	% CHANGE
-100								
-50								
-25								
-10								
BASE	-.17756		-.17756		-5.3392		0	
	-2.8702		2.8702		0		0	
+10								
+25								
+50								
+100								

TABLE 9C

LATERAL SENSITIVITY ANALYSIS OF ψ NUMERATOR NON-DIMENSIONAL ROOTS FOR A GENERALIZED UNDERWATER VEHICLE, VARYING K'_v ±100%

% VAR	ROOT 1	% CHANGE	ROOT 2	% CHANGE	ROOT 3	% CHANGE
-100	-.18836	1.7	-.18836	1.7	-1.0220	.06
	-2.8715	.19	2.8715	.19	0	
-50	-.18679	.84	-.18679	.84	-1.0217	.03
	-2.8637	.09	2.8637	.09	0	
-25	-.18601	.42	-.18601	.42	-1.0215	.01
	-2.8674	.05	2.8674	.05	0	
-10	-.18554	.17	-.18554	.17	-1.0215	.01
	-2.8665	.02	2.8665	.02	0	
BASE	-.18523		-.18523		-1.0214	
	-2.8665		2.8660		0	
+10	-.18491	-.17	-.18491	-.17	-1.0213	-.01
	-2.8654	-.02	2.8654	-.02	0	
+25	-.18445	-.42	-.18445	-.42	-1.0212	-.02
	-2.8646	-.05	2.8648	-.05	0	
+50	-.18367	-.84	-.18367	-.84	-1.0211	-.03
	-2.8632	-.17	2.8632	-.10	0	
+100	-.18212	-1.7	-.18212	-1.7	-1.0208	-.06
	-2.8605	-.19	2.8605	-.19	0	

TABLE 9D

LATERAL SENSITIVITY ANALYSIS OF ϕ NUMERATOR NON-DIMENSIONAL ROOTS FOR A GENERALIZED UNDERWATER VEHICLE, VARYING K'_v ±100%

% VAR	ROOT 1	% CHANGE	ROOT 2	% CHANGE
-100	-2.5597	44.3	1.8986	-62.0
	0		0	
-50	-2.1734	22.5	2.8880	-42.2
	0		0	
-25	-1.9719	11.2	3.7285	-25.4
	0		0	
-10	-1.8520	4.4	4.4205	-11.5
	0		0	
BASE	-1.7735		4.9963	
	0		0	
+10	-1.6986	-4.3	5.6911	13.9
	0		0	
+25	-1.5854	-10.6	7.0373	40.9
	0		0	
+50	-1.4135	-20.3	10.654	113.2
	0		0	
+100	-1.1287	-36.4	44.415	783.0
	0		0	

% VAR	ROOT 2	% CHANGE
+60	12.969	
	0	
+70	16.211	
	0	
+80	21.049	
	0	
+84	23.717	
	0	
+88	27.028	
	0	
+92	31.245	
	0	
+96	36.792	
	0	

* A third set of real and imaginary roots exists, which has a base ±100% variation value of zero.

3. & 4. This coefficient is evaluated in a similar fashion to that of $M'_{\dot{w}}$. It is the representation of added mass effects acting on moment arms from the cg.

$$K'_{\dot{v}_b} = -Y'_{\dot{v}_b} \frac{Z_{cb}}{\ell} .$$

As noted before, it is not uncommon for the upper and lower vertical tail fins to be of different size and shape. Also, since the cg is generally below the body axis of symmetry, there are unequal moment arms to the centroids of the upper and lower fins even if the fins are symmetric about the center line. The vertical tail surfaces' contribution to $K'_{\dot{v}}$ is written

$$K'_{\dot{v}_t} = -\frac{1}{\ell} \{Y'_{\dot{v}_{uvt}} Z_{uct} + Y'_{\dot{v}_{\ell vt}} Z_{\ell ct}\}$$

$$= K'_{\dot{v}_{uvt}} + K'_{\dot{v}_{\ell vt}} .$$

Z_{uct} = distance from the x-axis to the centroid of the upper vertical tail

$Z_{\ell ct}$ = distance from the x-axis to the centroid of the lower vertical tail.

Note: The vertical tail fins are assumed to lie in the xz-plane.

The complete expression, then, is written

$$K'_{\dot{v}} = K'_{\dot{v}_b} + K'_{\dot{v}_t} .$$

Any other vertical surfaces that can be approximated as flat plates lying in the xz-plane can be treated similarly to the upper and lower vertical tail surfaces.

$\underline{K'_{\dot{p}}}$

1. Moments additional to the I_x moment of inertia resisting angular acceleration in roll are included in the term $K'_{\dot{p}}$. This added moment of inertia is one that has no Lamb coefficient[1] for the body contribution. This is because a homogeneous body of revolution can rotate about its axis of symmetry and not experience any forces from an inviscid fluid.

---

[1] ibid.

2. Tables 10A through 10D present the results of a sensitivity analysis of nondimensional roots of the characteristic equation (transfer function denominator) and v, ψ, and ϕ (numerators) for a generalized underwater vehicle, varying $K'_{\dot{p}}$ from -100 percent to +100 percent.

3. Since $\dot{p}$, angular acceleration in roll, is defined about the x-axis passing through the cg, there will be some added moment effect of the body due to an added mass effect acting at the cb. It is written as

$$K'_{\dot{p}_b} = Y'_{\dot{v}_b} \frac{Z^2_{cb}}{\ell^2} .$$

Any surface projecting radially from the vehicle (such as tail fins, bowplanes, etc.) will contribute to the added moment effect represented by $K'_{\dot{p}}$. Each surface contributes in two ways. One is as an added mass acting on a moment arm from the x-axis. The general form for this is the same as the body contribution above. Considering any "flat plate" surface, such as the upper vertical tail fin, this term would be written

$$K'_{\dot{p}_{uvt}} = Y'_{\dot{v}_{uvt}} \frac{Z^2_{uct}}{\ell^2} .$$

The other form of contribution to $K'_{\dot{p}}$ is by the individual added moment of inertia of the flat plate rotating about an axis parallel to the x-axis but passing through the centroid of the flat plate. Again, we turn to Malvestuto and Gale[6] for experimental data on flat plates with varying dihedral angle and taper ratio. For rotation about an axis in the plane of the plate, parallel to the chord, and passing through the centroid, the equation is

$$I_{x_a} = - \frac{\pi\rho}{48} D_\lambda D_\Gamma k'_p c^2 b^3$$

where k'_p is the coefficient of added moment of inertia for a flat plate plotted in Figure 25, D_λ is the correction factor for taper ratio plotted in Figure 36, and D_Γ is the correction factor for dihedral angle plotted in Figure 37. Thus, for any "flat plate" surface such as the upper vertical tail fin

$$K'_{\dot{p}_{uvt}} = \frac{1}{\frac{1}{2}\rho\ell^5} I_{x_a} + Y'_{\dot{v}} \frac{Z^2_{uct}}{\ell^2} .$$

---

[6] ibid.

(Text Continued on Page 54)

TABLE 10A

LATERAL SENSITIVITY ANALYSIS OF CHARACTERISTIC EQUATION NON-DIMENSIONAL ROOTS FOR A GENERALIZED UNDERWATER VEHICLE, VARYING K'_p ±100%

% VAR	ROOT 1	% CHANGE	ROOT 2	% CHANGE	ROOT 3	% CHANGE	ROOT 4	% CHANGE
-100^R_I	- .18551 -2.8740	1.1 .52	- .18551 2.8740	1.1 .52	-4.1971 0	.002		
-50^R_I	- .18453 -2.8666	.52 .26	- .18453 2.8666	.52 .26	-4.1971 0	.002		
-25^R_I	- .18405 -2.8629	.26 .13	- .18405 2.8629	.26 .13				
-10^R_I	- .18376 -2.8607	.10 .05	- .18376 2.8607	.10 .05				
$BASE^R_I$	- .18357 -2.8592		- .18357 2.8592		-4.1970 0		- .84717 0	*
$+10^R_I$	- .18338 -2.8578	- .10 - .05	- .18338 2.8578	- .10 - .05				
$+25^R_I$	- .18309 -2.8556	- .26 - .13	- .18309 2.8556	- .26 - .13				
$+50^R_I$	- .18261 -2.8519	- .52 - .26	- .18261 2.8519	- .52 - .26				
$+100^R_I$	- .18167 -2.8447	-1.0 - .51	- .18167 2.8447	-1.0 - .51	-4.1969 0	-.002	- .84716 0	-.001

* A fifth set of real and imaginary roots exists, which has a base ±100% variation value of zero.

TABLE 10B

LATERAL SENSITIVITY ANALYSIS OF V NUMERATOR NON-DIMENSIONAL ROOTS FOR A GENERALIZED UNDERWATER VEHICLE, VARYING K'_p ±100%

% VAR	ROOT 1	% CHANGE	ROOT 2	% CHANGE	ROOT 3	% CHANGE	ROOT 4	% CHANGE
-100^R_I	- .17936 -2.8851	1.0 .52	- .17936 2.8851	1.0 .52	-5.3389 0	-.006		
-50^R_I	- .17846 -2.8776	.51 .26	- .17846 2.8776	.51 .26	-5.3391 0	-.002		
-25^R_I	- .17801 -2.8739	.25 .13	- .17801 2.8739	.25 .13				
-10^R_I	- .17774 -2.8717	.10 .05	- .17774 2.8717	.10 .05				
$BASE^R_I$	- .17756 -2.8702		- .17756 2.8702		-5.3392 0		0 0	
$+10^R_I$	- .17738 -2.8687	- .10 - .05	- .17738 2.8687	- .10 - .05	-5.3393 0	.002		
$+25^R_I$	- .17711 -2.8665	- .25 - .13	- .17711 2.8665	- .25 - .13				
$+50^R_I$	- .17667 -2.8628	- .50 - .26	- .17667 2.8628	- .50 - .26	-5.3394 0	.004		
$+100^R_I$	- .17579 -2.8555	-1.0 - .51	- .17579 2.8555	-1.0 - .51	-5.3396 0	.007		

TABLE 10C

LATERAL SENSITIVITY ANALYSIS OF ψ NUMERATOR NON-DIMENSIONAL ROOTS FOR A GENERALIZED UNDERWATER VEHICLE, VARYING K'_p ±100%

% VAR	ROOT 1	% CHANGE	ROOT 2	% CHANGE	ROOT 3	% CHANGE
-100^R_I	- .18716 -2.8808	1.0 .52	- .18716 2.8808	1.0 .52		
-50^R_I	- .18619 -2.8734	.52 .26	- .18619 2.8734	.52 .26		
-25^R_I	- .18571 -2.8697	.26 .13	- .18571 2.8697	.26 .13		
-10^R_I	- .18542 -2.8675	.10 .05	- .18542 2.8675	.10 .05		
$BASE^R_I$	- .18523 -2.8660		- .18523 2.8660		-1.0214 0	
$+10^R_I$	- .18503 -2.8645	- .11 - .05	- .18503 2.8645	- .11 - .05		
$+25^R_I$	- .18475 -2.8623	- .26 - .13	- .18475 2.8623	- .26 - .13		
$+50^R_I$	- .18427 -2.8587	- .52 - .25	- .18427 2.8587	- .52 - .25		
$+100^R_I$	- .18333 -2.8514	-1.0 - .51	- .18333 2.8514	-1.0 - .51		

TABLE 10D

LATERAL SENSITIVITY ANALYSIS OF ϕ NUMERATOR NON-DIMENSIONAL ROOTS FOR A GENERALIZED UNDERWATER VEHICLE, VARYING K'_p ±100%

% VAR	ROOT 1	% CHANGE	ROOT 2	% CHANGE	ROOT 3	% CHANGE
-100^R_I						
-50^R_I						
-25^R_I						
-10^R_I						
$BASE^R_I$	-1.7735 0		4.9963 0		0 0	
$+10^R_I$						
$+25^R_I$						
$+50^R_I$						
$+100^R_I$						

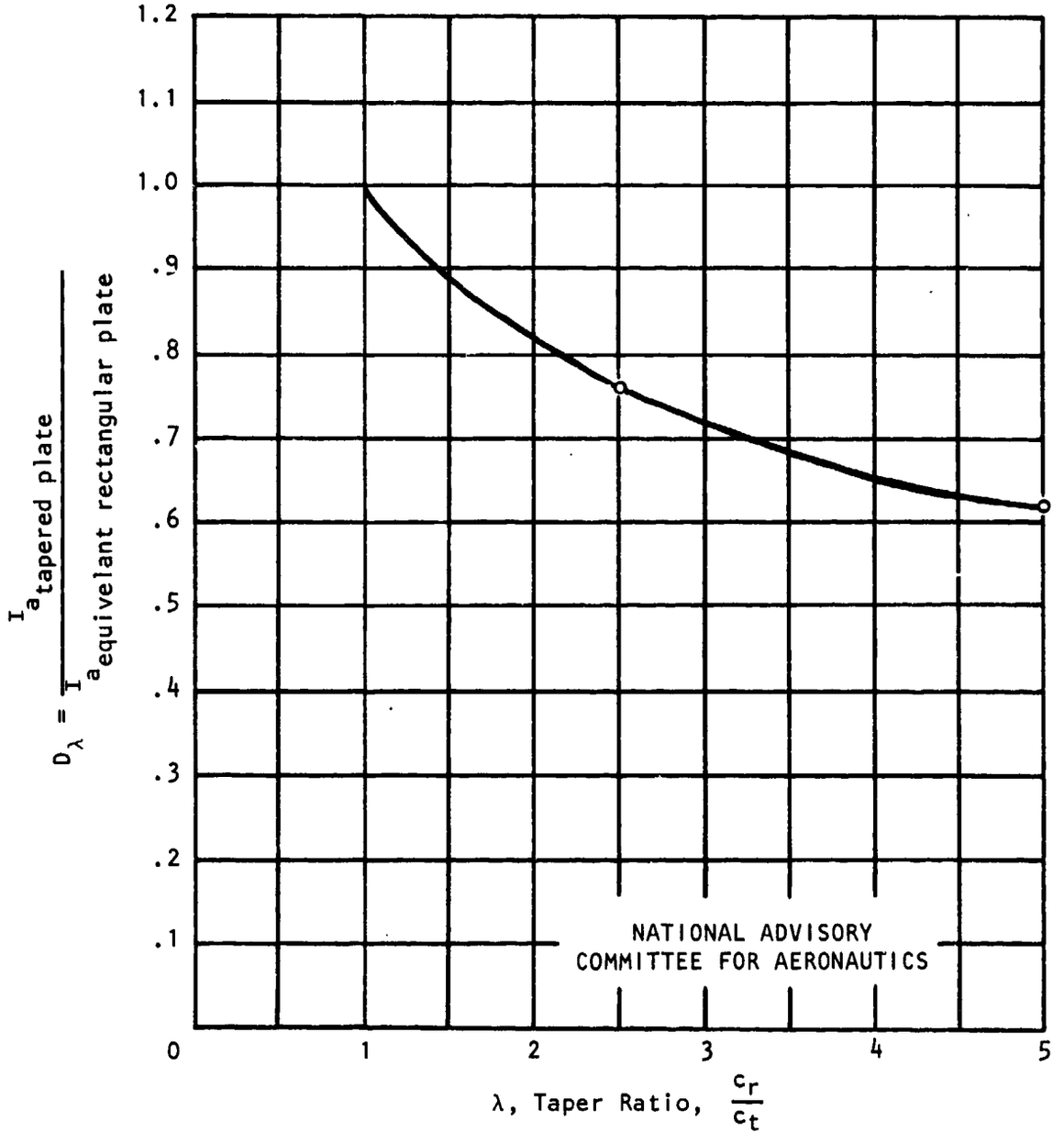

FIGURE 36. DEPENDENCE OF THE ADDITIONAL MOMENT OF INERTIA ON TAPER RATIO

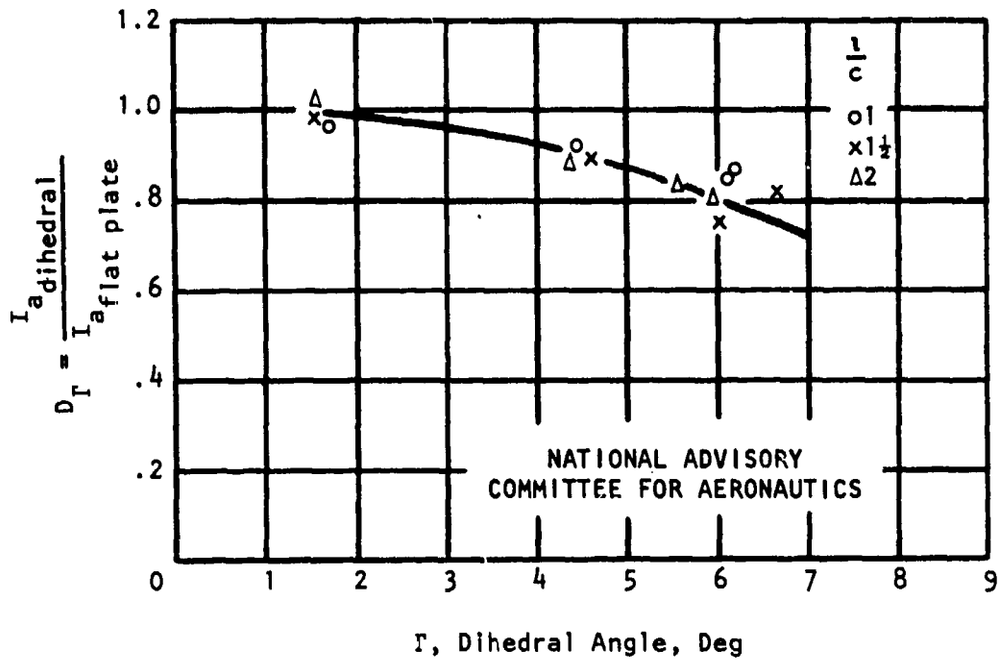

FIGURE 37. VARIATION OF THE ADDITIONAL MOMENTS OF INERTIA OF A SINGLE PLATE WITH DIHEDRAL ANGLE

The first term is often negligible compared to the second. The complete expression for a common vehicle would be

$$K'_{\dot{p}} = K'_{\dot{p}_b} + K'_{\dot{p}_{uvt}} + K'_{\dot{p}_{\ell vt}} .$$

$K'_{\dot{r}}$

1. Rolling moments caused by angular accelerations in yaw are represented by $K'_{\dot{r}}$.

2. Tables 11A through 11D present the results of a sensitivity analysis of nondimensional roots of the characteristic equation (transfer function denominator) and v, ψ, and ϕ (numerators) for a generalized underwater vehicle, varying $K'_{\dot{r}}$ from -100 percent to +100 percent.

3. $K'_{\dot{r}}$ arises in the same manner as the $K'_{\dot{v}}\dot{v}$ term except that the linear acceleration normal to the vertical surfaces is the result of an angular acceleration in yaw acting about the z-axis.

(Text Continued on Page 56)

TABLE 11A

LATERAL SENSITIVITY ANALYSIS OF CHARACTERISTIC EQUATION NON-DIMENSIONAL ROOTS FOR A GENERALIZED UNDERWATER VEHICLE, VARYING K'_{Y_r} ±100%

% VAR	ROOT 1	% CHANGE	ROOT 2	% CHANGE	ROOT 3	% CHANGE	ROOT 4	% CHANGE
-100^R_I	-.18346 -2.8594	-.06 .007	-.18346 2.8594	-.06 .007	-4.1966 0	-.01	-.84716 0	
-50^R_I	-.18351 -2.8593	-.03 .003	-.18351 2.8593	-.03 .003	-4.1968 0	-.005	-.84716 0	-.001
-25^R_I	-.18354 -2.8593	-.02 .003	-.18354 2.8593	-.02 .003	-4.1969 0	-.002		
-10^R_I	-.18356 -2.8592	-.005 0	-.18356 2.8592	-.005 0	-4.1970 0	0		
$BASE^R_I$	-.18357 -2.8592		-.18357 2.8592		-4.1970 0		-.84717 0	
$+10^R_I$	-.18358 -2.8592	.005 0	-.18358 2.8592	.005 0	-4.1971 0	.002		
$+25^R_I$	-.18360 -2.8592	.02 0	-.18360 2.8592	.02 0	-4.1971 0	.002		
$+50^R_I$	-.18362 -2.8591	.03 -.003	-.18362 2.8591	.03 -.003	-4.1972 0	.005		
$+100^R_I$	-.18368 -2.8590	.06 -.007	-.18368 2.8590	.06 -.007	-4.1975 0	.01		

* A fifth set of real and imaginary roots exists, which has a base ±100% variation value of zero.

TABLE 11B

LATERAL SENSITIVITY ANALYSIS OF V NUMERATOR NON-DIMENSIONAL ROOTS FOR A GENERALIZED UNDERWATER VEHICLE, VARYING K'_{Y_r} ±100%

% VAR	ROOT 1	% CHANGE	ROOT 2	% CHANGE	ROOT 3	% CHANGE	ROOT 4	% CHANGE
-100^R_I	-.17781 -2.9703	.14 .003	-.17781 2.9703	.14 .003	-6.3409 0	.03		
-50^R_I	-.17769 -2.9702	.07 0	-.17769 2.9702	.07 0	-6.3401 0	.02		
-25^R_I	-.17762 -2.9702	.03 0	-.17762 2.9702	.03 0	-6.3397 0	.009		
-10^R_I	-.17758 -2.9702	.01 0	-.17758 2.9702	.01 0	-6.3394 0	.004		
$BASE^R_I$	-.17756 -2.9702		-.17756 2.9702		-6.3392 0		0 0	
$+10^R_I$	-.17753 -2.9702	-.02 0	-.17753 2.9702	-.02 0	-6.3391 0	-.002		
$+25^R_I$	-.17749 -2.9702	-.04 0	-.17749 2.9702	-.04 0	-6.3388 0	-.007		
$+50^R_I$	-.17743 -2.9702	-.07 0	-.17743 2.9702	-.07 0	-6.3384 0	-.01		
$+100^R_I$	-.17730 -2.9701	-.15 -.003	-.17730 2.9701	-.15 -.003	-6.3376 0	-.03		

TABLE 11C

LATERAL SENSITIVITY ANALYSIS OF ψ NUMERATOR NON-DIMENSIONAL ROOTS FOR A GENERALIZED UNDERWATER VEHICLE, VARYING K'_{Y_r} ±100%

% VAR	ROOT 1	% CHANGE	ROOT 2	% CHANGE	ROOT 3	% CHANGE
-100^R_I						
-50^R_I						
-25^R_I						
-10^R_I						
$BASE^R_I$	-.18523 -2.8660		-.18523 2.8609		-1.0214 0	
$+10^R_I$						
$+25^R_I$						
$+50^R_I$						
$+100^R_I$						

TABLE 11D

LATERAL SENSITIVITY ANALYSIS OF ϕ NUMERATOR NON-DIMENSIONAL ROOTS FOR A GENERALIZED UNDERWATER VEHICLE, VARYING K'_{Y_r} ±100%

% VAR	ROOT 1	% CHANGE	ROOT 2	% CHANGE	ROOT 3	% CHANGE
-100^R_I	-1.7874 0	.78	5.3241 0	6.6		
-50^R_I	-1.7803 0	.38	5.1545 0	3.2		
-25^R_I	-1.7769 0	.19	5.0740 0	1.6		
-10^R_I	-1.7746 0	.07	5.0271 0	.62		
$BASE^R_I$	-1.7735 0		4.9963 0		0 0	
$+10^R_I$	-1.7721 0	-.08	4.9659 0	-.61		
$+25^R_I$	-1.7701 0	-.19	4.9211 0	-1.5		
$+50^R_I$	-1.7668 0	-.38	4.8483 0	-3.0		
$+100^R_I$	-1.7602 0	-.75	4.7036 0	-5.7		

$$K'_{\dot{r}} = K'_{\dot{v}_{uvt}} \frac{(X_{nuvt} - X_{ncg})}{\ell} + K'_{\dot{v}_{\ell vt}} \frac{(X_{n\ell vt} - X_{ncg})}{\ell}$$

where

X_{nuvt} = distance from nose to upper vertical tail surface centroid, positive aft

$X_{n\ell vt}$ = distance from nose to lower vertical tail surface centroid, positive aft.

$N'_{\dot{v}}$

1. Linear accelerations in the y-direction causing yawing moments give rise to the stability derivative $N'_{\dot{v}}$ to describe these resulting moments.

2. Tables 12a through 12D present the results of a sensitivity analysis of nondimensional roots of the characteristic equation (transfer function denominator) and v, ψ, and ϕ (numerators) for a generalized underwater vehicle, varying $N'_{\dot{v}}$ from -100 percent to +100 percent.

3. Primarily due to the vertical tail surfaces, a vehicle changing drift angle will experience a restoring force proportional to $\dot{v}$ (resulting from $\dot{\beta}$). $N'_{\dot{v}}$ is the term representing this force.

4. $$N'_{\dot{v}_b} = -Y'_{\dot{v}_b} \frac{(X_{ncb} - X_{ncg})}{\ell}$$

$$N'_{\dot{v}_t} = -Y'_{\dot{v}_{uvt}} \frac{(X_{nuvt} - X_{ncg})}{\ell} - Y'_{\dot{v}_{\ell vt}} \frac{(X_{n\ell vt} - X_{ncg})}{\ell} .$$

$N'_{\dot{p}}$

1. Yawing moments caused by angular accelerations in roll are represented in the vehicular equation of motion by $N'_{\dot{p}}$.

2. Tables 13A through 13D present the results of a sensitivity analysis of nondimensional roots of the characteristic equation (transfer function denominator) and v, ψ, and ϕ (numerators) for a generalized underwater vehicle, varying $N'_{\dot{p}}$ from -100 percent to +100 percent.

3. & 4. Equation (9) shows

$$N'_{\dot{p}} = K'_{\dot{r}} .$$

(Text Continued on Page 59)

TABLE 12A

LATERAL SENSITIVITY ANALYSIS OF CHARACTERISTIC EQUATION NON-DIMENSIONAL ROOTS FOR A GENERALIZED UNDERWATER VEHICLE, VARYING $N'_{\dot{v}}$ ±100%

% VAR	ROOT 1	% CHANGE	ROOT 2	% CHANGE	ROOT 3	% CHANGE	ROOT 4	% CHANGE
-100^R_I	-.18352 -2.8591	-.02 -.003	-.18353 2.8591	-.02 -.003	-4.1855 0	-.27	-.84530 0	.25
-50^R_I	-.18355 -2.8592	-.01 0	-.18355 2.8592	-.01 0	-4.1913 0	-.14	-.84623 0	.13
-25^R_I	-.18356 -2.8592	-.005 0	-.18356 2.8592	-.005 0	-4.1941 0	-.07	-.84770 0	.06
-10^R_I	-.18356 -2.8592	-.005 0	-.18356 2.8592	-.005 0	-4.1959 0	-.03	-.84738 0	.02
$BASE^R_I$	-.18357 -2.8592		-.18357 2.8592		-4.1970 0		-.84717 0	
$+10^R_I$	-.1835 -2.8592	0 0	-.18357 2.8592	0 0	-4.1982 0	.03	-.84695 0	-.03
$+25^R_I$	-.18358 -2.8593	.005 .003	-.18358 2.8593	.005 .003	-4.1999 0	.07	-.84664 0	-.06
$+50^R_I$	-.18359 -2.8593	.01 .003	-.18359 2.8593	.01 .003	-4.2028 0	.14	-.84610 0	-.13
$+100^R_I$	-.18361 -2.8593	.02 .003	-.18361 2.8593	.02 .003	-4.2085 0	.27	-.84505 0	-.25

* A fifth set of real and imaginary roots exists, which has a base ±100% variation value of zero.

TABLE 12B

LATERAL SENSITIVITY ANALYSIS OF V NUMERATOR NON-DIMENSIONAL ROOTS FOR A GENERALIZED UNDERWATER VEHICLE, VARYING $N'_{\dot{v}}$ ±100%

% VAR	ROOT 1	% CHANGE	ROOT 2	% CHANGE	ROOT 3	% CHANGE	ROOT 4	% CHANGE
-100^R_I								
-50^R_I								
-25^R_I								
-10^R_I								
$BASE^R_I$	-.17756 -2.8702		-.17756 2.8702		-5.3302 0		0 0	
$+10^R_I$								
$+25^R_I$								
$+50^R_I$								
$+100^R_I$								

TABLE 12C

LATERAL SENSITIVITY ANALYSIS OF ψ NUMERATOR NON-DIMENSIONAL ROOTS FOR A GENERALIZED UNDERWATER VEHICLE, VARYING $N'_{\dot{v}}$ ±100%

% VAR	ROOT 1	% CHANGE	ROOT 2	% CHANGE	ROOT 3	% CHANGE
-100^R_I	-.18519 -2.8660	-.02 0	-.18519 2.8660	-.02 0	-1.0133 0	-.79
-50^R_I	-.18521 -2.8660	-.01 0	-.18521 2.8660	-.01 0	-1.0173 0	-.40
-25^R_I	-.18522 -2.8660	-.005 0	-.18522 2.8660	-.005 0	-1.0191 0	-.20
-10^R_I	-.16522 -2.8660	-.005 0	-.18522 2.8660	-.005 0	-1.0206 0	-.08
$BASE^R_I$	-.18523 -2.8660		-.18523 2.8660		-1.0214 0	
$+10^R_I$	-.18523 -2.8660	0 0	-.18523 2.8660	0 0	-1.0222 0	.08
$+25^R_I$	-.18524 -2.8660	.005 0	-.18524 2.8660	.005 0	-1.0234 0	.20
$+50^R_I$	-.18525 -2.8660	.01 0	-.18525 2.8660	.01 0	-1.0255 0	.41
$+100^R_I$	-.18527 -2.8660	.02 0	-.18527 2.8660	.02 0	-1.0296 0	.81

TABLE 12D

LATERAL SENSITIVITY ANALYSIS OF ϕ NUMERATOR NON-DIMENSIONAL ROOTS FOR A GENERALIZED UNDERWATER VEHICLE VARYING $N'_{\dot{v}}$ ±100%

% VAR	ROOT 1	% CHANGE	ROOT 2	% CHANGE	ROOT 3	% CHANGE
-100^R_I	-1.7567 0	-.95	5.0384 0	.84		
-50^R_I	-1.7661 0	-.47	5.0173 0	.42		
-25^R_I	-1.7693 0	-.24	5.0068 0	.21		
-10^R_I	-1.7718 0	-.10	5.0005 0	.08		
$BASE^R_I$	-1.7735 0		4.9953 0		0 0	
$+10^R_I$	-1.7752 0	.10	4.9921 0	-.08		
$+25^R_I$	-1.7777 0	.24	4.9858 0	-.21		
$+50^R_I$	-1.7819 0	.47	4.9753 0	-.42		
$+100^R_I$	-1.7905 0	.96	4.9543 0	-.84		

TABLE 13A

LATERAL SENSITIVITY ANALYSIS OF CHARACTERISTIC EQUATION NON-DIMENSIONAL ROOTS FOR A GENERALIZED UNDERWATER VEHICLE, VARYING N'_p ±100%

% VAR	ROOT 1	% CHANGE	ROOT 2	% CHANGE	ROOT 3	% CHANGE	ROOT 4	% CHANGE
-100^R_I	-.18367 -2.8591	.05 -.003	-.18367 2.8591	.05 -.003	-4.1974 0	.01		
-50^R_I	-.18362 -2.8592	.03 0	-.18362 2.8592	.03 0	-4.1972 0	.005		
-25^R_I	-.18359 -2.8592	.01 0	-.18359 2.8592	.01 0	-4.1971 0	.002		
-10^R_I	-.18358 -2.8592	.006 0	-.18356 2.8592	.005 0	-4.1971 0	.002		
$BASE^R_I$	-.18357 -2.8592		-.18357 2.8592		-4.1970 0		-.84717 0	
$+10^R_I$	-.18356 -2.8592	-.005 0	-.18356 2.8592	-.005 0	-4.1970 0	0		
$+25^R_I$	-.18354 -2.8593	-.02 .003	-.18354 2.8593	-.02 .003	-4.1969 0	-.002		
$+50^R_I$	-.18352 -2.8593	-.03 .003	-.18352 2.8593	-.03 .003	-4.1968 0	-.005		
$+100^R_I$	-.18347 -2.8594	-.05 .007	-.18347 2.8594	-.05 .007	-4.1966 0	-.01	-.84716 0	-.001

* A fifth set of real and imaginary roots exists, which has a base ±100% variation value of zero.

TABLE 13B

LATERAL SENSITIVITY ANALYSIS OF V NUMERATOR NON-DIMENSIONAL ROOTS FOR A GENERALIZED UNDERWATER VEHICLE, VARYING N'_p ±100%

% VAR	ROOT 1	% CHANGE	ROOT 2	% CHANGE	ROOT 3	% CHANGE	ROOT 4	% CHANGE
-100^R_I	-.17767 -2.8700	.04 -.007	-.17763 2.8700	.04 -.007	-5.3399 0	.01		
-50^R_I	-.17759 -2.8701	.02 -.003	-.17759 2.8701	.02 -.003	-5.3396 0	.007		
-25^R_I	-.17758 -2.8702	.01 0	-.17758 2.8702	.01 0	-5.3394 0	.004		
-10^R_I	-.17757 -2.8702	.006 0	-.17757 2.8702	.006 0	-5.3393 0	.002		
$BASE^R_I$	-.17756 -2.8702		-.17756 2.8702		-5.3392 0		0 0	
$+10^R_I$	-.17755 -2.8702	-.006 0	-.17755 2.8702	-.006 0	-5.3392 0	0		
$+25^R_I$	-.17754 -2.8702	-.01 0	-.17754 2.8702	-.01 0	-5.3391 0	-.002		
$+50^R_I$	-.17752 -2.8703	-.02 .003	-.17752 2.8703	-.02 .003	-5.3389	-.006		
$+100^R_I$	-.17749 -2.8703	-.04 .003	-.17749 2.8703	-.04 .003	-5.3386 0	-.01		

TABLE 13C

LATERAL SENSITIVITY ANALYSIS OF ψ NUMERATOR NON-DIMENSIONAL ROOTS FOR A GENERALIZED UNDERWATER VEHICLE, VARYING N'_p ±100%

% VAR	ROOT 1	% CHANGE	ROOT 2	% CHANGE	ROOT 3	% CHANGE
-100^R_I	-.18517 -2.8659	-.03 -.003	-.18517 2.8659	-.03 -.003		
-50^R_I	-.18520 -2.8659	-.02 -.003	-.18520 2.8659	-.02 -.003		
-25^R_I	-.18521 -2.8660	-.01 0	-.18521 2.8660	-.01 0		
-10^R_I	-.18522 -2.8660	-.005 0	-.18522 2.8660	-.005 0		
$BASE^R_I$	-.18523 -2.8660		-.18523 2.8660		-1.0214 0	
$+10^R_I$	-.18523 -2.8660	0 0	-.18523 2.8660	0 0		
$+25^R_I$	-.18524 -2.8660	.005 0	-.18524 2.8660	.005 0		
$+50^R_I$	-.18525 -2.8660	.01 0	-.18525 2.8660	.01 0		
$+100^R_I$	-.18528 -2.8661	.03 .003	-.18528 2.8661	.03 .003		

TABLE 13D

LATERAL SENSITIVITY ANALYSIS OF ϕ NUMERATOR NON-DIMENSIONAL ROOTS FOR A GENERALIZED UNDERWATER VEHICLE, VARYING N'_p ±100%

% VAR	ROOT 1	% CHANGE	ROOT 2	% CHANGE	ROOT 3	% CHANGE
-100^R_I						
-50^R_I						
-25^R_I						
-10^R_I						
$BASE^R_I$	-1.7725 0		1.9263 0		0 0	
$+10^R_I$						
$+25^R_I$						
$+50^R_I$						
$+100^R_I$						

$N'_{\dot{r}}$

1. Yawing moments additional to I_z are denoted $N'_{\dot{r}}$. This is the added moment of inertia term whose longitudinal counterpart is $M'_{\dot{q}}$.

2. Trajectory simulation and yaw moment percent contribution plots in Figures 38 and 39 illustrate its significance to vehicular motion during various maneuvers. The root locus plots in Figures 40, 41 and 42 illustrate the wide variation in the locations of the poles due to variation in $N'_{\dot{r}}$. Tables 14A through 14D present the results of a sensitivity analysis of nondimensional roots of the characteristic equation (transfer function denominator) and v, ψ, and ϕ (numerators) for a generalized underwater vehicle varying $N'_{\dot{r}}$ from -100 percent to +100 percent.

3. & 4. Like $M'_{\dot{q}}$, there are two parts to the $N'_{\dot{r}}$ body contribution

$$N'_{\dot{r}_b} = \frac{-K'_b I_{z_{df}}}{\frac{1}{2}\rho \ell^5} + Y'_{\dot{v}_b} \frac{(X_{ncb} - X_{ncg})^2}{\ell^2}$$

for an axisymmetric vehicle body $I_{z_{df}} = I_{y_{df}}$. Again, similar to $M'_{\dot{q}_t}$, the upper vertical tail fin contribution is

$$N'_{\dot{r}_{uvt}} = -\frac{1}{\frac{1}{2}\rho \ell^5} \frac{(K'_p \pi \rho b^{2} c^{2} 3)}{48} + Y'_{\dot{v}_{uvt}} \frac{(X_{nuvt} - X_{ncg})^2}{\ell^2} .$$

The lower vertical tail fin is identical in form. The complete expression, then, is written $N'_{\dot{r}} = N'_{\dot{r}_b} + N'_{\dot{r}_{uvt}} + N'_{\dot{r}_{\ell vt}}$.

SUMMARY

A compilation of methods for analytically predicting the acceleration hydrodynamic coefficients from the geometric and mass distribution characteristics of underwater vehicles has been presented. A theoretical development from potential flow theory is given to show the equivalences among acceleration and coupled terms. The detailed discussion of each coefficient presented includes descriptions intended to provide the reader with an understanding of the physical relationships involved.

(Text Continued on page 63)

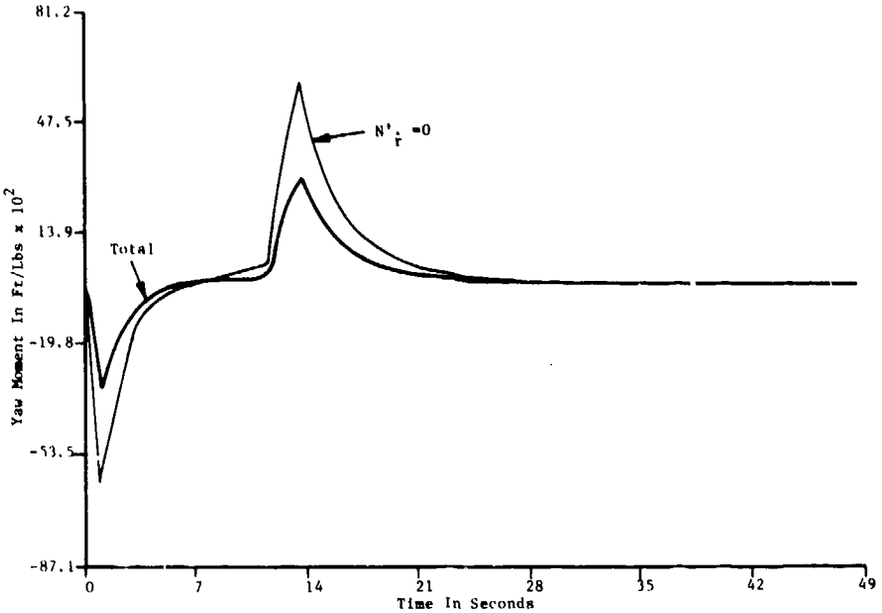

FIGURE 38. TRAJECTORY SIMULATION PLOT OF $N'_{\dot{r}}$ CONTRIBUTION TO YAW MOMENT DURING A δ_r = ±30° TURN REVERSAL MANEUVER

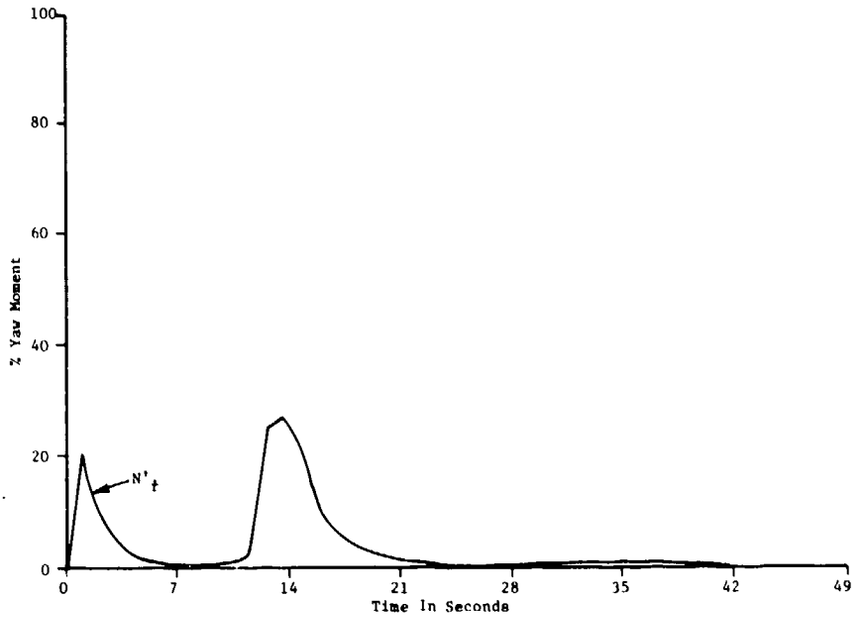

FIGURE 39. PERCENT CONTRIBUTION OF $N'_{\dot{r}}$ TO YAW MOMENT DURING A δ_r = ±30° TURN REVERSAL MANEUVER

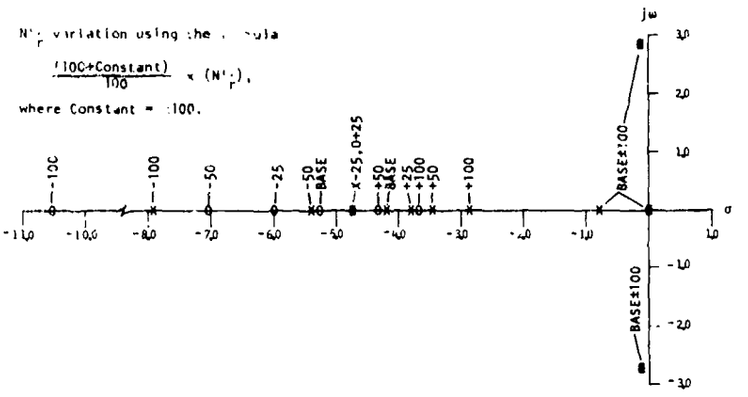

FIGURE 40. ROOT LOCUS PLOT OF v/δ_r FOR A GENERALIZED UNDERWATER VEHICLE, VARYING N'_r

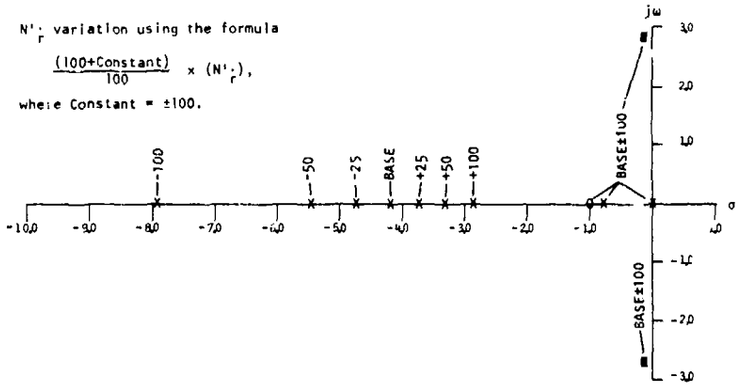

FIGURE 41. ROOT LOCUS PLOT OF v/δ_r FOR A GENERALIZED UNDERWATER VEHI VARYING N'_r

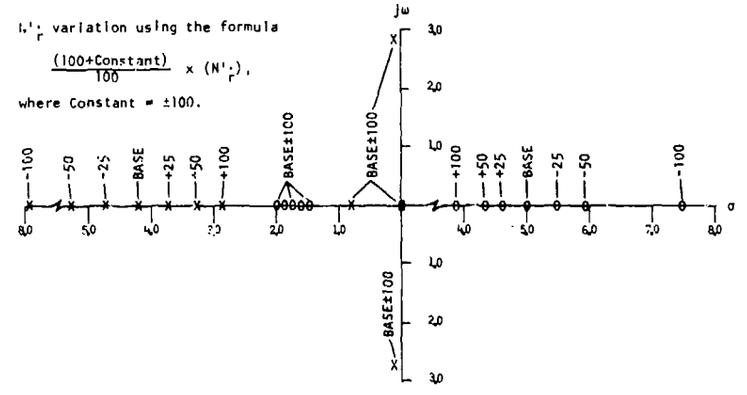

FIGURE 42. ROOT LOCUS PLOT OF r/δ_r FOR A GENERALIZED UNDERWATER VEHICLE, ARYING N'_r

TABLE 14A

LATERAL SENSITIVITY ANALYSIS OF CHARACTERISTIC EQUATION NON-DIMENSIONAL ROOTS FOR A GENERALIZED UNDERWATER VEHICLE, VARYING N'_r ±100%

% VAR	ROOT 1	% CHANGE	ROOT 2	% CHANGE	ROOT 3	% CHANGE	ROOT 4	% CHANGE
-100^R_I	-.18160 -2.8605	-1.1 .05	-.18160 2.8605	-1.1 .05	-7.8987 0	88.2	-.96170 0	.63
-50^R_I	-.18256 -2.8597	-.65 .02	-.18256 2.8597	-.65 .02	-5.4761 0	30.5	-.84956 0	.08
-25^R_I	-.18307 -2.8594	-.37 .007	-.18307 2.8594	-.37 .007	-4.7513 0	13.5	-.81539 0	.14
-10^R_I	-.18337 -2.8593	-.11 .003	-.18337 2.9593	-.11 .003	-4.4027 0	4.9	-.84787 0	.06
$BASE^R_I$	-.18357 -2.8592		-.18357 2.3592		-4.1970 0		-.94219 0	
$+10^R_I$	-.18376 -2.8592	.10 0	-.18376 2.8592	.10 0	-4.0104 0	-4.4	-.84656 0	-.06
$+25^R_I$	-.18405 -2.8591	.26 -.003	-.18405 2.8591	.26 -.003	-3.7601 0	-10.4	-.84187 0	-.15
$+50^R_I$	-.18451 -2.8590	.51 -.007	-.18451 2.8590	.51 -.007	-3.4088 0	-18.9	-.84450 0	-.32
$+100^R_I$	-.18533 -2.8590	.95 -.007	-.18532 2.8590	.95 -.007	-2.8709 0	-31.6	-.84748 0	-.67

* A fifth set of real and imaginary roots exists, which has a base +100% variation value of zero.

TABLE 14B

LATERAL SENSITIVITY ANALYSIS OF V NUMERATOR NON-DIMENSIONAL ROOTS FOR A GENERALIZED UNDERWATER VEHICLE, VARYING N'_r ±100%

% VAR	ROOT 1	% CHANGE	ROOT 2	% CHANGE	ROOT 3	% CHANGE	ROOT 4	% CHANGE
-100^R_I	-.17981 -2.8717	1.3 .05	-.17981 2.8717	1.3 .05	-10.473 0	96.2		
-50^R_I	-.17865 -2.8711	.56 .03	-.17865 2.8711	.56 .03	-7.0710 0	32.4		
-25^R_I	-.17802 -2.8706	.28 .01	-.17802 2.8706	.28 .01	-6.0840 0	13.9		
-10^R_I	-.17773 -2.8704	.10 .007	-.17773 2.8704	.10 .007	-5.6141 0	5.1		
$BASE^R_I$	-.17756 -2.8702		-.17756 2.8702		-5.3392 0		0 0	
$+10^R_I$	-.17749 -2.8700	-.09 -.007	-.17740 2.8700	-.09 -.007	-5.0902 0	-4.7		
$+25^R_I$	-.17717 -2.8697	-.22 -.02	-.17717 2.8697	-.22 -.02	-4.7574 0	-10.9		
$+50^R_I$	-.17686 -2.8692	-.39 -.03	-.17686 2.8692	-.39 -.03	-4.2902 0	-19.6		
$+100^R_I$	-.17641 -2.8683	-.65 -.07	-.17641 2.8683	-.65 -.07	-3.5866 0	-32.8		

TABLE 14C

LATERAL SENSITIVITY ANALYSIS OF ϕ NUMERATOR NON-DIMENSIONAL ROOTS FOR A GENERALIZED UNDERWATER VEHICLE, VARYING N'_r ±100%

% VAR	ROOT 1	% CHANGE	ROOT 2	% CHANGE	ROOT 3	% CHANGE
-100^R_I						
-50^R_I						
-25^R_I						
-10^R_I						
$BASE^R_I$	-.18433 -2.8680		-.18433 2.8680		-2.0814 0	
$+10^R_I$						
$+25^R_I$						
$+50^R_I$						
$+100^R_I$						

TABLE 14D

LATERAL SENSITIVITY ANALYSIS OF ϕ NUMERATOR NON-DIMENSIONAL ROOTS FOR A GENERALIZED UNDERWATER VEHICLE, VARYING N'_r ±100%

% VAR	ROOT 1	% CHANGE	ROOT 2	% CHANGE	ROOT 3	% CHANGE
-100^R_I	-2.1486 0	15.5	7.5033 0	50.2		
-50^R_I	-1.8945 0	8.8	5.8335 0	18.8		
-25^R_I	-1.8307 0	3.2	5.4132 0	8.3		
-10^R_I	-1.7956 0	1.2	5.1528 0	3.1		
$BASE^R_I$	-1.7735 0		4.9983 0		0 0	
$+10^R_I$	-1.7522 0	-1.2	4.8515 0	-2.9		
$+25^R_I$	-1.7217 0	-2.9	4.6537 0	-6.9		
$+50^R_I$	-1.6746 0	-5.6	4.3665 0	-12.6		
$+100^R_I$	-1.5917 0	-10.3	3.9106 0	-21.7		

Results of sensitivity analyses are presented to show the relative contributions of each coefficient to the equations of motion. A discussion of the important assumptions involved in mathematically computing each coefficient is given, along with the analytical expression used to compute each coefficient. An example case (Appendix B) is given to show a comparison between computed coefficients and experimental data.

Table 15 presents a summary of the sensitivity analyses conducted for each acceleration coefficient. These results are for ±100 percent coefficient variation. It can be seen in Table 15 that five coefficients make major contributions to the vehicle dynamics. These are $Z'_{\dot{w}}$, $M'_{\dot{q}}$, $Y'_{\dot{v}}$, $K'_{\dot{v}}$, and $I'_{\dot{r}}$. Variations of ±100 percent change both the numerator and denominator roots by better than 50 percent, except for $K'_{\dot{v}}$. Changes in $K'_{\dot{v}}$ significantly effect only the roll numerator, $N_{\delta_r}^{\phi}$. It should be noted that the $\dot{v}$ terms, such as $K'_{\dot{v}}$ and $Y'_{\dot{v}}$, do not affect the v-numerator because no v-term appears in the v-numerator. This is easily seen when one applies Cramer's rule to form the transfer functions[9]. This same observation can be made about each of the other numerators; i.e. no w-term in the w-numerator.

[9] Naval Coastal Systems Laboratory Technical Report 287-76, *Development of the Equations of Motion and Transfer Functions for Underwater Vehicles*, by D. E. Humphreys, July 1976.

TABLE 15

ROOT SENSITIVITY ANALYSES FOR DERIVATIVE VARIATION OF ±100%
(Sheet 1 of 2)

LONGITUDINAL DERIVATIVE ROOT VARIATION PERCENTAGES

f	CHAR. EQUATION		U NUMERATOR		W NUMERATOR		θ NUMERATOR	
	Derivative Variation		Derivative Variation		Derivative Variation		Derivative Variation	
	-100%	+100%	-100%	+100%	-100%	+100%	-100%	+100%
X'_u	0	0	0	0	0	0	3.30%	-3.10%
	3.30%	-3.10%	0	0	3.30%	-3.10%	0	0
	0	0	0	0	0	0		
min.	0	0						
	-0.12%	0.12%	-0.21%	0.23%	0	0	0	0
	0	0	88.30%	-32.30%	0	0	97.00%	-33.00%
	91.20%	-32.50%	4.00%	-0.98%	0	0		
maj.	2.40%	-0.58%						
M'_w	-0.01%	0.01%	-0.02%	0.02%	0	0	0	0
	0	0	0.43%	-0.42%	0	0	-0.79%	0.79%
	0.27%	-0.27%	-0.44%	0.43%	0	0		
neg.	-0.29%	0.29%						

LONGITUDINAL DERIVATIVE ROOT VARIATION PERCENTAGES

f	CHAR. EQUATION		U NUMERATOR		W NUMERATOR		θ NUMERATOR	
	Derivative Variation		Derivative Variation		Derivative Variation		Derivative Variation	
	-100%	+100%	-100%	+100%	-100%	+100%	-100%	+100%
$Z'_{\dot{q}}$	-0.007%	0.007%	-0.008%	0.01%	0.02%	-0.03%	0	0
	0	0	0.21%	-0.21%	0	0	0	0
	0.18%	-0.18%	-0.23%	0.23%	-4.00%	4.30%		
min.	-0.21%	0.21%						
$M'_{\dot{q}}$	-0.52%	0.53%	-0.68%	0.71%	-0.30%	0.30%	0	0
	0	0	1.20%	-1.50%	0	0	0	0
	0.68%	-0.85%	88.40%	-31.50%	97.10%	-33.10%		
maj.	89.10%	-31.80%						

LATERAL DERIVATIVE ROOT VARIATION PERCENTAGES

f	CHAR. EQUATION		V NUMERATOR		Y NUMERATOR		φ NUMERATOR	
	Derivative Variation		Derivative Variation		Derivative Variation		Derivative Variation	
	-100%	+100%	-100%	+100%	-100%	+100%	-100%	+100%
Y'_v	† -3.90%	1.10%	0	0	* -1.50%	0.07%	24.00%	-11.30%
	† -3.90%	1.10%	0	0	* -1.50%	0.07%	640.40%	-40.40%
	2.10%	-0.51%	0	0	96.90%	-33.00%	0	0
	91.50%	-32.50%	0	0				
maj.	0	0						
K'_v	†† 4.40%	-4.30%	0	0	** 1.70%	-1.70%	44.30%	-36.40%
	†† 4.40%	-4.30%	0	0	** 1.70%	-1.70%	-62.00%	789.00%
	-0.05%	0.05%	0	0	0.06%	-0.06%	0	0
	0.16%	-0.16%	0	0				
maj.	0	0						
N'_v	††† -0.02%	0.02%	0	0	*** -0.02%	0.02%	-0.95%	0.96%
	††† -0.02%	0.02%	0	0	*** -0.02%	0.02%	0.84%	-0.84%
	-0.27%	0.27%	0	0	-0.79%	0.80%	0	0
	0.25%	-0.25%	0	0				
neg.	0	0						

IMAGINARY ROOT VARIATIONS: † -0.10 to 0.10; * -0.20 to 0.09; †† 0.15 to -0.15;
** 0.19 to -0.19; ††† -0.003 to 0.003; *** 0

TABLE 15

(Sheet 2 of 2)

LATERAL DERIVATIVE ROOT VARIATION PERCENTAGES

ƒ		CHAR. EQUATION		V NUMERATOR		Y NUMERATOR		♦ NUMERATOR	
		Derivative Variation		Derivative Variation		Derivative Variation		Derivative Variation	
		-100%	+100%	-100%	+100%	-100%	+100%	-100%	+100%
Y'ρ	†	-1.00%	1.00%	* 3.40%	-3.30%	# -0.91%	0.90%	0	0
	†	-1.00%	1.00%	* 3.40%	-3.30%	# -0.91%	0.90%	0	0
		0.03%	-0.03%	0.71%	-0.70%	-0.07%	0.07%	0	0
		-0.06%	0.06%	0	0				
neg.		0	0						
K'ρ	††	1.10%	-1.00%	†† 1.00%	-1.00%	†† 1.00%	-1.00%	0	0
	††	1.10%	-1.00%	†† 1.00%	-1.00%	†† 1.00%	-1.00%	0	0
		0.002%	-0.002%	-0.006%	0.007%	0	0	0	0
		0	-0.001%	0	0				
neg.		0	0						
N'ρ	†††	0.05%	-0.05%	*** 0.04%	-0.04%	### -0.03%	0.03%	0	0
	†††	0.05%	-0.05%	*** 0.04%	-0.04%	### -0.03%	0.03%	0	0
		0.01%	-0.01%	0.01%	-0.01%	0	0	0	0
		0	-0.001%	0	0				
neg.		0	0						

IMAGINARY ROOT VARIATIONS: † 0.24 to -0.24; * 0.13 to -0.13; # 0.26 to -0.26; †† 0.52 to -0.51; ††† -0.003 to 0.007; *** -0.007 to 0.003; ### -0.003 to 0.003

LATERAL DERIVATIVE ROOT VARIATION PERCENTAGES

ƒ		CHAR. EQUATION		V NUMERATOR		Y NUMERATOR		♦ NUMERATOR	
		Derivative Variation		Derivative Variation		Derivative Variation		Derivative Variation	
		-100%	+100%	-100%	+100%	-100%	+100%	-100%	+100%
Y'r	†	-0.05%	0.05%	* 0.06%	-0.07%	0	0	-0.27%	0.26%
	†	-0.05%	0.05%	* 0.06%	-0.07%	0	0	3.70%	-3.50%
		-0.19%	0.19%	-3.90%	4.20%	0	0	0	0
		0.15%	-0.15%	0	0				
min.		0	0						
K'r	††	-0.06%	0.06%	** 0.14%	-0.15%	0	0	0.78%	-0.75%
	††	-0.06%	0.06%	** 0.14%	-0.15%	0	0	6.60%	-5.70%
		-0.01%	0.01%	0.03%	-0.03%	0	0	0	0
		-0.001	0	0	0				
min.		0	0						
N'r	†††	-1.10%	0.95%	*** 1.30%	-0.65%	0	0	15.50%	-10.30%
	†††	-1.10%	0.95%	*** 1.30%	-0.65%	0	0	50.20%	-21.70%
		88.20%	-31.60%	96.20%	-32.80%	0	0	0	0
		0.53%	-0.67%	0	0				
maj.		0	0						

IMAGINARY ROOT VARIATIONS: † 0.003 to 0; * -0.003 to 0.003; †† 0.007 to -0.007; ** 0.003 to -0.003; ††† 0.05 to -0.007; *** 0.05 to -0.07

APPENDIX A

DERIVATION OF HYDRODYNAMIC COEFFICIENTS RELATIONSHIPS FROM ENERGY EQUATIONS

Beginning with the momentum equations given in Equations (1) and (2) in the body of this report, a derivation is given here for the complete expressions, showing the equalities and relationships between all of the acceleration and nonlinear hydrodynamic coefficients possible for a vehicle moving in an infinite, inviscid, fixed fluid with zero circulation.

A summary of the identities and relationships derived is presented on Page A-6 with simplifications arising from vehicle symmetry on Page A-8.

Note: The hydrodynamic coefficients in parenthesis with a subscript are added together to get the value of the parenthesized hydrodynamic coefficient, e.g.,

$$X_{rq} = (X_{rq})_1 + (-X_{rq})_2$$

$$X_{rq} = (M) + (-N)$$

$$X_{rq} = M - N \ .$$

X-FORCE, SURGE

$$-X = \frac{d}{dt}\frac{\delta T_f}{\delta u} - r\frac{\delta T_f}{\delta v} + q\frac{\delta T_f}{\delta w}$$

$$\frac{d}{dt}\frac{\delta T_f}{\delta u} = A\dot{u} + B'\dot{w} + C'\dot{v} + L\dot{p} + G\dot{r} - G'\dot{r} + H\dot{q} + H'\dot{q}$$

$$-r\frac{\delta T_f}{\delta v} = -Brv - A'rw - C'ru - Mrq - Frr - F'rr - Hrp + H'rp$$

$$q\frac{\delta T_f}{\delta w} = Cqw + A'qv + B'qu + Nqr + Fqq - F'qq + Gqp + G'qp$$

letting $F_1 = F + F'$, $F_2 = F - F'$, $G_1 = G + G'$, $G_2 = G - G'$, $H_1 = H + H'$,

$H_2 = H - H'$

$$X = -A\dot{u} - B'\dot{w} - C'\dot{v} - L\dot{p} - G_2\dot{r} - H_1\dot{q} + Brv + A'rw + C'ru +$$

$$Mrq + F_1rr + H_2rp - Cqw - A'qv - B'qu - Nqr - F_2qq - G_1qp$$

$A = -X_{\dot{u}}$ $\quad A' = X_{rw} = -X_{qv}$ $\quad L = -X_{\dot{p}}$ $\quad F_1 = X_{rr}$ $\quad F_2 = -X_{qq}$

$B = X_{rv}$ $\quad B' = -X_{\dot{w}} = -X_{qu}$ $\quad M = (X_{rq})_1$ $\quad G_1 = -X_{qp}$ $\quad G_2 = -X_{\dot{r}}$

$C = -X_{qw}$ $\quad C' = -X_{\dot{v}} = X_{ru}$ $\quad N = -(X_{qr})_2$ $\quad H_1 = -X_{\dot{q}}$ $\quad H_2 = X_{rp}$

Other resulting relations: $X_{rq} = M - N$.

Y-FORCE, SWAY

$$-Y = \frac{d}{dt}\frac{\delta T_f}{\delta v} \quad -p\frac{\delta T_f}{\delta w} + r\frac{\delta T_f}{\delta u}$$

$$\frac{d}{dt}\frac{\delta T_f}{\delta v} = B\dot{v} + A'\dot{w} + C'\dot{u} + M\dot{q} + F\dot{r} + F'\dot{r} + H\dot{p} - H'\dot{p}$$

$$-p\frac{\delta T_f}{\delta w} = -Cpw - A'pv - B'pu - Npr - Fpq + F'pq - Gpp - G'pp$$

$$r\frac{\delta T_f}{\delta u} = Aru + B'rw + C'rv + Lrp - Grr - G'rr + Hrq + H'rq$$

$$Y = -B\dot{v} - A'\dot{w} - C'\dot{u} - M\dot{q} - F_1\dot{r} - H_2\dot{p} + Cpw + A'pv + B'pw + Npr +$$

$$F_2pq + G_1pp - Aru - B'rw - C'rv - Lrp - G_2rr - H_1rg$$

$A = -Y_{ru}$ $\quad A' = -Y_{\dot{w}} = Y_{pv}$ $\quad M = -Y_{\dot{q}}$ $\quad F_1 = -Y_{\dot{r}}$ $\quad F_2 = Y_{pq}$

$B = -Y_{\dot{v}}$ $\quad B' = -Y_{rw} = Y_{pu}$ $\quad N = (Y_{pr})_1$ $\quad G_1 = Y_{pp}$ $\quad G_2 = -Y_{rr}$

$C = Y_{pw}$ $\quad C' = -Y_{\dot{u}} = -Y_{rv}$ $\quad L = (-Y_{rp})_2$ $\quad H_1 = -Y_{rq}$ $\quad H_2 = -Y_{\dot{p}}$

Other resulting relations: $Y_{rp} = N - L$.

Z-FORCE, HEAVE

$$-Z = \frac{d}{dt}\frac{\delta T_f}{\delta w} - q\frac{\delta T_f}{\delta u} + p\frac{\delta T_f}{\delta v}$$

$$\frac{d}{dt}\frac{\delta T_f}{\delta w} = C\dot{w} + A'\dot{v} + B'\dot{u} + N\dot{r} + F'\dot{q} + G\dot{p} + G'\dot{p}$$

$$-q\frac{\delta T_f}{\delta u} = -Aqu - B'qw - C'qv - Lqp - Gqr + G'qr - Hqq - H'qq$$

$$p\frac{\delta T_f}{\delta v} = Bpv + A'pw + C'pu + Mpq + Fpr + F'pr + Hpp - H'pp$$

$$Z = -C\dot{w} - A'\dot{v} - B'\dot{u} - N\dot{r} - F_2\dot{q} - G_1\dot{p} + Aqu + B'qw + C'qv + Lqp + G_2qr + H_1qq - Bpv - A'pw - C'pu - Mpq - F_1pr - H_2pp$$

$A = Z_{qu}$ $\quad A' = -Z_{\dot{v}} = -Z_{pw}$ $\quad L = (Z_{qp})_1$ $\quad F_1 = -Z_{pr}$ $\quad F_2 = -Z_{\dot{q}}$

$B = -Z_{pv}$ $\quad B' = Z_{qw} = -Z_{\dot{u}}$ $\quad M = (-Z_{pq})_2$ $\quad G_1 = -Z_{\dot{p}}$ $\quad G_2 = -Z_{qr}$

$C = -Z_{\dot{w}}$ $\quad C' = Z_{qv} = -Z_{pu}$ $\quad N = -Z_{\dot{r}}$ $\quad H_1 = Z_{qq}$ $\quad H_2 = -Z_{pp}$

Other resulting relations: $Z_{pq} = L - M.$

K-MOMENT, ROLL

$$K = -\frac{d}{dt}\frac{\delta T_f}{\delta p} + w\frac{\delta T_f}{\delta v} - v\frac{\delta T_f}{\delta w} + r\frac{\delta T_f}{\delta q} - q\frac{\delta T_f}{\delta r}$$

$$-\frac{d}{dt}\frac{\delta T_f}{\delta p} = -P\dot{p} - Q'\dot{r} - R'\dot{q} - L\dot{u} - G_1\dot{w} - H_2\dot{v}$$

$$w\frac{\delta T_f}{\delta v} = Bwv + A'ww + C'wu + Mwq + F_1wr + H_2wp$$

$$-v\frac{\delta T_f}{\delta w} = Cvw - A'vv - B'vu - Nvr - F_2vq - G_1vp$$

$$r\frac{\delta T_f}{\delta q} = Qrq + P'rr + R'rp + Mrv + F_2rw + H_1ru$$

$$-q\frac{\delta T_f}{\delta r} = Rqr - P'qq - Q'qp - Nqw - F_1qv - G_2qu$$

$A' = K_{ww} = -K_{vv}$ $\quad L = -K_{\dot{u}}$ $\quad F_1 = (K_{wr})_1 = (-K_{qv})_1$

$B = (K'_{wv})_1$ $\quad B' = -K_{vu}$ $\quad M = (K_{wq})_1 = (K_{rv})_1$ $\quad G_1 = K_{vp} = -K_{\dot{w}}$

$C = (-K_{vw})_2$ $\quad C' = K_{wu}$ $\quad N = (-K_{vr})_2 = (-K_{qw})_2$ $\quad H_1 = K_{ru}$

$F_2 = (-K_{vq})_2 = (K_{rw})_2$ $\quad P = -K_{\dot{p}}$ $\quad P' = K_{rr} = -K_{qq}$

$G_2 = -K_{qu}$ $\quad Q = (K_{rq})_1$ $\quad Q' = -K_{\dot{r}} = -K_{qp}$

$H_2 = -K_{\dot{v}} = K_{wp}$ $\quad R = (-K_{qr})_2$ $\quad R' \quad -K_{\dot{q}} = K_{rp}$

Other resulting relations: $K_{wv} = B - C$

$K_{vr} = M - N$

$K_{qw} = M - N$

$K_{rw} = F_1 + F_2 = 2F$

$K_{vq} = -F_1 - F_2 = -2F$

$K_{qr} = Q - R$

M-MOMENT, PITCH

$$M = \frac{d}{dt}\frac{\delta T_f}{\delta q} + u\frac{\delta T_f}{\delta w} - w\frac{\delta T_f}{\delta u} + p\frac{\delta T_f}{\delta r} - r\frac{\delta T_f}{\delta p}$$

$$-\frac{d}{dt}\frac{\delta T_f}{\delta q} = -Q\dot{q} - P'\dot{r} - R'\dot{p} - M\dot{v} - F_2\dot{w} - H_1\dot{u}$$

$$u\frac{\delta T_f}{\delta w} = Cuw + A'uv + B'uu + Nur + F_2uq + G_1up$$

$$-w\frac{\delta T_f}{\delta u} = -Awu - B'ww - C'wv - Lwp - G_2wr - H_1wq$$

$$p \frac{\delta T_f}{\delta r} = Rpr + P'pq + Q'pp + Npw + F_1pv + G_2pu$$

$$-r \frac{\delta T_f}{\delta p} = - Prp - Q'rr - R'rq - Lru - G_1rw - H_2rv$$

$A = (-M_{wu})_1$ $\quad A' = M_{uv}$ $\quad L = (-M_{wp})_1 = (-M_{ru})_1$ $\quad F_1 = M_{pv}$

$B' = -M_{ww} = M_{uu}$ $\quad M = -M_{\dot{v}}$ $\quad G_1 = (M_{up})_1 = (-M_{rw})_1$

$C = (M_{uw})_2$ $\quad C' = -M_{wv}$ $\quad N = (M_{pw})_2 = (M_{ur})_2$ $\quad H_1 = -M_{\dot{u}} = -M_{wq}$

$F_2 = -M_{\dot{w}} = M_{uq}$ $\quad P = (-M_{rp})_1$ $\quad P' = -M_{\dot{r}} = M_{pq}$

$G_2 = (-M_{wr})_2 = (M_{pu})_2$ $\quad Q = -M_{\dot{q}}$ $\quad Q' = -M_{rr} = M_{pp}$

$H_2 = -M_{rv}$ $\quad R = (M_{pr})_2$ $\quad R' = -M_{\dot{p}} = -M_{rq}$

Other resulting relations:

$$M_{wv} = C - A$$

$$M_{pw} = N - L$$

$$M_{ru} = N - L$$

$$M_{pu} = G_1 + G_2 = 2G$$

$$M_{rw} = -G_1 - G_2 = -2G$$

$$M_{rp} = R - P \quad .$$

N-MOMENT, YAW

$$N = - \frac{d}{dt} \frac{\delta T_f}{\delta r} + v \frac{\delta T_f}{\delta u} - u \frac{\delta T_f}{\delta v} + q \frac{\delta T_f}{\delta p} - p \frac{\delta T_f}{\delta q}$$

$$-\frac{d}{dt}\frac{\delta T_f}{\delta r} = -R\dot{r} - P'\dot{q} - Q'\dot{p} - N\dot{w} - F_1\dot{v} - G_2\dot{u}$$

$$v\frac{\delta T_f}{\delta u} = Avu + B'vw + C'vv + Lvp + G_2vr + H_1vq$$

$$-u\frac{\delta T_f}{\delta v} = -Buv - A'uw - C'uu - Muq - F_1ur - H_2up$$

$$q\frac{\delta T_f}{\delta p} = Pqp + Q'qr + P'qq + Lqu + G_1qw + H_2qv$$

$$-p\frac{\delta T_f}{\delta q} = -Qpq - P'pr - R'pp - Mpv - F_2pw - H_1pu$$

$A = (N_{vu})_1$ $\quad A' = N_{uw}$ $\quad L = (N_{vp})_1 = (N_{qu})_1$ $\quad F_1 = -N_{\dot{v}} = -N_{ur}$

$B = (-N_{uv})_2$ $\quad B' = N_{vw}$ $\quad M = (-N_{uq})_2 = (-N_{pv})_2$ $\quad G_1 = N_{qw}$

$C' = N_{vv} = -N_{uu}$ $\quad N = -N_{\dot{w}}$ $\quad H_1 = (N_{vq})_1 = (-N_{pu})_1$

$F_2 = -N_{pw}$ $\quad P = (N_{qp})_1$ $\quad P' = -N_{\dot{q}} = -N_{pr}$

$G_2 = -N_{\dot{u}} = N_{vr}$ $\quad Q = (-N_{pq})_2$ $\quad Q' = -N_{\dot{p}} = N_{qr}$

$H_2 = (-N_{up})_2 = (N_{qv})_2$ $\quad R = -N_{\dot{r}}$ $\quad R' = N_{qq} = -N_{pp}$

Other Resulting relations: $N_{vu} = A - B$

$N_{vp} = L - M$

$N_{qu} = L - M$

$$N_{vq} = H_1 + H_2 = 2H$$

$$N_{pu} = -H_1 - H_2 = -2H$$

$$N_{pq} = P - Q$$

$$A = -X_{\dot{u}} = -Y_{ru} = Z_{qu} = (-M_{wu})_1 = (N_{vu})_1$$

$$B = -Y_{\dot{v}} = X_{rv} = -Z_{pv} = (K_{wv})_1 = (-N_{uv})_2$$

$$C = -Z_{\dot{w}} = -X_{qw} = Y_{pw} = (-K_{vw})_2 = (M_{uw})_2$$

$$A' = -Z_{\dot{v}} = Y_{\dot{w}} = X_{rw} = -X_{qv} = Y_{pv} = -Z_{pw} = K_{ww} = -K_{vv} = M_{uv} = N_{uw}$$

$$B' = -X_{\dot{w}} = -Z_{\dot{u}} = -X_{qu} = -Y_{rw} = Y_{pu} = Z_{qw} = -K_{vu} = -M_{ww} = M_{uu} = N_{vw}$$

$$C' = -X_{\dot{v}} = -Y_{\dot{u}} = X_{ru} = -Y_{rv} = Z_{qv} = -Z_{pu} = K_{wu} = -M_{wv} = N_{vv} = -N_{uu}$$

$$L = -X_{\dot{p}} = -K_{\dot{u}} = (Z_{qp})_1 = (-Y_{rp})_1 = (-M_{wp})_1 = (-M_{ru})_1 = (N_{vp})_1 = (N_{qu})_1$$

$$M = -Y_{\dot{q}} = -M_{\dot{v}} = (X_{rq})_1 = (-Z_{pq})_2 = (K_{wq})_1 = (K_{rv})_1 = (-N_{uq})_2 = (-N_{pv})_1$$

$$N = -Z_{\dot{r}} = -N_{\dot{w}} = (-X_{qr})_2 = (Y_{rp})_2 = (-K_{vr})_2 = (-K_{qw})_2 = (M_{pw})_2 = (M_{ur})_2$$

$$F_1 = Y_{\dot{r}} = -N_{\dot{v}} = X_{rr} = -Z_{pr} = (K_{wr})_1 = (K_{qv})_1 = M_{pv} = -N_{ur}$$

$$G_1 = -Z_{\dot{p}} = -K_{\dot{w}} = -X_{qp} = Y_{pp} = K_{vp} = (M_{up})_1 = (-M_{rw})_1 = N_{qw}$$

$$H_1 = -X_{\dot{q}} = -M_{\dot{u}} = -Y_{rq} = Z_{qq} = K_{ru} = -M_{wq} = (N_{vq})_1 = (-N_{pu})_1$$

$$F_2 = -Z_{\dot{q}} = -M_{\dot{w}} = -X_{qq} = Y_{pq} = (K_{vq})_2 = (K_{rw})_2 = M_{uq} = -N_{pw}$$

$$G_2 = -X_{\dot{r}} = -N_{\dot{u}} = -Y_{rr} = -Z_{qr} = -K_{qu} = (-M_{wr})_2 = (M_{pu})_2 = N_{vr}$$

$$H_2 = -Y_{\dot{p}} = -K_{\dot{v}} = X_{rp} = -Z_{pp} = K_{wp} = -M_{rv} = (-N_{up})_2 = (N_{qv})_2$$

$$P = -K_{\dot{p}} = (-M_{rp})_1 = (N_{qp})_1$$

$$Q = -M_{\dot{q}} = (K_{rq})_1 = (-N_{pq})_2$$

$$R = -N_{\dot{r}} = (-K_{qr})_2 = (M_{pr})_2$$

$$P' = -M_{\dot{r}} = -N_{\dot{q}} = K_{rr} = -K_{qq} = M_{pq} = -N_{pr}$$

$$Q' = -K_{\dot{r}} = -N_{\dot{p}} = -K_{qp} = -M_{rr} = M_{pp} = N_{qr}$$

$$R' = -K_{\dot{q}} = -M_{\dot{p}} = K_{rp} = -M_{rq} = N_{qq} = -N_{pp}$$

When xz-plane symmetry exists, then the following coefficients are zero; A', C', P', R', L, M, N, G, G'.

Table A1 gives a summary of force and moment coefficients for a body with xz-plane of symmetry. When xy-plane symmetry exists, then the following coefficients are zero; A', B', P', Q', L, M, N, H, H'.

When the yz-plane symmetry exists, then the following coefficients are zero; B', C', Q', R', L, M, N, F, F'.

When two planes of symmetry exist, all of the terms that are zero in the single plane cases are zero.

TABLE A1
(Sheet 1 of 2)

POTENTIAL FLOW FORCE AND MOMENT HYDRODYNAMIC COEFFICIENTS FOR BODY WITH XZ PLANE SYMMETRY

	X	Y	Z	K	M	N
$\dot{u}$	$X_{\dot{u}}$	Ø	$X_{\dot{w}}$	Ø	$X_{\dot{q}}$	Ø
$\dot{v}$	Ø*	$Y_{\dot{v}}$	Ø	$Y_{\dot{p}}$	Ø	$Y_{\dot{r}}$
$\dot{w}$	$X_{\dot{w}}$	Ø	$Z_{\dot{w}}$	Ø	$Z_{\dot{q}}$	Ø
$\dot{p}$	Ø	$Y_{\dot{p}}$	Ø	$K_{\dot{p}}$	Ø	$K_{\dot{r}}$
$\dot{q}$	$X_{\dot{q}}$	Ø	$Z_{\dot{q}}$	Ø	$M_{\dot{q}}$	Ø
$\dot{r}$	Ø	$Y_{\dot{r}}$	Ø	$K_{\dot{r}}$	Ø	$N_{\dot{r}}$
u^2	—**	—	—	—	$-X_{\dot{w}}$	Ø
uv	—	—	—	$X_{\dot{w}}$	Ø	$Y_{\dot{v}} - X_{\dot{u}}$
uw	—	—	—	Ø	$X_{\dot{u}} - Z_{\dot{w}}$	Ø
up	—	$-X_{\dot{w}}$	Ø	—	Ø	$X_{\dot{q}} + Y_{\dot{p}}$
uq	$X_{\dot{w}}$	—	$-X_{\dot{u}}$	Ø	$-Z_{\dot{q}}$	Ø
ur	Ø	$X_{\dot{u}}$	—	$-X_{\dot{q}}$	Ø	$Y_{\dot{r}}$
v^2	—	—	—	Ø	—	Ø
vw	—	—	—	$Z_{\dot{w}} - Y_{\dot{v}}$	Ø	$-X_{\dot{w}}$
vp	—	Ø	$Y_{\dot{v}}$	Ø	$-Y_{\dot{r}}$	Ø
vq	Ø	—	Ø	$Y_{\dot{r}} + Z_{\dot{q}}$	—	$-(X_{\dot{q}} + Y_{\dot{p}})$
vr	$-Y_{\dot{v}}$	Ø	—	Ø	$Y_{\dot{p}}$	Ø
w^2	—	—	—	Ø	$X_{\dot{w}}$	Ø
wp	—	$-Z_{\dot{w}}$	Ø	$-Y_{\dot{p}}$	Ø	$Z_{\dot{q}}$
wq	$Z_{\dot{w}}$	—	$-X_{\dot{w}}$	Ø	$X_{\dot{q}}$	Ø
wr	Ø	$X_{\dot{w}}$	—	$-(Y_{\dot{r}} + Z_{\dot{q}})$	Ø	—

TABLE A1

(Sheet 2 of 2)

	X	Y	Z	K	M	N
p^2	—	Ø	$Y_{\dot{p}}$	—	$-K_{\dot{r}}$	Ø
pq	Ø	$-Z_{\dot{q}}$	Ø	$K_{\dot{r}}$	Ø	$M_{\dot{q}} - K_{\dot{p}}$
pr	$-Y_{\dot{p}}$	Ø	$Y_{\dot{r}}$	Ø	$K_{\dot{p}} - N_{\dot{r}}$	Ø
q^2	$Z_{\dot{q}}$	—	$-X_{\dot{q}}$	Ø	—	Ø
qr	Ø	$X_{\dot{q}}$	Ø	$N_{\dot{r}} - M_{\dot{q}}$	Ø	$-K_{\dot{r}}$
r^2	$-Y_{\dot{r}}$	Ø	—	Ø	$K_{\dot{r}}$	—

*Coefficient zero because of xz symmetry

**Coefficient not present for arbitrary body with no planes of symmetry

APPENDIX B

COMPARISON OF ANALYTICAL PREDICTIONS WITH EXPERIMENTAL DATA

In this appendix hydrodynamic coefficients of an operational U.S. Navy submersible, obtained at the David Taylor Naval Ship Research and Development Center are compared to corresponding data calculated by the methods set forth in the body of this report. Table B1 lists those 15 acceleration coefficients generally considered to be important, their experimental and calculated values, and the percent difference between the two. Percent difference in this table was obtained as follows:

$$\frac{\text{Experimental - Calculated}}{\text{Experimental}}$$

As can be seen in Table B1, percent difference is significant in only four of the 15 cases, that is, those above 12 percent.

Three of those six coefficients ($M_{\dot{w}}$, $Z_{\dot{q}}$, and $K_{\dot{p}}$) have been shown in sensitivity analyses illustrated in the body of this report to be of relatively minor significance.

Some questions exist concerning the validity of using the PMM experimental technique to obtain roll derivatives, and specifically, in this case, the fourth problem coefficient listed in table, K_v .

It should be noted that not all of the coefficients obtained by DTNSRDC were measured. Some by necessity were calculated. Those marked with an asterisk in Table B1 were calculated by some DTNSRDC method and not by NCSL methods.

TABLE B1

COMPARISON OF CALCULATED VERSUS EXPERIMENTALLY-DETERMINED COEFFICIENTS OF AN OPERATIONAL SUBMERSIBLE

Coef.	Experiment	Calculation	% Error
$M_{\dot{w}}$	-.16800E-03	-.60300E-04	64.0
$Z_{\dot{w}}$	-.10110E-01	-.10100E-01	0.1
$M_{\dot{q}}$	-.49900E-03	-.54880E-03	10.0
$Z_{\dot{q}}$	-.17100E-03	-.60300E-04	65.0
$K_{\dot{p}}^*$	-.33000E-05	-.21500E-06	93.0
$Y_{\dot{v}}$	-.10880E-01	-.10001E-01	8.0
$X_{\dot{u}}^*$	-.20900E-03	-.18500E-03	11.5
$K_{\dot{v}}$	-.51000E-04	-.28500E-04	44.0
$N_{\dot{r}}$	-.48400E-03	-.53570E-03	10.7
X_{wq}^*	-.10110E-01	-.10100E-01	0.1
X_{vr}^*	.10880E-01	.10001E-01	8.0
Y_{wp}^*	.10110E-01	.10100E-01	0.1
N_{pq}^*	-.49600E-03	-.54900E-03	10.7
Z_{vp}^*	-.10880E-01	-.10001E-01	8.1
M_{rp}^*	.48070E-03	.53550E-03	11.4

APPENDIX C

DESCRIPTION OF TYPICAL HYDRODYNAMIC VEHICLE USED FOR SENSITIVITY ANALYSIS

This appendix contains a physical description of the underwater vehicle used as the subject of this report. Table C1 is a listing of pertinent geometric facts describing the vehicle, and Tables C2 through C6 list calculated derivatives, moments and symmetry terms. Figure C1 is a set of orthographic projections illustrating the vehicle.

TABLE C1

SUBJECT UNDERWATER VEHICLE GEOMETRY

BARE HULL

Vehicle Total Length, Ft.	.23534E 02
Hull Maximum Cross-Sectional Area, Ft^2	.78824E 01
Vehicle Total Weight, LBF	.79482E 04
Vehicle IXX Moment of Inertia, Slug-Ft^2	.82148E 04
Vehicle IYY Moment of Inertia, Slug-Ft^2	.21616E 06
Vehicle IZZ Moment of Inertia, Slug-Ft^2	.21616E 06
Vehicle Displacement Weight, LBF.	.79482E 04
Displaced Fluid IYY Moment of Inertia, Slug-Ft^2	.21616E 06
X-Distance from Nose to C.G., Ft.	.10391E 02
X-Distance from Nose to C.B., Ft.	.10391E 02
Z-Distance from C.G. to C.B., Ft.	-.10000E 00
Bare Hull Wetted Area, Ft^2.	.18421E 03
Bare Hull Lateral Area, Ft^2	.58070E 02
Bare Hull Volume, Ft^3	.12411E 03

TAIL STRUCTURE

Overall

X-Distance from Nose to A.C. of Tail, Ft.	.21298E 02
Z-Location of A.C. of Tail WRT C.G.	-.10000E 00
Sweep Angle, Deg.	.00000E 00
Taper Ratio	.10000E 01
Effective Aspect Ratio.	.24020E 01
Exposed Span, Root to Tip, of Fins (each of 4), Ft.	.13200E 01

Horizontal Tail

Total Exposed Planform Area (2 fins), Ft^2	.29010E 01
Dihedral Angle, Deg	.00000E 00
Incidence Angle, Deg.	.00000E 00

Vertical Tail

Total Exposed Planform Area (each of 2 fins), Ft^2 .	.14510E 01

TABLE C2

S N A M E NON-DIMENSIONAL LONGITUDINAL STABILITY DERIVATIVES

XU	= -.21408E-02	ZU	= .0	MU	= .0
XW	= .0	ZW	= -.32464E-01	MW	= .25379E-02
XQ	= -.15275E-03	ZQ	= -.15275E-01	MQ	= -.73062E-02
XTH	= .0	ZTH	= .0	MTH	= -.29769E-03
XUD	= -.62385E-03	ZUD	= .0	MUD	= .0
XWD	= .0	ZWD	= -.18182E-01	MWD	= -.14340E-03
XQD	= .0	ZQD	= -.14340E-03	MQD	= -.83506E-03
XX	= .0	ZX	= .0	MX	= .0
XZ	= .0	ZZ	= .0	MZ	= .0
XDELT	= -.57867E-03	ZDELT	= -.57867E-02	MDELT	= -.28238E-02
	M = .19043E-01		IY = .93512E-03		

TABLE C3

NONLINEAR X-Z SYMMETRY TERMS

XUU = -.10704E-02	ZUU = .0	MUU = -.0
XWW = -.11127E 00	ZWW = .0	MWW = .0
XWQ = -.18182E-01		
XQQ = -.14340E-03		
XVV = -.11127E 00	ZVV = .0	MVV = .0
	ZVP = -.18182E-01	MVP = -.14350E-03
XVR = .18182E-01	ZVR = .0	MVR = .77258E-04
XRP = -.77258E-04	ZRP = .14350E-03	MRP = .83473E-03
XRR = -.14350E-03	ZRR = .0	MRR = -.60977E-06

TABLE C4

S N A M E NON-DIMENSIONAL LATERAL
STABILITY DERIVATIVES

YV = -.33046F-01	KV = -.15537E-03	NV = -.22682E-02
YP = -.17294E-03	KP = -.13896E-04	NP = .80153E-04
YR = .15280E-01	KR = .53435E-04	NR = -.73083E-02
YPHI = .0	KPHI = -.29769E-03	NPHI = .0
YPSI = .0	KPSI = .0	NPSI = .0
YVD = -.18182E-01	KVD = -.77258E-04	NVD = .14350E-03
YPD = .77258E-04	KPD = -.37211E-06	NPD = .60977E-06
YRD = .14350E-03	KRD = -.60977E-06	NRD = -.83511E-03
YY = .0	KY = .0	NY = .0
YDELT = .13285E-01	KDELT = .56451E-04	NDELT = -.64829E-02

TABLE C5

MASS MOMENTS OF INERTIA

M = .19043E-01		IXZ = .0	
IX = .35537E-04		IZ = .93512E-03	

TABLE C6

NONLINEAR X-Z SYMMETRY TERMS

YUU = .0	KUU = .0	NUU = .0
YWP = .18182E-01	KWP = -.77258E-04	NWP = -.14340E-03
	KQR = -.45882E-07	
	KVW = .21335E-06	
YPQ = .14340E-03		NPQ = -.83469E-03

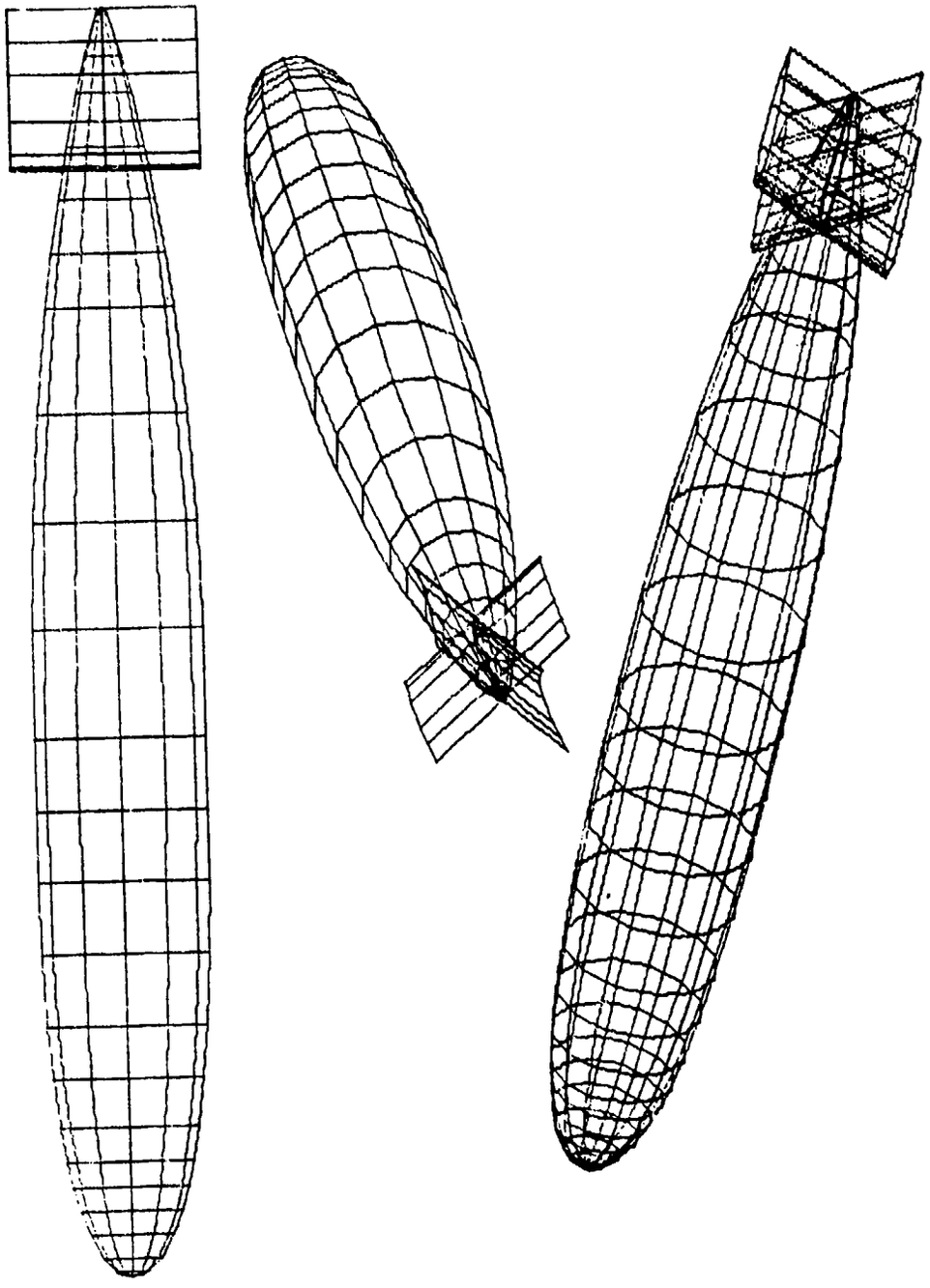

FIGURE C1. ORTHOGRAPHIC PROJECTIONS OF SUBJECT UNDERWATER VEHICLE

APPENDIX D

DESCRIPTION OF MANEUVERS USED IN TRAJECTORY SIMULATION

Figures D1 through D4 are time history plots of the four basic maneuvers used with the subject underwater vehicle to generate trajectory simulation and percent contribution plots of the various hydrodynamic coefficients discussed in the body of this report. These maneuvers were performed at a simulated vehicle speed of 14.35 feet per second.

The following definitions are provided to assist the reader in the interpretation of Figures D1 through D4.

DELS = Stern plane deflection, in degrees.

PITCH = Pitch angle, in degrees.

Z = Depth, in feet.

ALPHA = Angle of attack, in degrees.

DELR = Rudder deflection, in degrees.

BETA = Sideslip angle, in degrees.

R = Yaw rate, in degrees per second.

PHI = Roll angle, in degrees.

Y = Off-track distance, in feet.

X = Along-track distance, in feet.

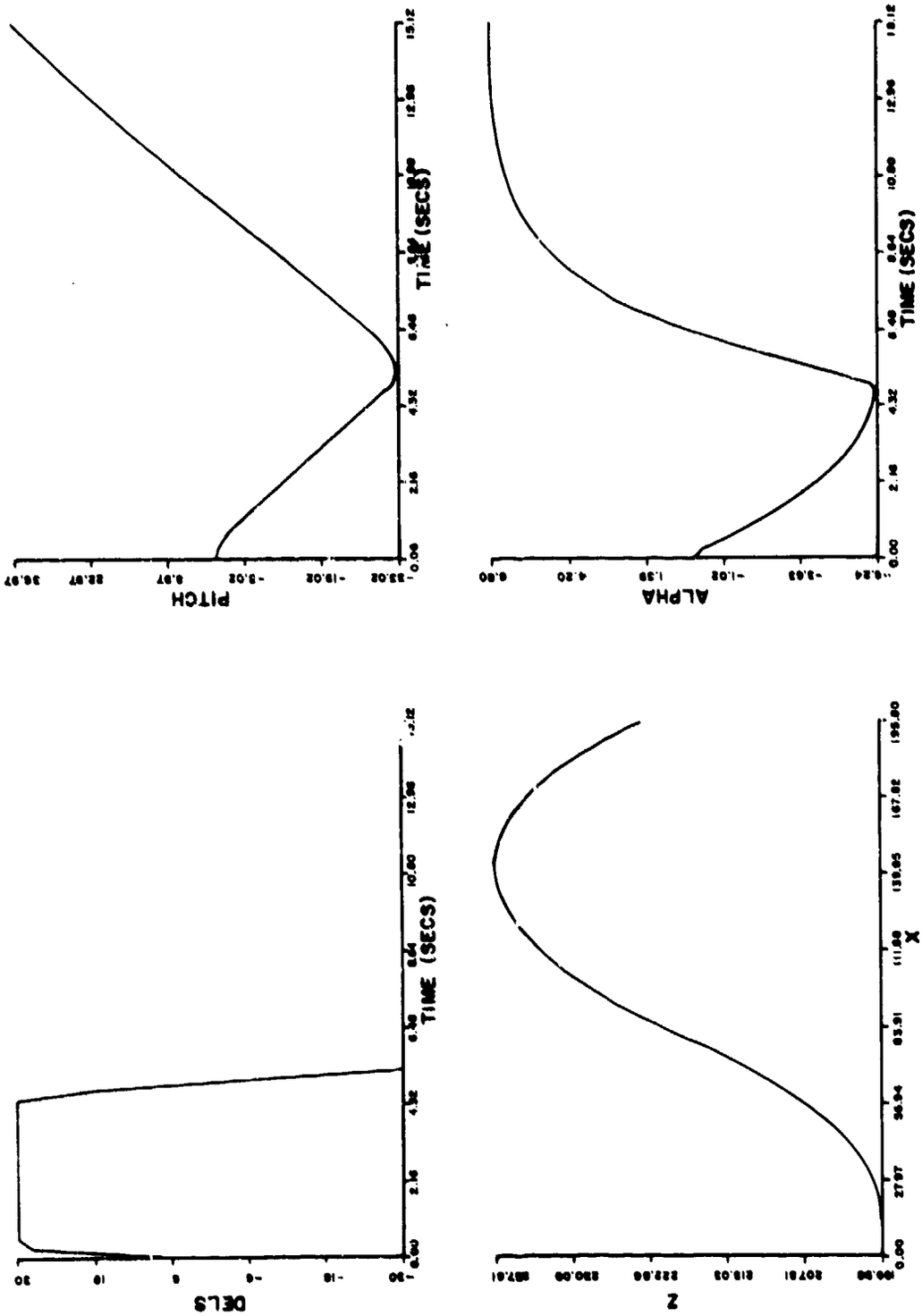

FIGURE D1. $\delta_s = \pm 30°$ DIVE/CLIMB MANEUVER TIME HISTORY PLOT

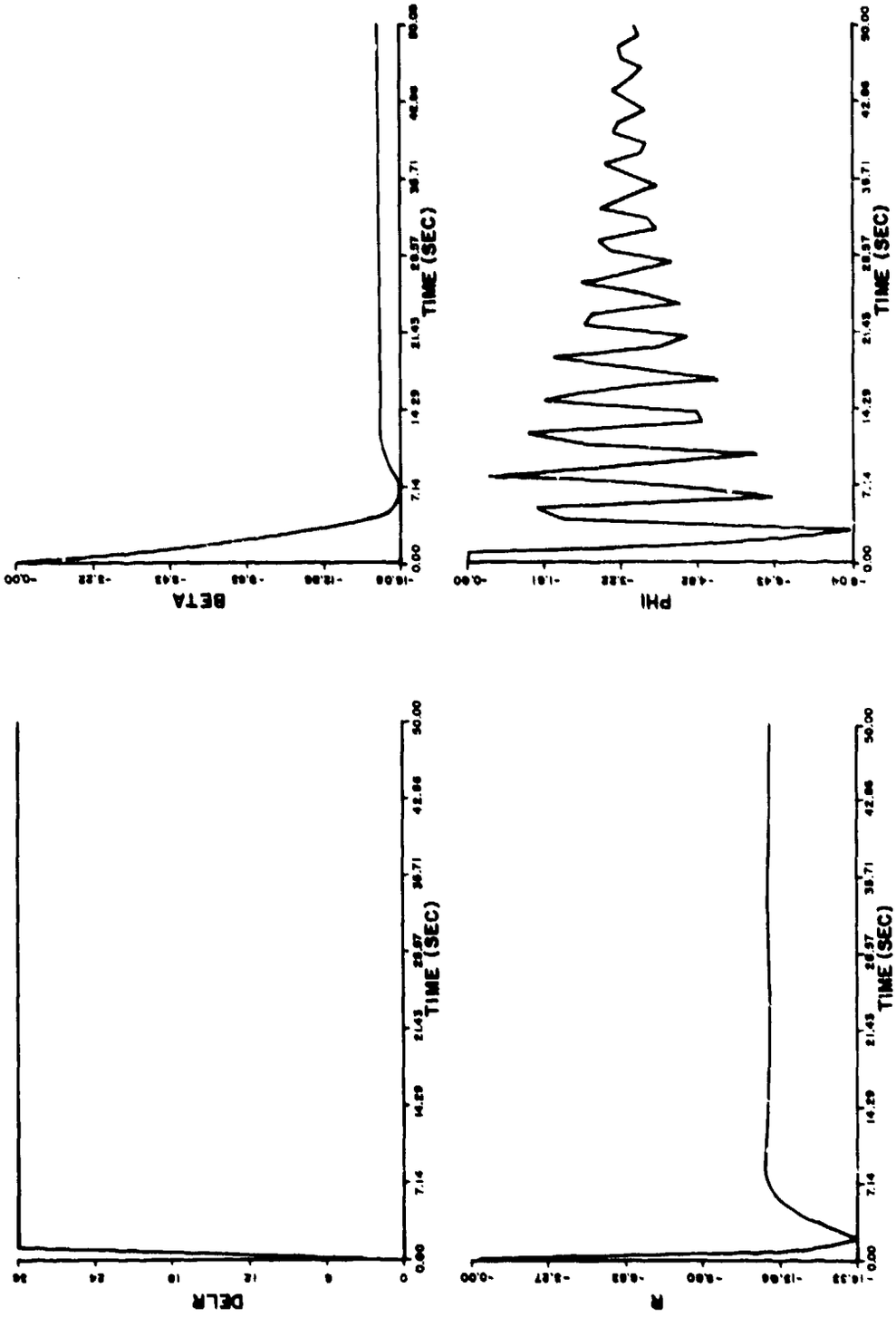

FIGURE D2. δ_r=30° STEADY TURN TIME HISTORY PLOT
(Sheet 1 of 2)

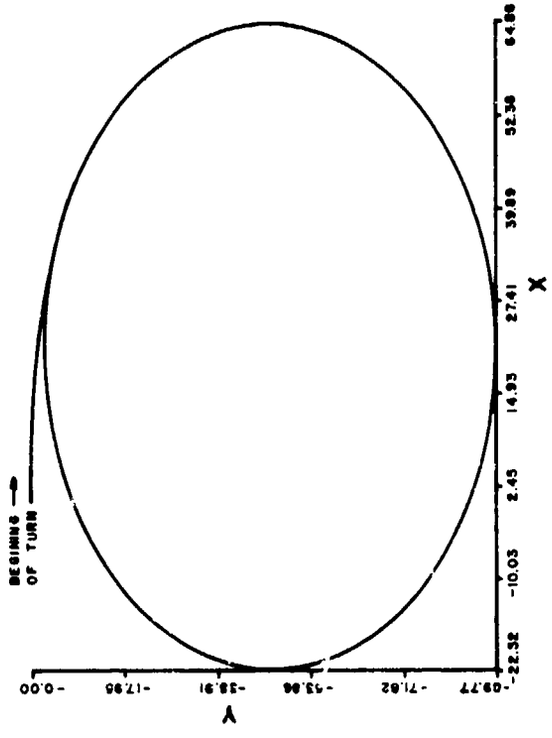

TABLE D2
(Sheet 2 Of 2)

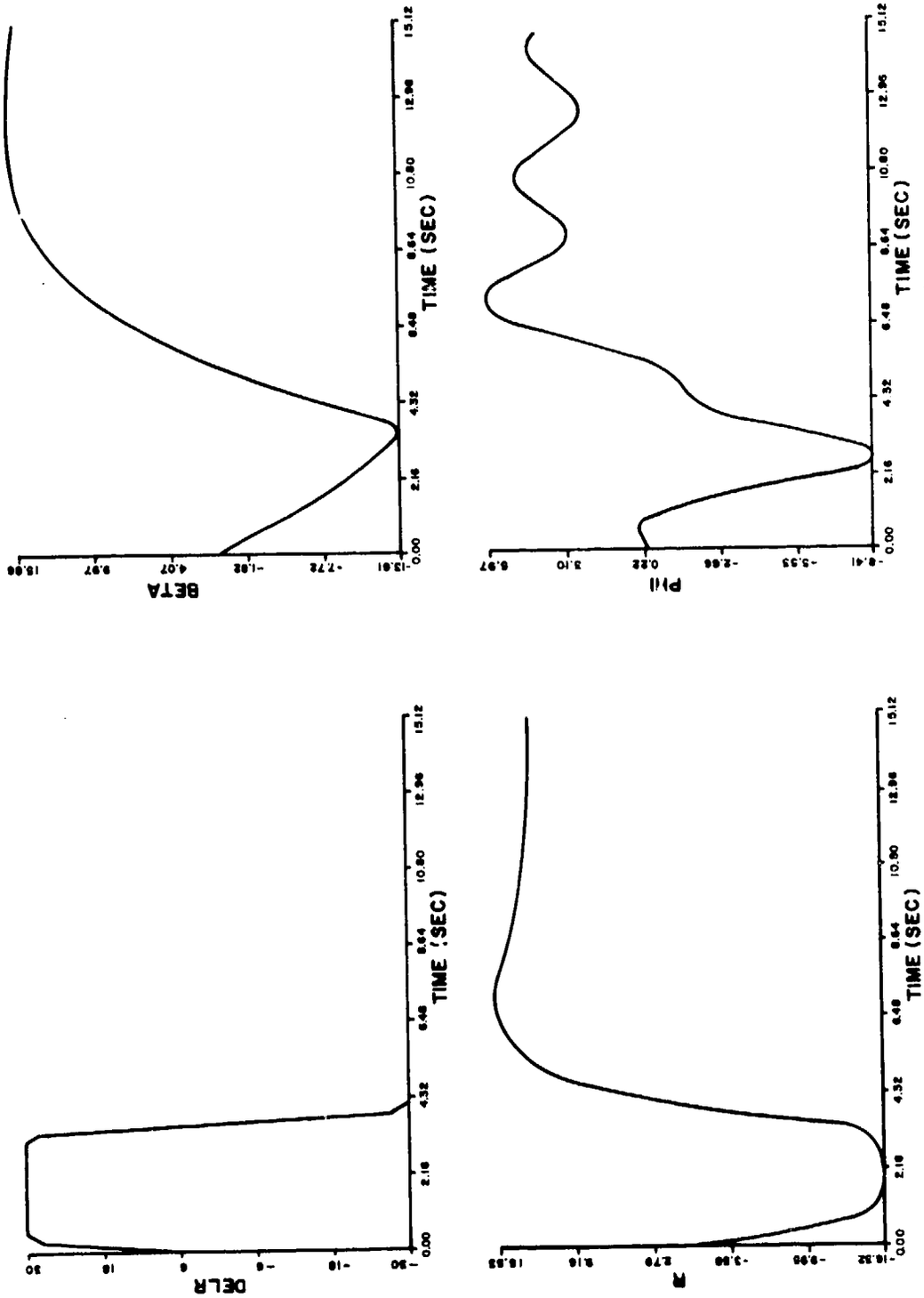

FIGURE D3. $\delta_r = \pm 30°$ TURN REVERSAL MANEUVER TIME HISTORY PLOT
(Sheet 1 of 2)

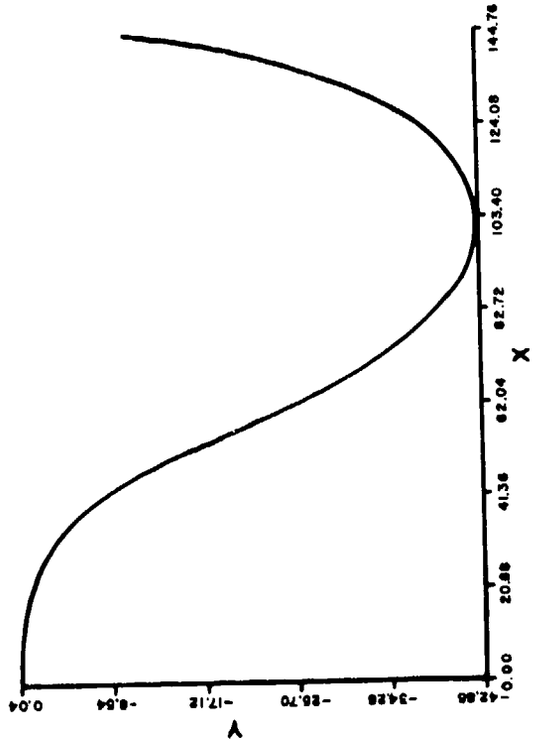

FIGURE D3
(Sheet 2 of 2)

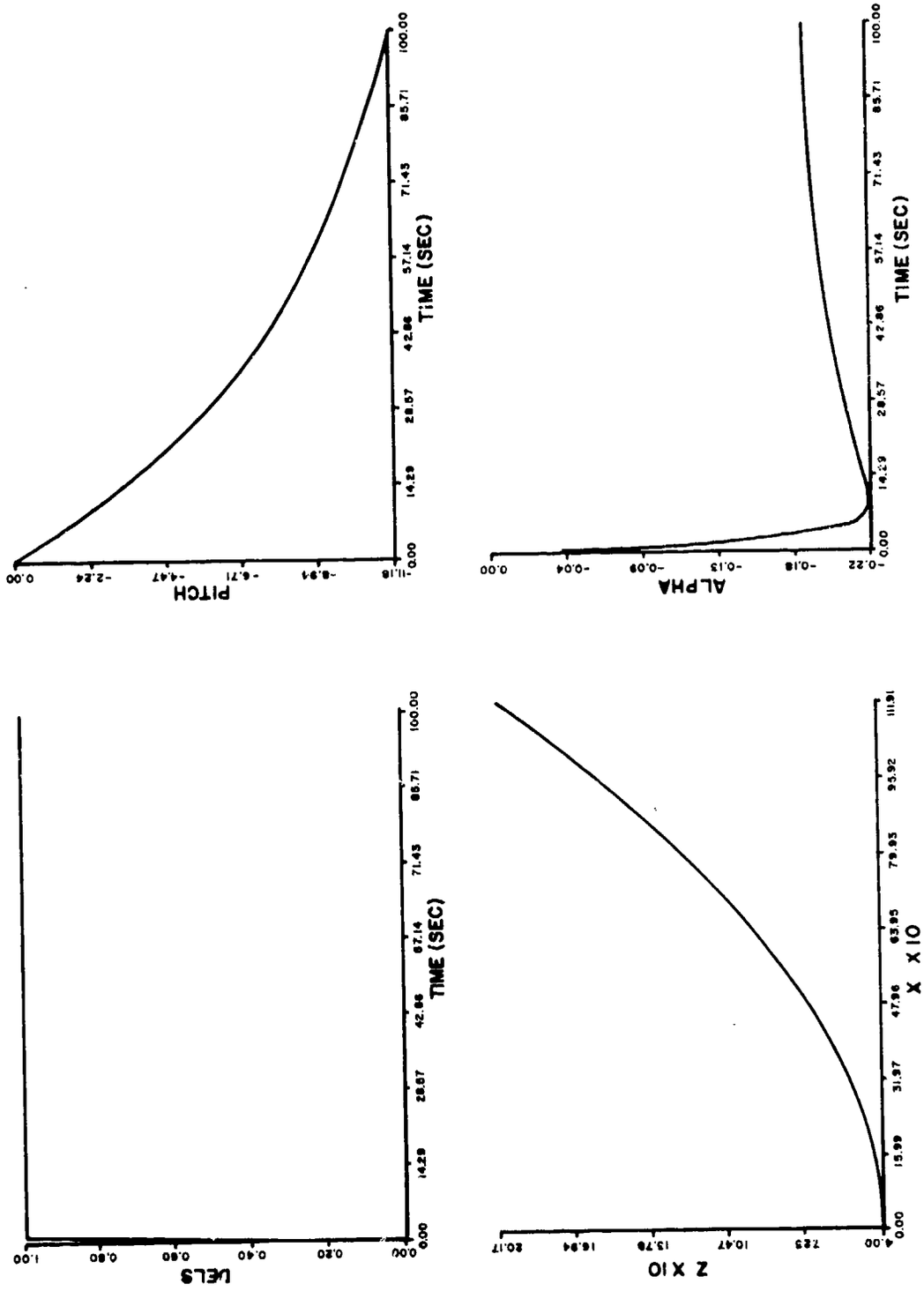

FIGURE D4. δ_s=1° STEADY DIVE TIME HISTORY PLOT

INITIAL DISTRIBUTION LIST
NCSC TR-[illegible]-78

Commander, Naval Sea Systems Command
(SEA 032, Mr. Sejd, Mr. Benen) (Copies 1-2)
(SEA 034) (Copy 3)
(SEA 035, Mr. Peirce) (Copy 4)
(SEA 99T) (Copy 5)
(PMS 393) (Copy 6)
(PMS 395) (Copy 7)
(Library) (Copy 8)
Chief of Naval Material
(MAT 08 T23, Mr. Remann, Mr. Vitus [illegible], Mr. Romano) (Copies 9-11)
Chief of Naval Operations (Copy 12)
Commander, Naval Ship Engineering Center
(Library) (Copy 13)
(Code 6136, Mr. Keane, Mr. Louis) (Copies 14-15)
Commander, David Taylor Naval Ship Research & Development Center, Bethesda
(Library) (Copy 16)
(Code 1564, Mr. Feldman) (Copy 17)
(Code 1548, Mr. Folli) (Copy 18)
Commanding Officer, Naval Underwater Systems Center
(Library) (Copy 19)
(Mr. Goodrich) (Copy 20)
(Mr. Nadolink) (Copy 21)
Commander, Naval Ocean Systems Center
(Code 5332) (Copy 22)
(Code 6302) (Copy 23)
(Library) (Copy 24)
Director, Naval Research Laboratory
(Library) (Copy 25)
Commander, Naval Surface Weapons Center, White Oak
(Library) (Copy 26)
Commander, Naval Surface Weapons Center, Dahlgren
(Library) (Copy 27)
Commander, Naval Weapons Center, China Lake
(Library) (Copy 28)
Superintendent, Naval Academy, Annapolis
(Library) (Copy 29)
Superintendent, Naval Postgraduate School, Monterey
(Library) (Copy 30)
Chief of Naval Research
(ONR 211 - Mr. Siegel) (Copy 31)
(ONR 438 - Mr. Cooper) (Copy 32)
(ONR 211 - Mr. Whitehead) (Copy 33)
Stevens Institute of Technology, Davidson Laboratory, Hoboken, NH 07030
(Library) (Copy 34)
(Mr. Al Strumpf) (Copy 35)
Applied Research Laboratory, Penn State University
(Library) (Copy 36)
(Mr. W. R. Wall) (Copy 37)
Applied Research Laboratory, University of Texas
(Library) (Copy 38)
Applied Physics Laboratory, Johns Hopkins University, Charles & 34th St., Baltimore, MD 21218
(Library) (Copy 39)
(W. Vane [illegible]) (Copy 40)
(Mr. Wozn[illegible]) (Copy 41)
Virginia Polytechnical Institute, Blacksburg, VA 24060
(Library) (Copy 42)
Massachusetts Institute of Technology, C[illegible]ge, MA 02139
(Library) (Copy 43)
(Mr. Abkowitz) (Copy 44)
Library of Congress, Washington, DC
(Science & Technology Library) (Copy 45)
Director, Woods Hole Oceanographic Institute (Copy 46)
Director, Scripps Institute of Oceanography (Copy 47)
Commanding Officer, Naval Ocean Research & Development Activity, Bay St. Louis, MS 39520 (Copy 48)
Society of Naval Architects & Marine Engineers (SNAME), 74 Trinity Pl., New York, NY 10006 (Copy 49)
Director of Defense Research & Engineering, Washington (Copy 50)
Director, Advanced Research Projects Agency, Washington (Copy 51)
The Analytical Sciences Corp., Six Jacob Way, Reading, MA 01867
(Library) (Copy 52)
Systems Control Institute, 1801 Page Mill Rd., Palo Alto, CA
[illegible]) (Copy 53)
Kansas University, Lawrence, Kansas 66044 (Copy 54)
Nielsen Engineering & Research, Inc., Mountain View, CA 940[illegible]
(J. Fidler) (Copy 55)
The Charles Stark Draper Laboratory, Cambridge, MA 02139
(Library) (Copy 56)
Director, Defense Documentation Center (Copies 57